



The
University
Of
Sheffield.

**Establishing the *Streptococcus pyogenes* model of infection in
the zebrafish embryo.**

By

Dimitrios Michailidis

A thesis submitted for the degree of Doctor of Philosophy

September 2019

Department of Molecular Biology and Biotechnology, University of Sheffield,
Western Bank, Sheffield, S10 2TN

Summary

Streptococcus pyogenes is a bacterium that colonises the human oropharynx asymptotically. It is also a common cause of mild skin and throat infections. These can develop into invasive tissue disease and post-immune sequelae. In order to understand how *S. pyogenes* causes disease, several animal models have been used. My study has developed and interrogated the zebrafish embryo systemic model of infection.

The first part of this work, involved analysis of the virulence of the H293 (*emm89*), H305 (*emm1*), and HSC5 (*emm14*) *S. pyogenes* strains, via zebrafish embryo survival assays. This revealed that H293 was the least virulent, and thus more amenable to study within experimental parameters. A study of bacterial population dynamics during infection suggested the presence of a bottleneck, where the immune system regulates growth of *S. pyogenes* for up to 8 hours post-infection. After this point, with an infectious dose that leads to approximately 50% host survival, either rapid bacterial growth and host mortality or decline in bacterial numbers was seen. Intravital microscopy revealed that phagocytes ingest *S. pyogenes* very early after infection, with macrophages containing more bacteria than neutrophils. Interestingly, by 8 hours post-infection, macrophages were found completely saturated with bacteria or empty, with concomitant extracellular *S. pyogenes*. The role of phagocytes as the immunological bottleneck was verified as their ablation led to uncontrolled bacterial proliferation. The role of other bacteria, and their products, in the initiation of *S. pyogenes* infection was then determined.

Based on my findings, I have established a temporal and spatial model of *S. pyogenes* infection in the zebrafish embryo. This sets the scene for the determination and analysis of host-pathogen interactions to aid the development of new control regimes.

Acknowledgements

To begin with, I would like to thank Prof. Simon Foster, the MRC CASE scholarship, and the University of Sheffield for giving me the opportunity to carry out my PhD. Thanks to Simon for helping me keep a productive pipeline with milestones throughout the project. I would also like to thank Dr Tomasz Prajsnar, whose input and guidance was vital to my PhD.

I am very grateful to all the members of the Foster lab for their scientific help, and to Dr Claire Turner, for providing me with two *Streptococcus pyogenes* strains, one of which ended up being the main strain of my project; H293. I am also grateful to Dr Turner for providing me with the CO₂ incubator as well as the heads up for using blood plates for *S. pyogenes*. In addition to that, I would like to thank the Renshaw lab for letting me use a few of their fish lines. I would also like to thank Dr Stefan Mesnage for his constructive criticism of my work via my yearly progress reports.

Finally, I would like to thank Felix Weis, Lucia Lafage and Oliver Carnell, for making my lab bay a fun place to be. I would also like to thank Piotr Szuta for teaching me fish injections as well as Josie Gibson and Josh Sutton for providing me with peptidoglycan as well as Josie helping me with the Johnston lab's microscope.

Abbreviations

°C	Degrees Celsius
BHI	Brain heart infusion
BSA	Bovine serum albumin
CFU	Colony forming units
dH ₂ O	Distilled water
DMSO	Dimethyl sulphoxide
DNA	Deoxyribonucleic acid
dpf	days post fertilisation
dpi	days post infection
Fc	fragment crystallisable domain of immunoglobulin molecules
Fg	Fibrinogen
g	Grams
GFP	Green fluorescent protein
hpi	Hours post infection
h	Hours
kV	Kilovolts
L	Litre
LWT	London wild-type
M	Molar
mg	Milligrams
mL	Millilitres
mM	Millimolar
min	Minutes
MO	Morpholino oligonucleotide
nL	nanolitre
nm	nanometre
OD ₆₀₀	Optical density at 600nm

PAMP	Pathogen-associated molecular pattern
PBS	Phosphate buffered saline
PG	Peptidoglycan
RNA	Ribonucleic acid
rpm	Revolutions per min
STSS	Streptococcal toxic shock syndrome
TCR	T-cell receptor
Tet	Tetracycline
THY	Todd-Hewitt broth
TLR	Toll-like receptor
TSB	Tryptone Soya broth
v/v	Volume for volume
WT	Wild-type
w/v	Weight for volume

Table of Contents

Summary.....	i
Acknowledgements	ii
Abbreviations	iii
Table of Contents.....	v
List of Figures.....	xi
List of Tables.....	xiii
Chapter 1: Introduction.....	1
1.1 <i>S. pyogenes</i> classification.....	1
1.2 <i>S. pyogenes</i> infections.....	2
1.2.1 Tissue tropism.....	2
1.2.2 Carriage	3
1.2.3 Non-invasive infections.....	5
1.2.4 Invasive infections	6
1.2.5 Autoimmune sequelae.....	9
1.2.6 <i>Emm</i> global epidemiology	10
1.3 <i>S. pyogenes</i> virulence factors	13
1.3.1 Surface-associated virulence factors	13
1.3.1.1 M protein.....	13
1.3.1.2 SpyCEP	14
1.3.1.3 Hyaluronic acid capsule	16
1.3.2 Secreted virulence factors	18
1.3.2.1 SpeB.....	18
1.3.2.2 Streptolysins	21
1.3.2.3 Complement inhibitors	22
1.3.2.4 IgG degrading proteins	24

1.3.3 Virulence genes and regulation	25
1.4 <i>S. pyogenes</i> interactions with the immune system.....	34
1.4.3 <i>S. pyogenes</i> TLR recognition	34
1.4.4 <i>S. pyogenes</i> and phagocytes	37
1.4.5 Adaptive immune system	38
1.5 Animal models for <i>S. pyogenes</i> infection	40
1.5.1 Mice	42
1.5.2 Primates.....	47
1.5.3 Zebrafish.....	49
1.5.4 Invertebrates	54
1.7 Population dynamics	54
1.8 Exploring the effect of commensals in <i>S. pyogenes</i> infection.....	55
1.9 Aims of the project.....	59
Chapter 2: Materials and Methods	60
2.1 Bacterial media.....	60
2.1.1 Todd-Hewitt 0.2% w/v yeast (THY) broth.....	60
2.1.2 Columbia horse Blood Agar (CBA)	60
2.1.3 Luria-Bertani (LB) broth.....	61
2.1.4 Brain Heart Infusion (BHI) broth	61
2.1.5 Electroporation medium	61
2.2 Antibiotics	62
2.3 Bacterial strains.....	62
2.3.1 <i>Streptococcus pyogenes</i> strains.....	62
2.3.2 <i>Escherichia coli</i> strains.....	63
2.3.3 <i>Staphylococcus aureus</i> strains.....	64
2.3.4 <i>Micrococcus luteus</i> strains	64

2.4 Plasmids	64
2.5 Buffers and solutions	65
2.5.1 Phosphate buffered saline (PBS)	65
2.5.2 QIAGEN buffers	65
2.5.2.1 QIAGEN Buffer P1	65
2.5.2.2 QIAGEN Buffer P2	65
2.5.2.3 QIAGEN Buffer P3	66
2.5.2.4 QIAGEN Buffer EB.....	66
2.5.2.5 QIAGEN Buffer TE	66
2.5.2.6 QIAGEN Buffer QBT	66
2.5.2.7 QIAGEN Buffer QC	67
2.5.2.8 QIAGEN Buffer QF	67
2.5.2.9 QIAGEN Buffer N3, PB, PE	67
2.6 Chemical dyes	68
2.7 Determination of bacterial cell density.....	68
2.7.1 Spectrophotometric measurement (OD ₆₀₀)	68
2.7.2 Cell counts (CFU mL ⁻¹).....	68
2.8 DNA Purification techniques	69
2.8.1 Plasmid preparation from <i>S. aureus</i>	69
2.9 Transformation of <i>S. pyogenes</i>	70
2.9.1 Preparing electro-competent <i>S. pyogenes</i> cells.....	70
2.9.2 Electroporation of DNA into competent <i>S. pyogenes</i> cells	70
2.10 Zebrafish lines	71
2.11 Zebrafish husbandry	71
2.12 Zebrafish media	72
2.12.1 E3 (x10).....	72
2.12.2 Methylcellulose.....	72
2.13 Zebrafish anaesthesia.....	73
2.14 Microinjections of <i>S. pyogenes</i> into zebrafish embryos	73

2.15 Determination of zebrafish embryo mortality following infection	74
2.16 Determination of <i>S. pyogenes</i> growth <i>in vivo</i>	74
2.17 Fixation of embryos	75
2.18 Microscopy	75
2.18.1 Mounting of zebrafish	75
2.18.2 Imaging of zebrafish	75
2.19 Chemical staining of <i>S. pyogenes</i>	76
2.20 Microinjections of morpholino oligonucleotides into zebrafish embryos	77
2.20.1 Morpholinos	77
2.20.2 Morpholino injections into zebrafish eggs	78
2.21 Neutrophil ablation via Metronidazole treatment	78
2.22 Macrophage ablation via Metronidazole treatment	78
2.22 Statistical analysis	79
Chapter 3: Developing the zebrafish embryo infection model for <i>S. pyogenes</i>	80
3.1 Introduction	80
3.1.1 Choosing an embryo age	80
3.1.2 Choosing an <i>S. pyogenes</i> strain	81
3.2 Aims of this chapter	82
3.3 Results	83
3.3.1 Determination of optimal infection point post-fertilisation	83
3.3.2 Investigation of HSC5 virulence in the zebrafish embryo model	86
3.3.3 HSC5 population dynamics <i>in vivo</i>	86
3.3.4 Investigation of H293 virulence in the zebrafish embryo model	88
3.3.5 H293 population dynamics <i>in vivo</i>	88
3.3.6 Investigation of H305 virulence in the zebrafish embryo model	90
3.3.7 H305 population dynamics <i>in vivo</i>	90

3.8 Discussion	92
3.8.1 Choosing the systemic model of infection.....	92
3.8.2 2-dpf embryos offer an amenable model to study <i>S. pyogenes</i> infection	92
3.8.3 H293 <i>S. pyogenes</i> strain allows for examination of the infection bottleneck	93
Chapter 4: Investigating host-pathogen interactions in the zebrafish embryo model of <i>S. pyogenes</i> infection	95
4.1 Introduction.....	95
4.2 Aims of this chapter	96
4.3 Results.....	97
4.3.1 pHrodo staining of <i>S. pyogenes</i> injected in zebrafish embryos.....	97
4.3.2 Creating fluorescently-labelled <i>S. pyogenes</i>	98
4.3.3 Whole fish microscopy of <i>S. pyogenes</i> during the initial and terminal stages of infection.....	101
4.3.4 Elucidating the involvement of macrophages and neutrophils during infection	105
4.3.5 Imaging the infection progression over the first 8 hpi.....	110
4.3.6 Myeloid depletion in zebrafish embryos via a <i>pu.1</i> morpholino	112
4.3.7 <i>irf8</i> knock-down in zebrafish larvae.....	115
4.3.8 Use of clodronate liposomes for macrophage ablation	117
4.3.9 Metronidazole treatment for effective ablation of neutrophils	120
4.4 Discussion	124
Chapter 5: Elucidation of population dynamics during <i>S. pyogenes</i> infection and the role of augmenting material	128
5.1 Introduction.....	128
5.2 Aims of this chapter	128
5.3 Results.....	129
5.3.1 Population dynamics during the <i>S. pyogenes</i> infection.....	129

5.3.2 Does the augmentation phenomenon occur during <i>S. pyogenes</i> infection? ...	134
5.3.2.1 The effect of the skin commensal <i>M. luteus</i> on <i>S. pyogenes</i> infection	134
5.3.2.3 Elucidation of the role of cell wall peptidoglycan in augmentation of <i>S. pyogenes</i> infection	136
5.3.2.3.2 Effect of <i>S. aureus</i> peptidoglycan on <i>S. pyogenes</i> infection.....	140
5.3.2.5 <i>In vivo</i> zebrafish imaging of <i>S. pyogenes</i> co-inoculated with <i>M. luteus</i> peptidoglycan	142
Chapter 6: General Discussion	150
6.1 Introduction.....	150
6.2 Setting up the model.....	152
6.3 Describing the <i>S. pyogenes</i> infection dynamics.....	152
6.4 Phagocytes mediate a temporary bottleneck during infection	153
6.5 <i>S. pyogenes</i> can replicate inside phagocytes	154
6.6 Pathogen population dynamics reveal polyclonality	155
6.7 Augmenting material does not affect <i>S. pyogenes</i> infection.....	155
6.8 <i>S. pyogenes</i> infection model hypothesis.....	156
6.9 Future directions.....	157
Chapter 7: References	162

List of Figures

Figure 1.1 Emm patterns and their tissue tropism groupings	4
Figure 1.2 Geographical distribution of the most prevalent invasive <i>S. pyogenes emm</i> types	12
Figure 1.3 Surface-associated <i>S. pyogenes</i> virulence factors	15
Figure 1.4 Secreted <i>S. pyogenes</i> virulence factors	19
Figure 1.5 Innate immune response against <i>S. pyogenes</i>	36
Figure 1.6 Animal models for analysis of <i>S. pyogenes</i> pathogenesis	41
Figure 3.1 Effect of embryo age on the <i>S. pyogenes</i> zebrafish infection model	87
Figure 3.2 Host-pathogen dynamics during zebrafish embryo infection with H293	89
Figure 3.3 Host-pathogen dynamics during zebrafish embryo infection with HSC5	91
Figure 3.4 Host-pathogen dynamics during zebrafish embryo infection with H305	93
Figure 4.1 pHrodo stained <i>S. pyogenes</i> was internalised by likely embryo phagocytes	99
Figure 4.2 Transformation confirmation of pMV158-GFP and pMV158m-Cherry in H293	100
Figure 4.3 Imaging of disseminated bacterial foci at 1 hpi after systemically challenging embryos with GFP-tagged <i>S. pyogenes</i>	103
Figure 4.4 Visualisation of <i>S. pyogenes</i> localisation at the terminal stage of infection versus a cleared infection	104
Figure 4.5 <i>S. pyogenes</i> is phagocytosed by both embryo macrophages and neutrophils	106
Figure 4.6 Phagocytosis of <i>S. pyogenes</i> by macrophages vs neutrophils	108
Figure 4.7 Macrophages are more efficient in phagocytosing <i>S. pyogenes</i> than neutrophils in the zebrafish systemic model of infection	109
Figure 4.8 Visualising <i>S. pyogenes</i> progression of infection via macrophage phagocytosis over 8 hours	111
Figure 4.9 <i>pu.1</i> knock-down zebrafish larvae are significantly more susceptible to <i>S. pyogenes</i>	114
Figure 4.10 <i>irf8</i> knock-down zebrafish larvae are more susceptible to <i>S. pyogenes</i>	116

Figure 4.11 Macrophages are required for a successful defence against <i>S. pyogenes</i>	119
Figure 4.12 Metronidazole treatment effectively ablates neutrophils	122
Figure 4.13 Metronidazole renders zebrafish embryos more susceptible to infection regardless of NTR expression	123
Figure 5.1 <i>S. pyogenes</i> population dynamics reveal polyclonality	131
Figure 5.2 Visualisation of <i>S. pyogenes</i> population dynamics	133
Figure 5.3 Skin commensal <i>M. luteus</i> has no effect on <i>S. pyogenes</i> infection.	135
Figure 5.4 Examining the effect of <i>M. luteus</i> cell wall peptidoglycan on <i>S. pyogenes</i> pathogenesis	139
Figure 5.5 <i>S. aureus</i> peptidoglycan has no effect on <i>S. pyogenes</i> virulence	141
Figure 5.6 Confocal microscopy of labelled <i>M. luteus</i> cell wall peptidoglycan in fixed zebrafish embryos	143
Figure 5.7 <i>In vivo</i> microscopy of labelled <i>M. luteus</i> peptidoglycan and <i>S. pyogenes</i> H293 co-injected in zebrafish larvae	145
Figure 5.8 Comparative microscopy of overwhelmed and healthy zebrafish embryos after injections with labelled <i>M. luteus</i> peptidoglycan and <i>S. pyogenes</i>	146
Figure 5.9 Comparative microscopy of zebrafish embryos challenged with a mixed inoculum of <i>S. pyogenes</i> -GPF and <i>M. luteus</i> peptidoglycan over 0.5, 5.5 and 18.5 hpi	147
Figure 6.1 Diagram of the <i>S. pyogenes</i> systemic model of infection	159

List of Tables

Table 2.1 List of <i>S. pyogenes</i> strains used in this study	63
Table 2.2 Chemical dyes used in this study	68
Table 2.3 Transgenic zebrafish lines used in this study	71
Table 2.4 Morpholinos used in this study	77

Chapter 1: Introduction

1.1 *S. pyogenes* classification

Streptococcus pyogenes, also known as Group A *Streptococcus* (GAS), is a Gram-positive β -hemolytic bacterium, within the phylum of Firmicutes, that is restricted to human hosts (Bessen, 2009). It can grow either in pairs (diplococci) or in chains, is non-motile, and a facultative anaerobe. One of the early ways of classifying the *Streptococci*, and that is still routinely used, is the Lancefield serological grouping system. Species-specific 'Lancefield' carbohydrates on the surface of the bacterium are detected using antisera that are specific to the antigen type. For instance, Group A *Streptococcus* can be classified as such after confirming antisera reaction with its 'type A' antigen, which is a highly conserved polysaccharide of *N*-acetyl- β -D-glucosamine anchored onto a polyrhamnose backbone (Reglinski and Sriskandan, 2015). Other types include B-D and F-H, while there are *Streptococci* that do not have these antigens, such as *Streptococcus pneumoniae*. Prior to the advent of molecular techniques, M type-specific antisera were used to distinguish different *S. pyogenes* serological M types. Now, sequencing the 5' variable region of the *emm* gene (coding for the M protein), that ends up forming the N-terminus of the M protein, is used instead. Although, more than 200 *emm* types have been identified, the ten most prevalent types comprise about 70% of invasive *S. pyogenes* infections (O'Loughlin et al., 2007, Luca-Harari et al., 2009, Bessen and Lizano, 2010). T typing can be used in addition to M typing for further characterisation of *S. pyogenes*

isolates, by serum recognition of the backbone subunit of the *S. pyogenes* pilus (T antigen) (Lancefield and Dole, 1946, Johnson et al., 2006).

1.2 *S. pyogenes* infections

The vast majority of reported *S. pyogenes* infections are either throat infections, with more than 600 million cases, or skin infections, with more than 100 million per annum (Carapetis et al., 2005). There are estimated to be 2 million new cases of *S. pyogenes* infections every year (Carapetis et al., 2005). Severe *S. pyogenes* diseases in total cause at least 500,000 deaths each year globally, with the greatest burden coming from rheumatic heart disease.

1.2.1 Tissue tropism

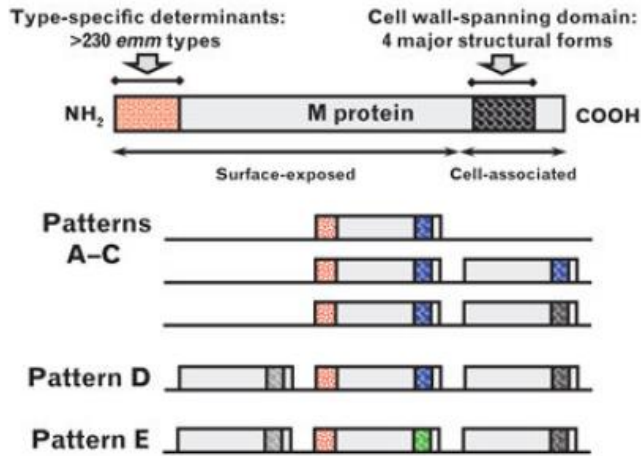
Many years of *S. pyogenes* epidemiology studies revealed a number of *S. pyogenes* *emm* types to be strongly associated with either pharyngitis (throat infection) or impetigo (superficial skin infection), rarely changing these observed tissue infection tendencies (McGregor et al., 2004, Bessen and Lizano, 2010). Other *emm* types were reported to consistently cause both infections. This alludes to some degree of specialisation within *S. pyogenes*. In order to systematically define these tissue tropisms, five *emm* patterns were assigned (A-E), based on sequence differences of the cell wall-spanning domain of the *emm* locus, and its close *emm*-like paralogs (Figure 1.1A) (Hollingshead et al., 1993, 1994). These *emm* patterns are strong

markers for tissue tropism with A-C being throat specialists, D being skin specialists, and E generalists (Figure 1.1B) (Bessen et al., 2008, Bessen 2009, Bessen and Lizano, 2010, Bessen, 2016).

1.2.2 Carriage

Many bacterial pathogens can asymptotically colonise the host, such as *S. pyogenes*, *Staphylococcus aureus*, and *Streptococcus pneumoniae* (Bogaert et al., 2004, Yazdankhah, 2004, Shaikh et al., 2010). Despite our many advances in understanding bacterial pathogenesis, it is still not known how and why these bacteria switch from carriage to the disease state. *S. pyogenes* usually colonises the naso- and oropharynx, and carriers can carry it regardless of any history of clinical symptoms (Martin, 2004). *S. pyogenes* has been reported to occur (carriage) in 5-15% in children (Shaikh et al., 2010). In general, the throat and skin areas of the human host are the primary reservoirs of *S. pyogenes*, and transmission occurs primarily via droplets originating from the throat, or direct skin contact (Mandell et al., 2005).

A



B

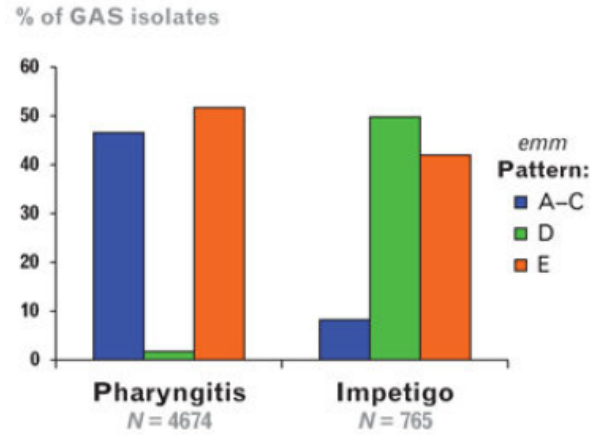


Figure 1.1 *Emm* patterns and their tissue tropism groupings

(A) Genetic map of the *emm* chromosomal region indicating *emm* genes, downstream or upstream *emm*-like genes, and their respective *emm* patterns.

(B) Categorisation of 5,439 *S. pyogenes* isolates according to pharyngitis or impetigo isolates, and their *emm* pattern.

Taken from (Bessen, 2016).

1.2.3 Non-invasive infections

Throat infections

The biggest reservoir of *S. pyogenes* in humans is Waldeyer's ring in the pharynx, a mucosal-associated lymphoid tissue that includes the tonsils (Watson et al., 2016). *S. pyogenes* can infect the human pharynx and cause pharyngitis or tonsillitis. 20-30% of all pharyngitis is being attributed specifically to *S. pyogenes* (Reglinski and Sriskandan, 2015). *Emm* types 1-4, 12, and 28, have been reported to be the most dominant types in the US and Canada causing these infections (Shulman et al., 2009). Pharyngitis symptoms include soreness of the throat as well as swollen lymph nodes and fever as the immune system attempts to combat the infection. Additionally, if the infecting *S. pyogenes* produces any superantigens, it can induce scarlet fever. This leads to inflammation of the tongue that gives the distinctive 'strawberry' patterning of scarlet fever, and is discussed in more detail below (Cunningham, 2000). Pharyngitis has also been associated with Acute Rheumatic Fever (ARF), an autoimmune sequela caused by *S. pyogenes*, discussed in 1.2.5.

Skin infections

Skin infections of *S. pyogenes* are classified according to how deep the infection has reached. The most common of such infections is (superficial) impetigo, and is characterised by skin lesions on the face or extremities, that are easily transmitted by contact (Stulberg, et al., 2002). Superficial impetigo pustules can lead into deep impetigo (ecthyma), when *S. pyogenes* penetrates the epidermis further and reaches the dermis (Kaplan, 2009). Although impetigo lesions are often painless and

heal without scarring, ecthyma ones can cause pain and prove scarring. Treatment with oral broad-spectrum antibiotics, such as flucloxacillin, should systemic ulceration arise, is suggested as it protects against potential co-infection with *Staphylococcus aureus* (Reglinski and Sriskandan, 2015). Skin infections have been linked to post-streptococcal glomerulonephritis (PSGN), discussed in more detail in 1.2.5.

1.2.4 Invasive infections

Many superficial infections can evolve into invasive infections that disseminate further into deeper tissue via bacteraemic spread, skin wounds, or insect bites (Cunningham, 2000).

Cellulitis

Cellulitis occurs when *S. pyogenes* invades the dermis and subcutaneous tissues, and causes inflammation. Oral or parenteral administration of penicillin combined with flucloxacillin is the first-line therapy for cellulitis (Reglinski and Sriskandan, 2015).

Necrotizing Fasciitis

Wounds, blunt trauma, and greater than first-degree burns, can predispose a patient to Necrotizing Fasciitis (NF), and allow *S. pyogenes* to penetrate deep into subcutaneous tissues progressively destroying fat and fascia (Bisno and Stevens, 1996). Its symptoms, in order of appearance, are diffuse swelling, fluid-filled bullae

and their later violet colouration, at the soft tissue of extremities. However, the swelling could also be associated to the original trauma, whereas the violet colour, to potential cellulitis. Hence, while correct diagnosis of NF is difficult, it is vital as antibiotic therapy alone is insufficient (Bisno and Stevens, 1996). Instead, it additionally requires drainage and surgical removal of the infected tissues.

Streptococcal Toxic Shock Syndrome

All *S. pyogenes* invasive infection types have been reported to be able to lead to Streptococcal Toxic Shock Syndrome (STSS). When *S. pyogenes* produces at least one superantigen, along with its other virulence factors, it induces a 'cytokine storm' mediated by the abnormally high numbers of activated T cells. This leads to hypotension and subsequent organ failures. STSS is identified when the following have all been observed: hypotension, at least two body system failures, and isolation of *S. pyogenes* from a normally sterile site (Reglinski and Sriskandan, 2015). STSS manifests early as fever, vomiting, and diarrhoea, all non-specific symptoms. 30-60% of patients succumb within 72 to 96 hours (Stevens, 2000). Use of adjunct intravenous immunoglobulin G (IVIG) therapy against STSS has been suggested, due to reported protection via a strong anti-SAg antibody response, however its usefulness has not been entirely proven (Shah, et al., 2009).

Scarlet Fever

Scarlet Fever (SF) is a disease that develops from an *S. pyogenes* throat infection and is thought to be caused by the production of superantigens (Cunningham, 2000). It is characterised by the inflammation of the tongue giving it a characteristic rash. Although, SF was one of the main diseases that led to *S. pyogenes*-associated deaths at the end of the 19th century, it later saw a decline as the living conditions improved and antibiotics were introduced (Krause, 2002). However, new cases have been emerging in Hong Kong and mainland China since 2011, as well as in the UK since 2014 (Davies et al., 2015, Brouwer et al., 2019, Lynskey et al., 2019).

The Hong Kong and China cases were found to be *emm12* and *emm1* lineages that had acquired prophage elements conferring expression of two superantigens, streptococcal superantigen A (SSA) and streptococcal pyrogenic exotoxin C (SpeC), the DNase Spd1, as well as multidrug resistance (Davies et al., 2015, Brouwer et al., 2019).

In 2016, England specifically saw an increase in invasive *S. pyogenes* infections along with its seasonal elevation of SF (Lynskey et al., 2019). Albeit a hypervirulent *emm1* strain being the most frequently reported cause of invasive *S. pyogenes* disease since the mid-1980s, the current upsurge of SF in the UK is being caused by many different *emm* types with *emm3*, *emm12*, *emm1*, and *emm4* dominating (Aziz and Kotb, 2008, Turner et al., 2016, Lamagni et al., 2018). Lynskey and colleagues reported a new prevalent group of *emm1* lineage (M1_{UK}), genetically

different from other pandemic *emm1* strains, was found to be the leading cause of both the 2014-2016 UK seasonal elevations of SF, as well as the increase in invasive infections (Lynskey et al., 2019). Specific mutations in the M1_{UK} lineage are linked to higher levels of expression of the streptococcal pyrogenic exotoxin A (SpeA), a phage-encoded superantigen that is both necessary for nasopharyngeal infection and proved a key factor for the epidemic spread of *emm1* in the 1980s (Kasper et al., 2014).

1.2.5 Autoimmune sequelae

S. pyogenes infections can also lead to post-infection immune sequelae. These diseases can severely damage different organ systems, such as the kidneys in post-streptococcal glomerulonephritis (PSGN), and joints and heart in Acute Rheumatic Fever (ARF) (Cunningham, 2016). Data from both diseases suggest that molecular mimicry between streptococcal antigens and specific host molecules is the underlying reason why the immune system attacks and damages the host itself. Both PSGN and ARF, which are believed to be caused by persistent *S. pyogenes* infection, can be prevented by timely antibiotic administration. As a result, they are generally no longer seen in high income countries, which is not the case for low and middle income countries. In both ARF and PSGN, the *S. pyogenes* antigen responsible for the molecular mimicry has been reported to be the M protein (Adderson et al., 1998, Cunningham, 2014). The M protein is structurally similar to human heart proteins, such as tropomyosin and myosin, in the case of ARF, while it

is also structurally similar to the kidney molecules collagen and laminin (Michael et al., 1966, Kefalides et al., 1986, Cunningham, 2000). PSGN is characterised by the presence of blood or sediments in urine, oedema, and high blood pressure, whereas RHD by the severe damage of the heart. PSGN and ARF have been reported to not coexist in the same host, which was also confirmed with different *emm* types being associated with each one specifically.

1.2.6 *Emm* global epidemiology

A recent review of *S. pyogenes* invasive disease epidemiology from Europe, USA and Canada (2000-2017) reported that *emm1* was the most common followed by *emm28*, 89, 3, 12, 4 and 6 (Gheradie et al. 2018) (Figure 1.2).

One of the most prevalent *S. pyogenes* genotypes globally is *emm/M1*, and the rise of the M1T1 hypervirulent isolate was reported at the same time as the resurgence of invasive *S. pyogenes* infections the last 30 years (Cole et al., 2011). One of the factors that gave M1T1 its virulence, and genetically differentiated it from previous M1 variants, was the acquisition of two new prophages (Cleary et al., 1998). This new event resulted in M1T1 being able to produce SpeA and the DNase Sda1. Additionally, M1T1 also acquired a 36-kb region of the M12 chromosome which had as a consequence the upregulation of SPN and Streptolysin O (SLO) (Sumbly et al., 2005, Azirk et al., 2005). Additionally, a spontaneous mutation in the genes of the control of virulence (CovRS) two-component system, *covR* or *covS*, has been

demonstrated to further increase the virulence and dissemination capability of this clone, since it can upregulate virulence factor expression including Sic, SLO, and SpyCEP (Cole et al., 2011).

From 2000 to 2017, *emm89* has been one of the most dominant genotypes causing invasive disease in high income countries (Figure 1.2). In Europe, it has been in the top 3 of *emm* types; in Portugal, France, Denmark, Iceland, Sweden and Finland. It has also been one of the most prevalent but fluctuating in Norway, Germany, and the UK. The genotype has also been reported to be one of the most occurring ones in the US (top 5 fluctuating) and Canada (top 2 from the Toronto/Peel and the province of Ontario) (Gherardi et al., 2018). There has been a dramatic increase in infections caused by *emm89* in the UK over the past 10 years which contributed to a rise in overall invasive *S. pyogenes* infections (Turner et al., 2015).

A



B



Figure 1.2 Geographical distribution of the most prevalent invasive *S. pyogenes* emm types

A map of the distribution of the most prevalent *S. pyogenes* emm types that caused invasive disease in Europe (A), and North America (B). Data from epidemiology studies from different countries was pooled together for the period 2000-2017. Taken from (Gherardi et al., 2018).

1.3 *S. pyogenes* virulence factors

1.3.1 Surface-associated virulence factors

1.3.1.1 M protein

The M protein is a cell wall-anchored protein that is fibrillar and is found on all *S. pyogenes* strains (Figure 1.3). It is one of the most studied virulence factors of *S. pyogenes*, and it has been found to have roles in adhesion, phagocytosis resistance, and interaction with neutrophils (McNamara et al., 2008). With regards to adhesion, *S. pyogenes* uses its M protein to bind to host cells or components of the extracellular matrix, including collagen and fibronectin (Dinkla et al., 2003, Smeesters et al., 2010, Bober et al., 2011). M protein can additionally interfere with opsonisation and phagocytosis by binding to host proteins, and subsequently recruiting them to cover the surface of *S. pyogenes*. More specifically, the C4b binding protein (C4BP), once recruited, still acts as a complement inhibitor (Johnsson et al., 1996, Johnsson et al., 1998, Berggard et al., 2001). Plasma components, like albumin and fibrinogen can also be bound, which protects against complement deposition (Carlsson et al., 2005, Smeesters et al., 2010).

The M protein was also found to maintain its important role in virulence even after being cleaved to its soluble form by either human proteases or the streptococcal cysteine protease SpeB. In this state, it can form a complex with fibrinogen

molecules that has been shown to bind to β 2-integrins on the surface of neutrophils causing the neutrophil to be activated and release heparin-binding protein (HBP) (Herwald et al., 2004, Macheboeuf et al., 2011). This release of HBP, leads to vascular leakage and hence sepsis and shock (Linder et al., 2009). Furthermore, it has been reported that M protein, in its cleaved form, has pro-inflammatory properties (Pahlman et al., 2006), as well as the ability to induce massive T-cell activation which consequently induces a 'cytokine' storm (Pahlman et al., 2008). Observations have also been made suggesting that the M protein may contribute to invasive *S. pyogenes* infections by interacting with endothelial and epithelial cells causing cytoskeletal rearrangements (Cue et al., 1998, Dombek et al., 1999).

1.3.1.2 SpyCEP

S. pyogenes cell envelope proteinase (SpyCEP), is a protease on the surface of *S. pyogenes* that cleaves and inactivates interleukin (IL)-8 (Edwards et al. 2005). This results in a decrease in neutrophil recruitment, neutrophil-induced bacterial killing, and dissemination (Zinkernagel et al., 2008, Kurupati et al., 2010). Although, generally residing on the surface of *S. pyogenes*, SpyCEP has also been reported to be readily released, and phagocytosed by endothelial cells to impede neutrophil migration to the site of infection (Reglinski and Sriskandan, 2015). SpyCEP is expressed in higher levels in invasive clinical isolates as opposed to non-invasive strains (Edwards et al., 2005, Turner et al., 2009).

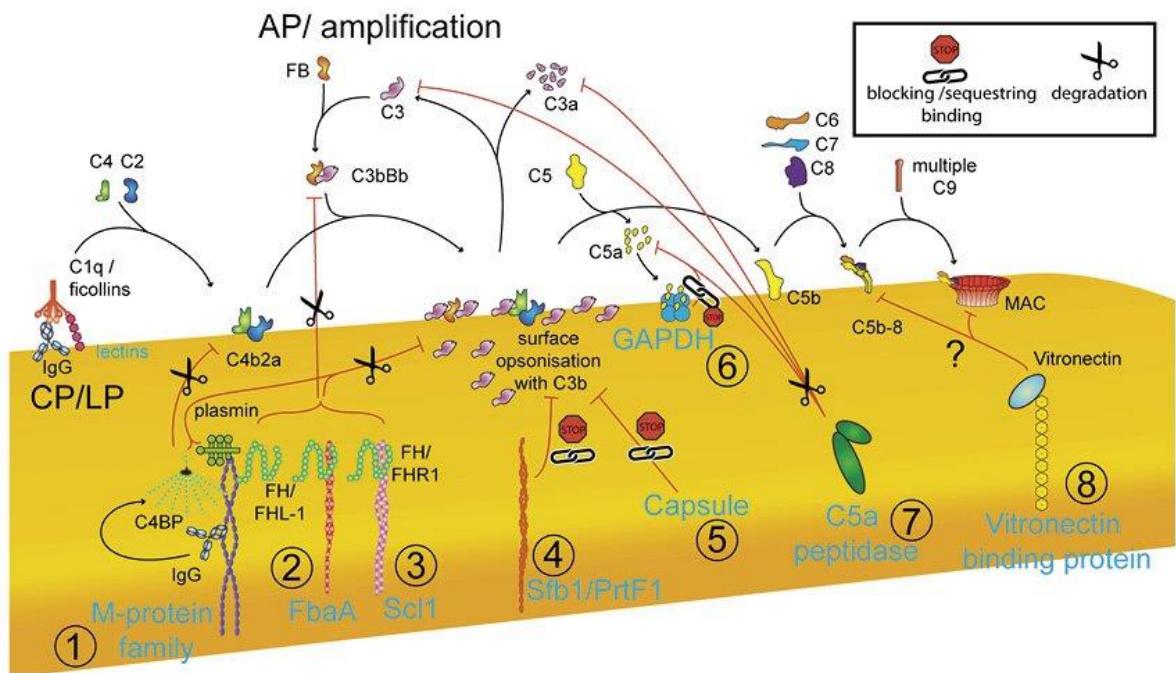


Figure 1.3 Surface-associated *S. pyogenes* virulence factors

Diagram of membrane-bound *S. pyogenes* evasins (written in blue), and their interactions with host proteins (written in black). **(1)**M proteins, **(5)**Hyaluronic capsule as described in Section 1.2.1. FbaA**(2)** and Scl1**(3)** bind Factor H (H), one of the complement inhibitors that targets the CP/LP and AP convertases. Fibronectin-binding protein Sfb1/PrtF1**(4)** impairs C3b deposition. **(6)**GAPDH is generally cytosolic, but has also been described to be sent to the bacterial surface. The CP C5a peptidase**(7)** cleaves C5a, C3, and C3a. Vitronectin-binding protein**(8)** has been reported to interfere with the MAC assembly, but its exact role as a *S. pyogenes* evasin is unknown, as indicated by the question mark. Taken from (Laabei and Ermert, 2018).

1.3.1.3 Hyaluronic acid capsule

The hyaluronic acid (HA) capsule is a viscous material made up of polymers of glucuronic acid and *N*-acetylglucosamine units (Cunningham, 2000). It is produced *de novo* and deposited on the surface of *S. pyogenes* covering it. Not all *emm* types have an HA capsule, as *emm4* and *emm22* lack the entire *hasABC* operon. Although, both HasA and HasB are needed for the synthesis of glucuronan, HasC is not (Alberti et al., 1998, Ashbaugh et al., 1998). A *hasB* homologue (*hasB2*) was found and was demonstrated to act as an additional UDP-glucose dehydrogenase for the production of HA (Cole et al., 2012). The second part of the HA repeating unit, *N*-acetylglucosamine, is synthesised as a by-product of cell wall production.

The HA capsule functions as a physical barrier for *S. pyogenes*, and hinders interactions between immune system effectors and pathogen-associated molecular patterns (PAMPs) on the surface of *S. pyogenes*, as well as being very important at establishing *S. pyogenes* during the initial stages of infection (Cunningham, 2000, Schragar et al., 1998). *S. pyogenes* HA is chemically identical to eukaryotic HA, found on cell surfaces, connective tissues, and the extracellular matrix, which allows the pathogen to mimic host antigens and evade the adaptive immune response (Cunningham, 2000, Cole et al., 2012). Furthermore, the HA capsule protects *S. pyogenes* from being coated with the cathelicidin antimicrobial

peptide LL-37 when trapped in neutrophil extracellular traps (NETs) (Cole et al., 2010). This promotes *S. pyogenes* survival by interfering with the role of LL-37 as a chemoattractant.

HA may be important for establishment of *S. pyogenes* during the initial stages of infection. The host cell surface HA receptor CD44 is present on the pharyngeal epithelium and the epidermis, and is upregulated during injury or inflammation (Schrager et al., 1998). *S. pyogenes* has been found to be able to bind to CD44 on human keratinocytes (Cunningham, 2000, Schrager et al., 1998). Hence, given the expression of CD44 in both skin and pharynx, and the conservation of *hasABC* in *S. pyogenes*, the HA-CD44 interaction might be key to the initial stages of infection. Hyper-encapsulated strains have been reported to cause extensive tissue damage at the site of infection and secondary bacteraemia in mice skin infection, whereas their isogenic acapsular clones induced a mild, self-resolving infection restricted at the site of infection (Schrager et al., 1996). This suggests that the HA capsule can play a key role in establishing *S. pyogenes* upon entry. Binding to CD44 was also found to trigger host cytoskeletal ruffling to initiate *S. pyogenes* movement into deeper tissues through or around the host cells (Cywes and Wessels, 2001). Nevertheless, despite all the data on the HA capsule, its definite role is yet to be understood.

1.3.2 Secreted virulence factors

1.3.2.1 SpeB

The streptococcal cysteine protease SpeB, is secreted as a 40 kDa inactive zymogen that is converted into its mature 28 kDa form via autocatalysis (Carroll and Musser, 2011). It is secreted by all sequenced strains, as seen in both mice and patients, but expression varies among *emm* types (Cole et al., 2011, Laabei and Ermert, 2019). A loss of function mutation of *speB* yielded reduced skin lesions, tissue damage, bacterial dissemination, and mortality in mice (Nelson et al., 2011). A study that analysed more than 9000 clinical isolates, reported that the overwhelming majority of the ones causing invasive disease secreted SpeB (Olsen et al., 2015). However, there are some isolates derived from *emm* types associated with invasive disease that do not produce SpeB (Chatellier et al., 2000, Flores et al., 2014).

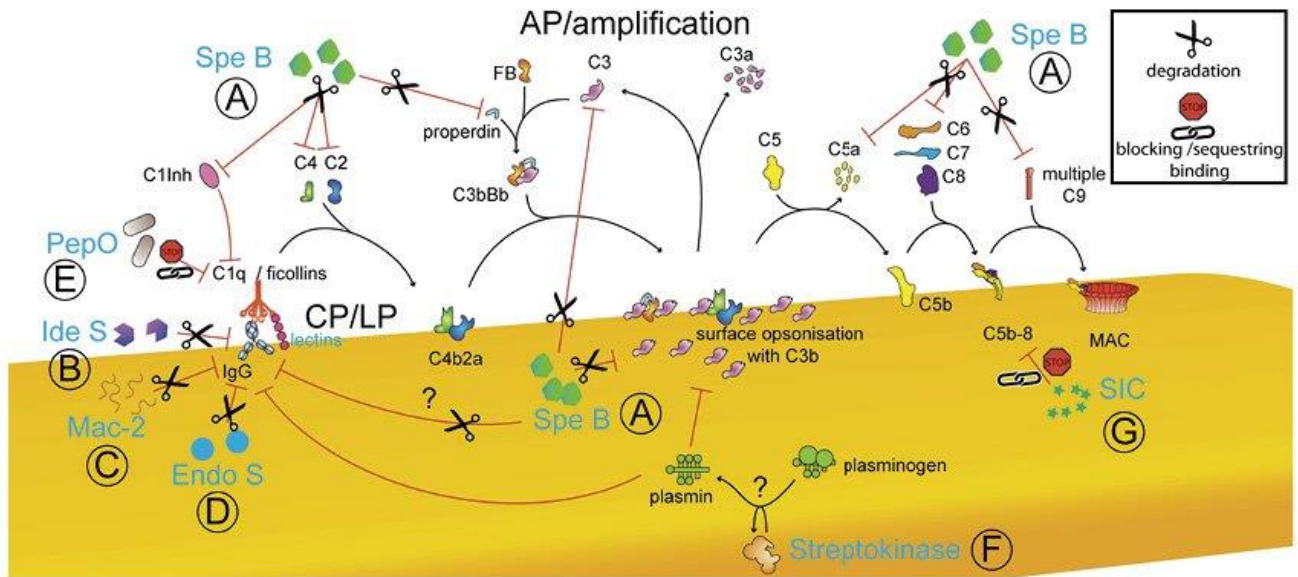


Figure 1.4 Secreted *S. pyogenes* virulence factors

Diagram of secreted *S. pyogenes* virulence factors (written in blue), and their interactions with host components (written in black) as described in Section 1.2.2. The action of SpeB on IgG remains elusive, as indicated by the question mark. Taken from (Laabei and Ermert, 2018).

SpeB is able to degrade both host and *S. pyogenes* virulence factors. Cleavage of E-cadherin and occludin, as well as ECM fibronectin and vitronectin, allows *S. pyogenes* to penetrate the epithelial barrier, and invade deeper tissues (Kapur et al., 1993, Sumitomo et al., 2013). SpeB can also hinder complement activation and neutrophil killing by degrading complement factors, such as the C1 inhibitor, C2, C3b, C5a, C9, and properdin (Figure 1.4) (Kuo et al., 2008, Terao et al., 2008, Honda-Ogawa et al., 2013). More specifically, a study showed that the absence of SpeB, resulted in increased deposition of C3 fragments on *S. pyogenes* A20 (Kuo et al., 2008). A20 is an M1T1 type, that was isolated from a patient with necrotizing fasciitis. A20 was found to be more resistant to neutrophil killing in SpeB-treated serum, when compared to normal serum, with the killing returning with the addition of purified C3. These observations were supported *in vivo* by a study reporting no detection of C3 (C3b) in sera from the sites of infection in STSS patients (Terao et al., 2008). Additionally, SpeB can degrade immunoglobulins, chemokines, fibrinogen, plasminogen, and the antimicrobial peptide LL-37 (Collin and Olsen 2001, Schmidtchen et al., 2002, Egesten et al., 2009, Nelson et al., 2011).

Virulence factors can also be proteolytically cleaved by SpeB suggesting that *S. pyogenes* can regulate its own virulence. SpeB can degrade the M protein, fibronectin-binding proteins, the plasminogen activator streptokinase, and the DNase Sda1 (Svensson et al., 2002, Cole et al., 2006, Walker et al., 2007, Sanderson-Smith et al., 2008, Nelson et al., 2011). In addition, SpeB has proteolytic activity against streptolysin O (SLO), the SpeF DNase (DNase B), glycolytic

enzymes, and the secreted inhibitor of complement (SIC) (Aziz et al., 2003, Terao et al., 2008, Honda-Ogawa et al., 2013). Plasmin-coated *S. pyogenes* can invade deeper tissues by breaking down tissues and extracellular matrix components. The lysis of the DNase Sda1 by SpeB also prevents *S. pyogenes* clearance from extracellular traps (Cole et al., 2006). Therefore, this significant control of virulence must be carried out by a complex system, but the underlying mechanisms are still elusive. It has been suggested that SpeB regulation is carried out by a combination of environmental cues and intrinsic regulators, including the regulator of protease B (RopB), the multiple gene regulator protein (Mga), and the CovRS system (Ribardo and McIver, 2006, Carroll and Musser, 2011).

1.3.2.2 Streptolysins

S. pyogenes causes vascular dysfunction, sepsis and toxic shock via superantigens and two secreted streptolysins; O (SLO) and S (SLS). These two hemolysins induce cell death of host red blood cells, neutrophils, and platelets via pore formation, as well as degrading epithelial junctions between host cells (Figure 1.4) (Goldmann et al., 2009, Timmer et al., 2009, Sumitomo et al., 2011).

SLO toxin is secreted and binds to the plasma membrane of host cells as a monomer. The monomers then oligomerise, and start transitioning through a few steps before they eventually create a circular pore complex with a diameter of 30 nm (Bhakdi et al., 1985, Feil et al., 2014).

SLS is produced and deposited on the *S. pyogenes* surface to then either be delivered on host cell membranes, to induce pore-forming-driven death, or bind calpain and E-cadherin to facilitate the breaking down of tight junctions (Sumitomo et al., 2011). A mechanism that has been recently elucidated however, is that of pore-forming-mediated cell death by SLS. High-resolution live cell imaging has shown that SLS pores disrupt band 3, an anion exchange protein, on the surface of erythrocytes, which causes a dramatic influx of Cl⁻ ions into the cell, and its subsequent lysis (Higashi et al., 2016). *In vivo* microscopy of embryo and adult zebrafish, and mice, revealed that *S. pyogenes* strain HSC5 producing SLS, is able to impede migration of neutrophils to the infection site, when compared to its SLS-mutant (Lin et al., 2009). This observation was also associated with decreased host survival for wild type HSC5.

1.3.2.3 Complement inhibitors

Endopeptidase O (PepO)

Endopeptidase O or PepO was shown to bind to C1q, an initiator of the classical complement pathway, at a higher affinity than IgG, preventing IgG from binding to C1q (Figure 1.4) (Honda-Ogawa et al., 2017). A *pepO* deletion mutant, proved to be more susceptible to the bactericidal activity of human serum *in vitro*. *In vivo*, *pepO* mutant-infected tissues showed reduced infection severity and higher complement activity in a mouse skin infection model. Hence, data suggests that *S. pyogenes* can evade the complement system by using PepO to prevent IgG from being engaged with C1q. Interestingly, a recent study identified PepO as a growth phase dependent

regulator of SpeB, using the *emm1* type *S. pyogenes* strain 5448 (Brouwer et al., 2018). They also confirmed the aforementioned *in vivo* observations when using a *pepO* mutant in mice. It is therefore unclear how much the susceptibility seen in the *pepO* mutant comes from its effects on SpeB or from its effects on C1q.

Streptococcal inhibitor of complement (SIC)

The thick outer wall of peptidoglycan of Gram-positive bacteria has been reported to confer resistance from the membrane attack complex (MAC)-mediated lysis (Joiner et al., 1983). Yet, the streptococcal inhibitor of complement (SIC) has been shown to interact with MAC directly *in vitro*, and was suggested to interfere with the complement system via MAC (Ferne-King et al., 2001). Although, it is still not known which one of these findings is relevant, SIC-deleted *S. pyogenes* strains exhibited reduced survival in saliva, a finding which was also seen in a mouse oropharyngeal infection model, hence there is a potential role of SIC for combatting the host immune system (Lukomski et al., 1999, Shelburne et al., 2005). SIC has only been found to be expressed by *emm1* strains.

A recent study reported that SIC binds to histones H3 and H4, and boosts pro-inflammatory cytokine production (Westman et al., 2018). SIC could bind to both H4 and TLR4 on monocytes and macrophages, and result in IL-6 production. Additional SIC ligands were found to induce an increased inflammatory response including LL-37, a neutrophil and eosinophil chemoattractant. Taken together with the previously mentioned studies, of SIC being needed for *S. pyogenes* to survive in saliva, the

authors hypothesised that SIC can both create a non-inflammatory and an overwhelmingly inflammatory environment, depending on whether *S. pyogenes* is colonising asymptotically or is causing invasive disease. More specifically, the highest levels of *sic* expression were seen when *S. pyogenes* was incubated in blood (Westman et al., 2018).

1.3.2.4 IgG degrading proteins

Immunoglobulin G (IgG) is the most ubiquitous antibody type in human serum, opsonises the bacteria, and activates the complement system via the classical way by binding to C1q at its Ig Fc region (Noris and Remuzzi, 2013, Laabei and Ermert, 2019). This engages the Fc γ receptors on phagocytes, and results in opsonophagocytosis and further chemoattraction. *S. pyogenes* can produce IdeS/Mac-1 and EndoS that can both neutralise this pathway.

IdeS/Mac-1

IdeS/Mac-1 owes its name to its homology with the α -subunit of human Mac-1, a leukocyte β 2 integrin (Lei et al., 2001). It is a 35-kDa cysteine endopeptidase that specifically binds to IgG, and is produced by many *S. pyogenes* strains (von Pawel-Rammingen, 2012). IdeS cleaves IgG at the lower region of the heavy chain, rendering Fc γ engagement impossible. The resulting antibody fragments can bind to *S. pyogenes*, but are unable to elicit a complement response, constituting a protective coat. IdeS/Mac-1 was reported to specifically bind to CD16 (Fc γ RIIIB) on

the membrane of human neutrophils and abrogate opsonophagocytosis and following production of reactive oxygen species (ROS) (Lei et al., 2001). This resulted in significantly higher *S. pyogenes* survival.

EndoS

EndoS is a 108-kDa endoglycosidase that targets the glycan at asparagine-297 of the heavy chain of IgG, required to interact with Fcγ receptors on the surface of phagocytes (Collin and Olsén, 2001b). This alludes to interference with classical activation of the complement via IgG. Whereas a study confirmed this, and reported that EndoS prevents binding of IgG to Fc receptors, and increases *S. pyogenes* survival in human blood *ex vivo* (Collin et al., 2002), another reported that mutagenesis of *ideS* or *EndoS* in M1T1 *S. pyogenes*, did not curtail resistance to phagocytosis or reduce virulence in a systemic mouse model of infection (Okumura et al., 2013). Therefore, these mechanisms are yet to be properly elucidated.

1.3.3 Virulence genes and regulation

Virulence Genes

The size of the *S. pyogenes* genome is about 1.9 Mb and sequencing the whole genome of 12 isolates indicated that more than 85% of all genes were conserved among the strains (Beres and Musser, 2007). These conserved genes, also known as the core genome, share a 98% nucleotide identity. Another approximately 10% of all genes, among the 12 isolates, was variable, and was comprised mainly of

mobile genetic elements, the majority of which were bacteriophage genomes (prophages) (Ferretti et al., 2001, Banks et al., 2004).

S. pyogenes virulence factor genes are scattered throughout the genome, unlike in pathogens such as *S. aureus* that has them grouped in pathogenicity islands. However, there are two pathogenicity island-like clusters; the *emm* cluster and the FCT region. The *emm* cluster is a group of *S. pyogenes* virulence factors located around the *emm* gene, coding for factors such the M protein, the C5a peptidase and SIC (Ferretti et al., 2001, Beres and Musser, 2007). Both the sequence and the chromosome location of the *emm* cluster have been shown to be highly conserved. The fibronectin-binding, collagen-binding, T antigen (FCT) region can be found in many *S. pyogenes* strains, and it carries genes for extracellular factors that promote attachment to human cells in the skin and pharynx (Bessen and Kalia, 2002, Mora et al., 2005, Abbot et al., 2007). The genes for pilin and full-length pilus protein production and cell wall attachment genes have been identified in this region (Telford et al., 2006). There have been reported at least nine variants of this region, which have also been linked to specific M types (Kratovac et al., 2007).

Mobile Genetic Elements

Mobile genetic elements (MGEs) are DNA sequences that encode proteins involved in the movement of genetic material from one bacterial chromosome to the next (Frost et al., 2005). They can be detected by their difference in G+C content compared to the genome they are found in, as well as from specific genetic elements they carry facilitating lateral gene transfer (Ferretti et al., 2001, Frost et al., 2005, Panchaud et al., 2009). There are three types of MGEs: insertion sequences (IS), prophages, and integrative and conjugative elements (ICEs) (Ferretti et al., 2001). Prophages are responsible for most of *S. pyogenes* strain to strain variations in virulence. They can often carry one or more genes for virulence, (Reglinski and Sriskandan, 2015). Examples of prophage and prophage-like element associated genes include ones expressing superantigens (*speA*, *speC*, , *speH*, *speI*, *speK*, *speL*, *ssa*), DNases (*spd1*, *mf2*, *mf3*, *mf4*), phospholipase A2 (*sla*), and macrolide resistance (*mefA*) (McShan and Nguyen, 2016). ICEs are DNA regions that can self-transmit between bacterial genomes via conjugative transfer (Burrus and Waldor, 2004). Twelve ICEs have been reported in *S. pyogenes*, expressing virulence determinants, antibiotic resistance genes, and antibiotics (Beres and Musser, 2007).

Virulence Gene Regulation: Standalone Regulators

Virulence gene regulation in *S. pyogenes* is coordinated by 12 highly conserved two-component systems, and at least 30 transcription regulators (Vega et al., 2016). They combine environmental cues with *S. pyogenes*' own metabolic state, and currently expressed genes, into a unified response.

Mga

Mga (multiple gene activator of *S. pyogenes*) is a transcriptional positive regulator that is highly conserved and is situated in the *emm* cluster having two alleles: *mga-1* and *mga-2* (Kreikemeyer et al., 2003, Hause and McIver, 2012). Its core regulon includes *emm* cluster virulence genes (*emm*, *scpA*, *sic*), the serum opacity factor gene (*sof*), and the streptococcal collagen-like protein genes (*scIA*, *scIB*). Mga is at its peak activity during the exponential growth phase under normal growth conditions, while also being induced in response to growth-limiting conditions, such as low iron and/or increased CO₂ concentrations, as well as higher temperatures (Vega et al., 2016). Hence, this data suggests that the timely upregulation of the colonisation and immune evasion factors controlled by Mga is important to enable *S. pyogenes* to progress into deeper tissues, after it has established the local infection. While Mga is active during exponential growth, there are other transcriptional regulators, such as ones from the RALP and Rgg families, that mostly act during the stationary growth phase (Vega et al., 2016). These factors have the ability to repress Mga when carbohydrate levels are low.

RALPs

The RALP (RofA-like protein) family is a group of four individual transcriptional regulators: RofA, Nra, RALP-3, and RALP-4/RivR. The RALP family is believed to drive *S. pyogenes* persistence during the stationary phase via upregulation of adhesins and downregulation of tissue damaging factors (Kreikemeyer et al., 2003). RofA and Nra have been studied the most and have been reported to exert their activity upon the FCT region. They both can repress SpeB and SLS transcription, while Nra can also silence SpeA (Panchaud et al., 2009, Siemens et al., 2012). Co-activation of RALPs and the fibronectin binding protein Sfb1, boosts attachment and penetration of host cells allowing *S. pyogenes* to switch from a colonisation to a persistence phenotype during stationary growth. In addition to being able to repress Mga, Nra can also exert such an activity on RALP-3, RALP-4, and Rgg/RopB (Podbielski et al., 1999, Kreikemeyer et al., 2007)

Rggs

The Rgg/GadR/MutR family of transcription factors are widespread in the Firmicutes phylum, and *S. pyogenes* expresses four paralogs: Rgg/Rgg1/RopB, ComR, Rgg2, and Rgg3 (Chang et al, 2011). All Rgg proteins affect gene expression during stationary growth. Rgg/RopB controls the expression levels of SpeB depending to the growth phase, with maximum production of SpeB at the stationary phase (Lyon et al., 1998, Chaussee et al., 1999, Unnikrishnan et al., 1999). It was also found to downregulate the transcription of genes including *speH* (superantigen), Mga targets (*sclA*, *emm*, *scpA*, *slo*), *ska*, the *hasABC* operon, and *mac* in NZ131 (M49) (Chaussee et al., 2002). For this reason, Rgg/RobB is believed to be able to

influence other regulator genes, such as *mga*, as well as genes from the two-component systems CovRS and FasBCAS/X (Vega et al., 2016). RopB was additionally found to affect the stationary phase expression of genes involved in metabolism (Chaussee et al., 2003, Chaussee et al., 2004, Dmitriev et al., 2006).

Rgg2 and Rgg3 (ordered according to their similarity to RopB) have been described as cytoplasmic quorum-sensing receptors, affecting virulence factor gene expression, via binding to signalling peptides, also known as autoinducers or pheromones (Chang et al., 2011, Federle, 2012). Adjacent to the *rgg2* and *rgg3* *S. pyogenes* genes, two short hydrophobic peptide (shp) sequences were found for each Rgg gene (Ibrahim et al., 2007). These shp peptide products later mature into pheromones that bind and activate their Rgg2 and Rgg3 targets (Chang et al., 2011). A similar DNA sequence was found near RopB coding for the SIP pheromone (Makthal et al., 2018). Moreover, the expression of these shp genes enhances biofilm production. Similar to Rgg2 and Rgg3 and their shp pheromones, ComR has been shown in *Streptococcus mutans* and *thermophilus* to be adjacent to *comS*, which expresses a pheromone that binds to the ComR regulator, and activates it (Federle, 2012). Federle reported in 2012, that ComR and ComS work the same way in *S. pyogenes*, albeit with no shown data.

Virulence Gene Regulation: Two-Component Systems

Two-component signal transduction systems (TCS) are comprised of two parts; signal detection and activation of a responder. The typical example of a TCS is one where a transmembrane histidine kinase binds to an external signal molecule, and in turn activates a response regulator that controls transcription (Kreikemeyer et al., 2003, Stock et al., 2012).

CovRS

The control of virulence (CovRS) system, first characterised as the capsule synthesis regulator (CsrRS), consists of the CovS sensor kinase situated on the surface of *S. pyogenes*, and the CovR response regulator in the cytoplasm (Levin and Wessels, 1998, Dalton and Scott, 2004). CovS detects extracellular stimuli, such as Mg²⁺ and host antimicrobial peptides, and subsequently phosphorylates and activates CovR. CovR in turn modulates the transcription of the target virulence genes, mainly facilitating transcriptional repression (Gryllos et al., 2003, Gryllos et al., 2008). CovRS is a master regulator of *S. pyogenes*, given that it was reported that it can negatively regulate up to 15% of all genes on the *S. pyogenes* chromosome, including those encoding for SpyCEP, EndoS, SLS, and SLO, but positively regulate *speB* (Heath et al., 1999, Graham, et al., 2002, Dalton and Scott, 2004). This master regulator was also demonstrated to be able to regulate Mga (Leday et al., 2008).

Furthermore, it was reported that CovR is able to modulate its regulon without CovS, since *covR* or *covS* mutants can have different phenotypes (Treviño et al., 2009, Sumbly et al., 2006, Shelburne et al., 2008). A number of studies observed hypervirulent *S. pyogenes* phenotypes that were linked to *covRS* mutations that yielded loss of SpeB synthesis and upregulation of HA capsule and other virulence factors (Aziz et al. 2004, Engleberg et al., 2004, Cole et al., 2006, Li et al., 2013). In the absence of SpeB, the Sda1 DNase, along with other virulence factors such as Streptokinase and M1, can be produced, turn host plasminogen to plasmin, and promote systemic spread (Aziz, et al., 2004, Cole et al., 2006, Kansal et al., 2000). Higher concentrations of Sda1 also enhances DNA degradation in NETs, which enables *S. pyogenes* to resist neutrophil killing at the site of infection (Buchanan et al., 2006, Sumbly et al., 2005). Neutrophils were specifically reported to drive the selection pressure for *covRS* mutations (Li et al., 2014).

FasBCA/X

In the FasBCA/X system in *S. pyogenes* (fibronectin/fibrinogen binding/hemolytic activity/streptokinase -Fas- regulator), FasB and FasC are two predicted histidine protein kinases (HPKs) that phosphorylate and activate the FasA response regulator (Kreikemeyer et al., 2001, Kreikemeyer et al., 2003, Liu et al., 2012). FasA triggers the expression of a small regulatory RNA downstream of the *fasBCA* operon, FasX, that base pairs with two target mRNAs: streptokinase (*ska*) and the first gene of the pilus production operon *cpa* (Ramirez-Peña et al., 2010, Liu et al, 2012). In the case of *ska*, FasX makes the mRNA more stable, which upregulates streptokinase

production, while binding to the *cpa* mRNA prevents ribosome binding and production of the collagen-binding minor pilus protein at the pilus tip. Additional activity FasBCA/X has been reported to have is repression of adhesin genes, *fbp54* and *mrp*, as well as upregulation of *sagA*, all in a growth-phase-dependent manner (Kreikemeyer et al, 2001). These opposing forces of gene regulation suggest that FasBCA/X is responsible for switching from a colonisation to a systemic spread phenotype.

Ihk/Irr

The Ihk/Irr TCS promotes *S. pyogenes* survival and persistence within phagocytes of the host innate immune system at the initial stages of infection, in a way that does not interfere with phagocytosis or ROS production in neutrophils (Voyich et al., 2003, Hertzén et al., 2012). It was also reported to be expressed at high levels during pharyngeal infections (Kreikemeyer et al., 2003, Voyich et al., 2003). In the early stages of infection, intracellular *S. pyogenes* was found to highly express *ihk* and *irr* along with the *hasABC* operon and genes involved in energy production (Hertzén et al., 2012). Over time, a decrease of this expression profile was noted with concomitant elevated levels of *covRS* transcription. Ihk/Irr can also drive the increased transcription of virulence genes, such as *sic*, *mac*, *speH*, *endoS*, *smeZ*, *speB* and *srtA* (Voyich et al., 2003, Voyich et al., 2004).

1.4 *S. pyogenes* interactions with the immune system

1.4.3 *S. pyogenes* TLR recognition

Pattern recognition receptors (PRRs) detect the presence of invading pathogens or damaged cells in a host when bound to pathogen-associated molecular patterns (PAMPs) (Takeuchi and Akira, 2010). One type of PRRs, the TLRs (transmembrane Toll-like receptors), are found not only in phagocytes, such as macrophages and neutrophils, but also in non-professional immune cells. Activation of TLRs is ligand-specific, and upregulates the transcription of specific pro-inflammatory genes, depending on the type of TLR. The signalling cascade that eventually activates those genes requires an adaptor that binds to their cytoplasmic Toll/IL-1R homology (TIR) domain (Akira and Takeuchi, 2006). One of the main adaptors, that binds to such domain, is the myeloid differentiation primary response protein (MyD88). MyD88 leads into a cascade that translocates NF- κ B into the nucleus, and eventually activates the specific transcription factor to upregulate the target pro-inflammatory cytokine genes. Cytokines, such as type I interferons (IFNs), interleukins (ILs), and tumour necrosis factors (TNFs), are proteins that mediate cell communication (O'Shea et al., 2002, Kleemann et al., 2008).

It has been reported that MyD88 is required for mounting a successful inflammatory response against *S. pyogenes* (Loof et al., 2008, 2010). It was found that in MyD88-deficient mice, production of TNF, IL-6, IL-12, and type I interferons (IFNs) was significantly lower (Gratz et al., 2008, 2011; Loof et al., 2008, 2010). This was associated with inability to recruit neutrophils, and a higher susceptibility to *S. pyogenes*. Furthermore, TNF is also produced downstream of TLR-induced MyD88, and results in rapid recruitment of macrophages (Mishalian et al., 2011).

In spite of all this data implicating MyD88 against *S. pyogenes*, it is still not clear which TLRs are engaged (Figure 1.5). A study showed that in mice, TLR2 and TLR13, albeit being redundant *in vitro*, are not *in vivo*, and are employed to engage and combat *S. pyogenes* (Fieber et al., 2015). TLR2 recognises *S. pyogenes* at first regardless of phagocytosis, and TLR13 then gets engaged after internalisation of *S. pyogenes*. Although TLR2, and its ligand specificity, is conserved between fish and mammals (Stein et al., 2007), TLR13 recognises 23S rRNA and is absent from both humans and zebrafish. It is present in all kingdoms, but is limited to only a few mammals, including mice and rats (Hidmark et al., 2012, Li and Chen, 2012, Oldenburg et al., 2012, Fieber et al., 2015). Despite the specific identity of human TLRs eluding us, MyD88 was demonstrated to induce the transcription of IFN- β and pro-inflammatory cytokines including TNF and IL-6.

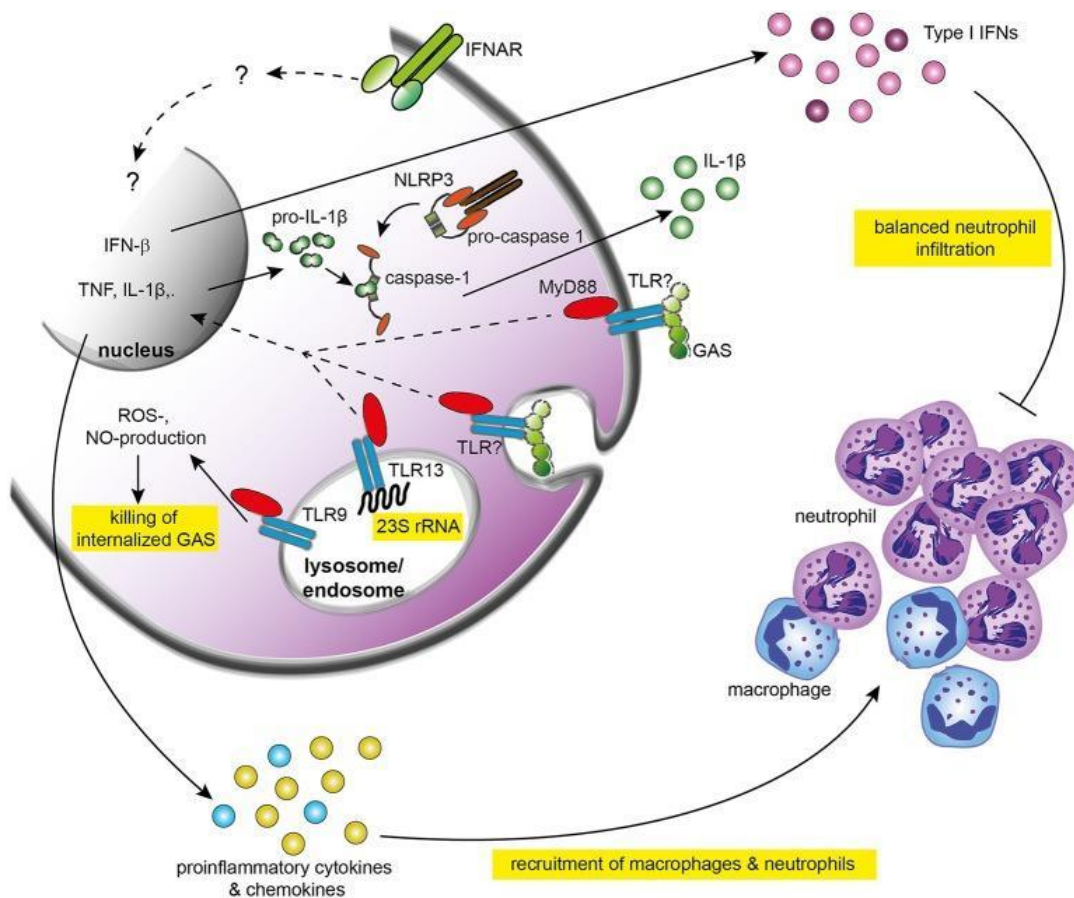


Figure 1.5 Innate immune response against *S. pyogenes*

S. pyogenes is recognised by yet unknown TLRs, that induce MyD88 signalling. MyD88 upregulates the transcription of cytokines, such as IFN- β , TNF, and IL-6, to promote inflammation. TNF promotes the migration of macrophages to the site of infection. IFN- β triggers Type I IFN signalling that eventually leads to a balanced migration of neutrophils in a process not yet identified. Upon *S. pyogenes* phagocytosis, *S. pyogenes* rRNA can bind to TLR13, and activate the innate immunity. TLR9 was also shown to drive ROS- and NO-killing of *S. pyogenes*. Recognition of *S. pyogenes* results in IL-1 β production in a NLRP3-dependent manner, the role of which has yet to be elucidated. Taken from (Fieber and Kovarik, 2014).

ROS: reactive oxygen species, NO: nitric oxide, NLRP3: NOD-like receptor family, IFNAR: type I IFN receptor 1.

1.4.4 *S. pyogenes* and phagocytes

Despite the complicated and robust mechanisms of the innate immune system, *S. pyogenes* has been demonstrated to persist not only within the professional phagocytes macrophages (Thulin et al., 2006, O'Neil et al., 2016) and neutrophils (Medina et al., 2003), but also within epithelial (Marouni and Sela, 2004, Kaplan et al., 2006), and endothelial cells (Amelung et al., 2011). A study looking at human macrophages reported that *S. pyogenes emm1* is able to replicate intracellularly (O'Neil et al., 2016). Macrophages were additionally shown to act a reservoir to harbour large numbers of viable *S. pyogenes*, during aggressive intravenous antibiotic treatment (Thulin et al., 2006). The M1 protein was additionally suggested to interfere with the fusion of enzymolytic vesicles with phagocytosed *S. pyogenes* (Staali et al., 2006; Hertzén et al., 2010).

Furthermore, a study showed that TNF- α deficient mice revealed a significant impairment of macrophage recruitment to the site of infection, whilst neutrophil numbers recruited were not affected (Mishalian et al., 2011). This was found in a cutaneous model resembling necrotizing fasciitis. In order to assert that the TNF- α deficiency leading to higher host susceptibility was macrophage-mediated, mice were depleted of macrophages. Whilst the number of neutrophils and tissue bacterial load remained the same, *S. pyogenes* dissemination was dramatically increased. This was reverted by replenishing the macrophages by either an

intravenous or subcutaneous injection. Hence, this study highlighted the importance of macrophages in restricting *S. pyogenes*.

1.4.5 Adaptive immune system

As most *S. pyogenes* infection models examine innate immunity, the role of the adaptive immune response, is much less explored (Fieber and Kovarik, 2014). Mice deficient in B and T cells (SCID) inoculated with *S. pyogenes*, yielded a similar survival to control mice, alluding to clearance of *S. pyogenes* relying more on the innate immune system, than the adaptive one (Medina et al., 2001; Goldmann et al., 2005b). However, due to the lack of data, there is a high chance that the role of the adaptive response is greatly underestimated. Patients lacking the TLR signalling adaptor MyD88, although being very susceptible to *S. pyogenes* during their early years, become more resistant in adulthood, which suggests that adaptive immunity might be able to substitute the innate to some degree (Von Bernuth et al., 2008). To further support this point, two mouse studies revealed a key involvement of IL-17-producing T helper (Th) 17 (or CD4+) cells in clearing *S. pyogenes* (Wang et al., 2010; Dileepan et al., 2011).

TGF- β 1 is a cytokine that is vital to the development of regulatory T cells (Tregs) and Th cells, that can be generated by many cell types, such as macrophages and dendritic cells (Wang et al., 2010). The first T cell type blocks immune attacks to self-antigens, whereas the latter, upregulates macrophage and neutrophil migration to the site of infection, resulting in the clearance of the pathogen. It was shown that production of TGF- β 1 was required for the development of Th cells and IL-17 production. These primed cells were then transferred into naive mice and enabled the mice to clear *S. pyogenes*. Another study uncovered that the need for IL-17 production for *S. pyogenes* clearance, was also dependent on IL-6 production, as IL-6-deficient mice were either highly more susceptible to infection or became long-term carriers (Dileepan et al., 2011).

1.5 Animal models for *S. pyogenes* infection

Animal models are an excellent platform for elucidating human pathogen infection at a holistic level, within the context of an organism, as opposed to focusing on a single isolated mechanism (*in vitro* models), or mathematical or computer models, which by their nature are simple and do not allow for the multiplicity of interactions. Animals can help identify virulence factors and mechanisms important to medical conditions caused by *S. pyogenes*, as well as interrogate host immune components important to combating the pathogen. One of the challenges with creating an *S. pyogenes* model reflects the diverse population of the species, and not many strains have been reported to be virulent in any given animal model (Bessen, 2009). As a consequence, when considering animal models for most human pathogens, it is important to know that no single strain can successfully recapitulate the exact infection progression observed in the human body milieu. Despite this limitation, animal models can still be used to study specific facets and mechanisms of the infectious process. In order to understand *S. pyogenes* infection, many animal models have been established (Figure 1.6). In the following sections, a variety of models of *S. pyogenes* infection will be discussed.

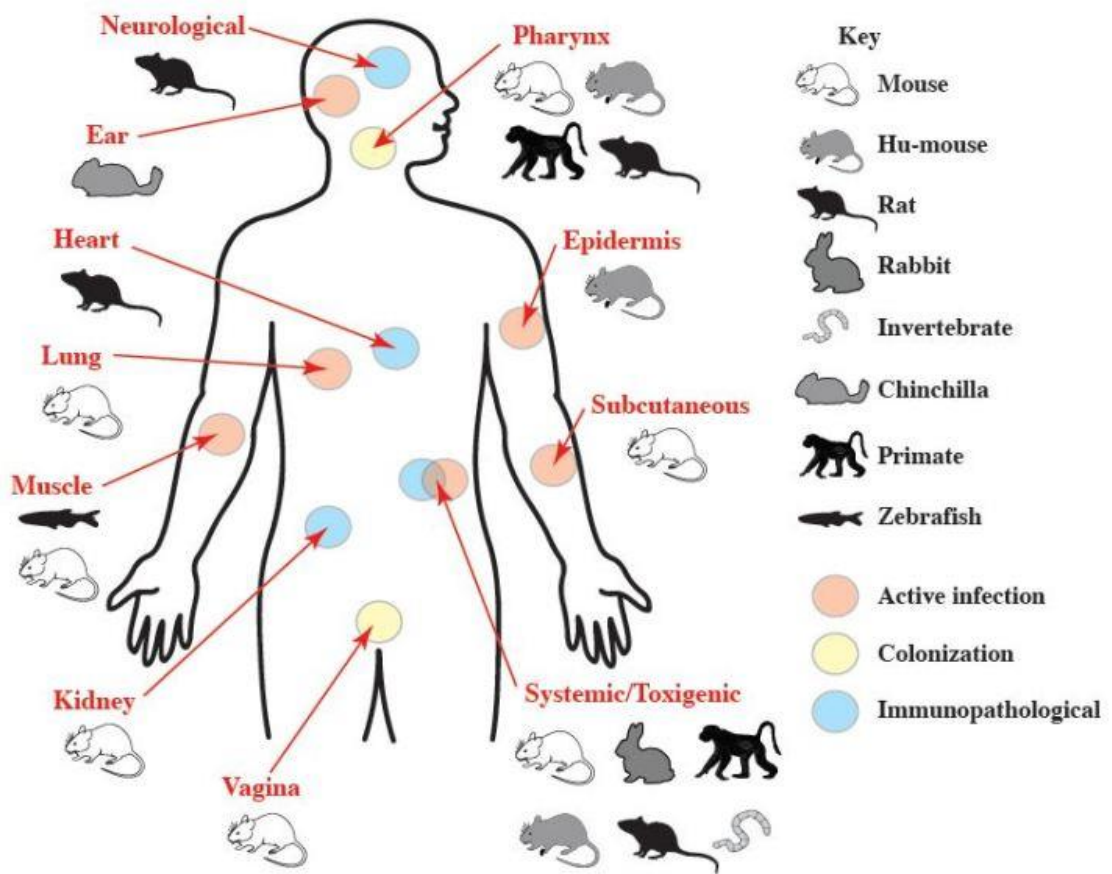


Figure 1.6 Animal models for analysis of *S. pyogenes* pathogenesis

The figure summarises the animal models that have been established to study *S. pyogenes* infection. The models are grouped according to the site of infection or colonisation as well as colour-labelled, indicating the type of host-pathogen interaction. The key for the animal model symbols is given on the right. Taken from (Watson et al., 2016).

1.5.1 Mice

Mice are the primary animal model for studying *S. pyogenes* infection, with many available inbred strains, the ability to knock-out genes or produce transgenic mice, and them being well-characterised genetically, being the biggest strengths of this model.

Pharyngeal Colonisation

Most experiments studying the interactions between *S. pyogenes* and the pharynx in an animal model have been the mouse (Gogos and Federle, 2019). This model is referred to as the pharyngeal or mucosal colonisation model, where a volume between 2.5 and 100 μL carrying 10^6 - 10^8 bacteria is inserted into the mice via inhalation from the nares (Watson et al., 2016). This allows for the bacteria to reach the nasopharynx, oropharynx, and nasal-associated lymphoid tissue (NALT). At larger volumes, bacteria can also reach the lungs. Bacterial burden is subsequently measured by CFU enumeration on plates with bacteria coming either from throat swab-inoculated saline or homogenised nasal tissue (Gogos and Federle, 2019).

Female FVB/n mice were challenged with 5 μL of 10^8 CFU of *emm75 S. pyogenes* or its isogenic ΔcovRS , and the competence of the two strains to persist over 21 days was examined (Alam et al., 2013). Nose pressing on plates to monitor bacterial burden revealed that the wild type persisted for longer when compared to ΔcovRS ,

which confirmed the role of CovRS in the successful *S. pyogenes* colonisation of the pharynx. This data further supports previous reports that pharyngeal isolates from patients rarely carry *covRS* mutations, unlike invasive isolates from patients (Liang et al., 2013, Galloway-Pena et al., 2018). This study utilised a new model for mouse pharyngeal infection discussed more below. Another study showcased the importance of SpeB, along with RopB, during *S. pyogenes* infection of the pharynx (Makthal et al., 2018). CFU counts from infected mice throat swabs showed that *speB*, *ropB* or the SIP pheromone gene deletions yielded smaller numbers of *S. pyogenes* over 7 days. This underlined the importance of not only SpeB for pharyngeal persistence, but also the one of cell-cell communication.

Mice have also been able to allow for analysis of immunisation against *S. pyogenes*. Anti-M protein secretory IgA was delivered into the nares of the mice, and was found to protect against systemic infection, following intranasal inoculation of *S. pyogenes* (Bessen and Fischetti, 1988). Active immunisation was also studied when peptide vaccines were delivered intranasally, and demonstrated protection (Olive et al., 2002, Olive et al., 2006).

One of the weaknesses of this mouse model is that rodents do not have a Waldeyer's ring homologue and hence tonsils, in their pharynx. As mentioned before, the importance of Waldeyer's ring is that it constitutes the biggest reservoir of *S. pyogenes* in humans (Watson et al., 2016). With that being said, mice have a

NALT that acts in an analogous manner to the human tonsils in that it drives mucosal immunity via uptake and response to pathogen antigens, as well as has zones of B and T cells (Csencsits et al., 1999). NALTs of mice challenged with *S. pyogenes* were observed to manifest similar symptoms to the human tonsils, both triggering greater numbers of CD4+ T cells producing IFN- γ and IL-6, with human tonsils also producing IL-4 and IL-5 (Kerakawauchi et al., 1997, Park et al., 2004, Dileepan et al., 2011).

Another limitation of this model is that pharyngeal infection in mice varies depending on mouse strain, age, sex, as well as inoculum volume, and *S. pyogenes* strain, which is why the Sriskandan lab published an optimised model assessing all aforementioned variables (Alam et al., 2013). This optimised variables are as follows: an inoculation volume of 5 μ L of *emm75* administered intranasally using a pipette, the use of FVB/n mice, and CFU enumeration coming from nares pressing on plates. Additionally, they found that *S. pyogenes* could persist longer in 5-week-old mice, compared to 10-week-old, and that generally males could be colonised better than females. The latter observation diminished at 5 weeks.

Subcutaneous Ulcer

In the subcutaneous ulcer model, mice are usually inoculated with 10^6 – 10^8 CFU in the tissue, and lesions appear by 8-12 hours post infection (Watson et al., 2016). One of the biggest strengths of this model is that it reproduces many of the aspects of *S. pyogenes* disease, namely a highly inflammatory localised lesion in soft tissue with great levels of bacterial proliferation, and recruitment of large numbers of leukocytes. These recruited cells are primarily composed of neutrophils that surround the bacteria and create an abscess-like structure (Brenot et al., 2004). Studies have shown that macrophages are vital to the formation of this structure, which keeps the infection local and prevents dissemination, with one study reporting IL-12-driven interferon-gamma (IFN- γ) plays a key role (Raeder, et al., 2000, Mishalian et al., 2011).

The surface area of the lesion, the time required to reach its maximum size, the time needed for the lesion to be resolved, and its formation or not, are all measurements used to assess virulence, for example between a mutant and its parent wild type (WT) strain (Watson et al., 2016). Other tests include lethality, weight monitoring, CFU recovery from the lesion, and for the *S. pyogenes* strains that disseminate and become systemic; CFU recovery from the spleen and inguinal lymph nodes. An example of such a strain that demonstrated enhanced virulence and a propensity to become systemic, is MGAS166, an *emm1* clinical isolate, with mutations in its CovRS system (Engleberg et al., 2001). Several mouse strains have been used in this model, including BALB/c and C57BL6, however a commonly used strain is the

SKH1 (Benavides et al., 2009). This mouse strain has a defect in its Hr gene, rendering it hairless.

Limitations include the histopathology, despite what was mentioned above, not closely resembling human diseases, such as impetigo, probably due to differences in the mouse cutaneous tissue anatomy, such as higher density of hair follicles and a thin epidermal layer.

Invasive Model

Sepsis is relatively rare, and usually manifests as a complication of a soft tissue infection (Reglinski and Sriskandan, 2014, Wong and Stevens, 2013). There are several ways to reproduce the sepsis model in mice; an intravenous (IV), intraperitoneal (IP), intramuscular (IM), intranasal (IN), or intratracheal (IT) inoculation. A dose of 10^5 - 10^6 CFU is generally used, and many *S. pyogenes* strains have been reported to be used successfully (Watson et al., 2016). IV deposits *S. pyogenes* directly into the bloodstream, while the other models require *S. pyogenes* to invade deeper tissue, and subsequently to become systemic. When focusing on the systemic infection model, following initial infection of the upper respiratory tract, it has been proposed that IT inoculations, might be more useful as compared to IN. This is because hosts challenged with *S. pyogenes* IT, present symptoms much faster, and most of them manifest bacteraemia following those symptoms (Husmann et al., 1996). Assessment of virulence is quantified by monitoring survival, and CFU

counts from the spleen, liver, lungs, and blood. Humanised mice (hu-mice) have also been raised to address the human-specificity of *S. pyogenes* virulence factor targets. For example, a hu-mouse expressing human plasminogen was created to study streptokinase (Sun et al., 2004).

1.5.2 Primates

Pharyngeal Colonisation

Rodent infection models are still far from resembling a human infection as murine nasopharyngeal tissue architecture is not the same. For that reason, non-human primate models have been developed, such as the baboon, chimpanzee, cynomolgus macaque, and the rhesus monkey (Watson et al., 2016). Strengths of the primate models include close resemblance of immune system factors and responses to humans, easier access to the site of infection, a more expansive list of usable *S. pyogenes* strains, and an extended persistence of *S. pyogenes* at the site of infection. Limitations to these models include very high expense, low availability, and the fact that although few of them, like chimpanzees develop strong pharyngeal pathology, others like baboons, do not (Virtaneva, et al., 2003, Friou, 1950).

In the baboon model, hosts are inoculated with 3×10^5 CFU of *emm3 S. pyogenes* by dribbling the inoculum over the posterior pharynx, which leads to *S. pyogenes* persistence for a minimum of six weeks (Ashbaugh et al., 2000). Acapsular or M-deficient *emm3* mutants, were unable to colonise the pharynx for more than two

weeks. Adding to this observation, another study showed that capsule production during the initial phases of pharyngeal colonisation (1 h post infection) was significantly upregulated, following delivery of *S. pyogenes* into the pharynx, using a moderately encapsulated *emm3* isolate (Gryllos et al., 2001).

Invasive Model

A sepsis model of baboons has been established, with injection of 10^{10} CFU of an *emm3* strain IV. Over the following 10 h, tests were carried out to analyse the progression of the infection, by the end of which mortality is close to 100% (Stevens et al., 1996). Those tests included body temperature, heart rate, arterial blood pressure, serum chemistry, and cytokine profiles.

1.5.3 Zebrafish

The complete analysis of the zebrafish (*Danio rerio*) genome, has revealed a high degree of both synteny with the human and similarities with the mammalian immune system (Postlethwait et al., 1999, Hsu, et al., 2004). Zebrafish have many orthologs of the human immune system, such as phagocytes, the complement system, cytokines, TLRs, and acquired immunity (Holland et al., 2002, Jault et al., 2004, Meijer et al., 2004, van der Vaart et al., 2012). All innate immune cells are present in zebrafish; macrophages, neutrophils, eosinophils, dendritic, and natural killer cells (Renshaw and Trede, 2012). Zebrafish macrophages and neutrophils have been reported to be morphologically and biochemically close to mammalian ones, with neutrophils being very unsuccessful at phagocytosing bacteria in fluid environments (Colucci-Guyon et al., 2011). The complement system also exists in zebrafish with orthologues of all its mammalian components. Acquired immunity wise, T cell receptor mRNA, secreted immunoglobulins, and T cell-dependent and -independent humoral responses also develop by 4 weeks post fertilisation (Lam et al., 2004). Zebrafish are inexpensive to maintain, and many available transgenic lines are commercially available (Nasevicius and Ekker, 2000).

Zebrafish, both adult and larvae (embryo), have been already used for several pathogenesis studies. *Burkholderia cenocepacia* (Deng et al., 2009), *Mycobacterium marinum* (Prouty et al., 2003, Swaim et al., 2006), *Staphylococcus aureus* (Lin et al., 2007, Kao et al., 2010), *Streptococcus iniae* (Neely et al., 2002,

Roca et al., 2008), and *Streptococcus suis* (Wu et al., 2008) are few of the pathogens that have been used in the zebrafish adult model. On the other hand, pathogens including *Bacillus subtilis* (Herbomel et al., 1999, Li et al., 2007), *B. cenocepacia* (Phennicie et al., 2010, Vergunst et al., 2010), *Escherichia coli* (Herbomel et al., 1999, van der Sar et al., 2003), *Haemophilus influenzae* (Phennicie et al., 2010), *M. marinum* (Davis et al., 2002), *Pseudomonas aeruginosa* (Brannon et al., 2009, Clatworthy et al., 2009), *S. aureus* (Prajnsar et al., 2008), and *Salmonella typhimurium* (van der Sar et al., 2003, Li et al., 2007) have been used to challenge embryos. *S. pyogenes* has mainly been used to challenge adult zebrafish however, Lin et al used embryos to demonstrate that SLS prevents neutrophil recruitment at the initial stages of infection (Lin et al., 2009). In this study, 10^5 CFU of wild type and SLS⁻ *S. pyogenes* were injected into the yolk sac of 1 dpf zebrafish to monitor survival, whereas 7 dpf fish were inoculated with 10^3 CFU to examine neutrophil recruitment.

Adult Myonecrosis Model

The adult zebrafish has been used to reproduce the myonecrosis model, with lack of immune cells being able to penetrate the lesion, large bacterial numbers at the site of infection, and big areas of necrotic tissue damage are all observed (Neely et al., 2002, Saralahti and Rämetsä, 2015). In the case of a strain switching from being resident to being systemic, CFU have been recovered from the spleen, but not from any other organs. Both intramuscular (IM) and intraperitoneal (IP) injections have been used to analyse this model, with the HSC5 *emm14* strain producing an LD₅₀ of

3×10^4 for IM, but 2.5×10^2 CFU for IP (Rosch et al., 2008). By 24 hours post infection (hpi), a lesion forms at the site of infection, which expands until the host succumbs at 36 to 96 hpi. To investigate the virulence of mutants, a dose 10 or 100 times the LD_{50} is used. Virulence in this model is examined by survival rates, and CFU recovered (Phelps et al., 2009). The strains that have been used in this model are the extensively used *emm14* type HSC5, and a the *emm49* NZ131 (Neely et al., 2003, Fisher et al., 2008).

Zebrafish Embryos

Zebrafish embryos can be an even stronger model for the following reasons. They can be easily genetically modified either by transiently knocking down genes via morpholino injections or by purchasing transgenic lines. Their small size also allows for large-scale screens. Another great advantage is the fact that the embryos grow *ex utero* and as a result, they can be used instead of adults in order to isolate and focus on the innate immune response. The zebrafish embryos are also transparent, allowing for fluorescent microscopy observations that allow for real-time pathogenesis studies of bacteria. However, one of the disadvantages of zebrafish is that the optimal temperature for the fish is 27-29 °C, 6-10 °C lower than the *S. pyogenes* natural host. At a temperature greater than 29 °C, zebrafish viability diminishes (van der Sal et al., 2004).

Injecting Embryos

A number of zebrafish embryo injection sites have been reported, including the axial vein near the blood islands, the yolk sac circulation valley, and the yolk sac/ball (Figure 1.8) (Prajsnar et al., 2008). One of the most common sites of infection, and the one used in this study, is the yolk sac circulation valley (Clatworthy et al., 2009). Embryos are anaesthetised using tricaine and are subsequently injected. Injections in the axial vein and the circulation valley deposit the inoculum directly into the bloodstream. Injections require a microinjector pump that deals minute amounts of air pressure, delivering volumes as low as 1 nL or less. The process also needs a manipulator to control the movement of the injection needle in a controlled fashion. Given the small size of both the embryos and needle, the experiments take place under a stereo microscope.

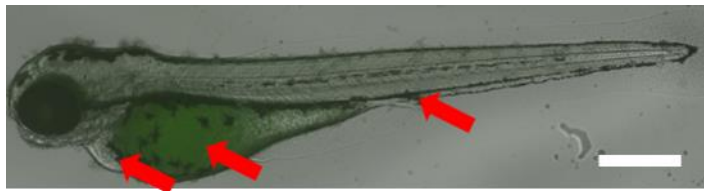


Figure 1.8 Potential injection sites in zebrafish embryos

The inoculum can be injected into, from left to right, the circulation valley, yolk, and axial vein. Scale bar represents 750 μm .

1.5.4 Invertebrates

Although, the mammalian models are biologically generally closer to humans, the logistics of maintaining these models along with the ethical issues have made alternative infection models more appealing. Invertebrate models have been widely used in infection studies as high-throughput screens for virulence (Sifri et al., 2003). Primarily due to ease of maintenance, low cost, high-throughput, amenable genetics etc. *Caenorhabditis elegans* has been used as a *S. pyogenes* infection model (Bolm et al., 2004, Jansen et al., 2002). Other reported invertebrate models for *S. pyogenes* are the silkworm *Bombyx mori*, and the waxworm *Galleria mellonella* (Kaito, et al., 2005, Loh, Adenwalla, Wiles, & Proft, 2013, Olsen, et al., 2010).

1.7 Population dynamics

There have been many studies analysing population dynamics during an infection (Grant et al., 2008, Prajsnar et al., 2012, Gerlini et al., 2014, Rego et al., 2014). Grant et al, used eight wild-type *Salmonella enterica* strains in a multi-organ study, and reported that soon after inoculation, bacterial phagocytosis and death, occurred with the subsequent replication of the survivors leading to independent subpopulations in different organs (Grant et al., 2008). A similar phenomenon was described by Gerlini et al where *Streptococcus pneumoniae* strains were used in mice in order to study bacteraemia. Collection and analysis of blood samples, following intravenous injections, showed that most outcomes were monoclonal

events (Gerlini et al., 2014). This suggested a single bacterial cell bottleneck as the potentiator of disease. In a *S. aureus* study by Prajsnar et al, it was demonstrated that professional phagocytes drive the pathogen through a very narrow population bottleneck that results in only a few bacteria escaping this control (Prajsnar et al., 2012). These survivors go on to form lesions and overwhelm the host. Additional population dynamics studies also exist with *Salmonella typhimurium* (Maier et al., 2014. Lim et al., 2014) as well as *Borrelia* species (Rego et al., 2014). All these reports collectively describe the population pressure effect (bottleneck), exerted on the pathogens, by the host immune defences. However, it seems that not all bottlenecks are as narrow as in *S. aureus*, as different pathogens interact with the host in different ways.

1.8 Exploring the effect of commensals in *S. pyogenes* infection

How hosts get infected with opportunistic pathogens, such as *S. pyogenes*, is an interesting and open question. These organisms live within a polymicrobial milieu from which they emerge to cause an infection, given the appropriate opportunity. This is often presented as a breach in innate defences, such as a wound. In such cases, the initial infectious dose is likely to be low, and in the presence of a range of other microbes and material. For example, the lungs of a Cystic Fibrosis patient can be co-infected by both *S. aureus* with *Pseudomonas aeruginosa* (Mashburn et al., 2005). This is true for *S. pyogenes*. In the context of the skin, an injury that leads to a *S. pyogenes* infection, could also have *S. aureus* or *Micrococcus luteus* present.

Although, commensals can confer additional protection against invading pathogens by creating a very competitive environment to colonise, they have been also shown to potentiate an infection. It was also reported that *Staphylococcus epidermidis* releases anti-inflammatory cytokines that neutralise monocyte pro-inflammatory cytokines (Laborel-Préneron et al., 2015). As this action of the monocytes is in response to *S. aureus*, *S. epidermidis* effectively dampens the host response. Furthermore, a phenomenon called augmentation, was described, in which the presence of a commensal organisms, or their cell wall peptidoglycan, results in enhanced virulence of *S. aureus* during infection in both zebrafish embryos and mice (Boldock et al., 2018).

The Augmentation Effect

Boldock et al, initially showed in 1 dpf zebrafish embryos that although a low dose of 150 CFU of *S. aureus* yielded about 90% survival, co-infection of this *S. aureus* dose with 2000 CFU of *M. luteus*, results in a significant decrease of survival down to 50% (Boldock et al., 2018). 50% host survival was noted at the *S. aureus* high dose of 1500 CFU, which shows that augmentation allows for a 10-fold decrease in the infectious dose. This is despite the fact that 2000 *M. luteus* alone does not cause any mortality. This augmentation effect was also observed when using a *S. aureus* virulence attenuated mutant (*pheP saeR*) instead of *M. luteus*. Albeit, *M. luteus* being cleared from the host, is still leads to an enhanced *S. aureus* virulence measured by host mortality and pathogen proliferation. *S. aureus* and *M. luteus* were confirmed to colocalise within phagocytes *in vivo*.

This phenomenon was subsequently tested and also seen in mice, where co-injecting 10^8 CFU of *Staphylococcus epidermidis* or *M. luteus* with the low dose of *S. aureus* (10^5 CFU), resulted in reduced mouse weight and increased *S. aureus* numbers in the liver. In mice, the infectious dose could be reduced by 1000-fold when mixing with an augmenting organism. Following experiments interrogated the molecular basis of augmentation. Heat-killed *M. luteus* was able to augment *S. aureus* virulence in zebrafish, hence the presence of a bacterial cellular component was hypothesised to be key for this mechanism. It was reported that infection could be augmented using insoluble cell wall peptidoglycan from *M. luteus*, *S. epidermidis*, *Bacillus subtilis*, *Curtobacterium flaccumfaciens*, and *S. aureus*. This suggest that there must be a conserved moiety driving this phenomenon.

Non-pathogen Interactions with the Immune System: Live Commensals

There have been numerous studies reporting that bacteria, other than the pathogen in question, can interact directly with either the host immune system or the pathogen itself. This has ramifications to the efficacy of the pathogen. For instance, although *S. epidermidis* has been known to be a relatively mild pathogen, Vandecandelaere et al., demonstrated that its serine proteases could break down *S. aureus* biofilms, leading to increased survival of *C. elegans* (Vandecandelaere et al., 2014). The same avirulent bacterium, was reported to restrict *Candida albicans* invasion via induction of T cells, when *C. albicans* was applied 11 days after (Naik et al., 2015).

On the contrary, the presence of *M. luteus* present at the time of infection with *S. aureus*, was reported to yield an increased level of host mortality. This allowed for the infectious dose of *S. aureus* to be decreased 10-fold in zebrafish, and 1000-fold in mice in the respective systemic models. (Boldock et al., 2018).

Non-pathogen Interactions with the Immune System: Adjuvants

The aforementioned augmentation effect, that occurred by co-injecting *S. aureus* with the skin commensal *M. luteus*, was also observed when *S. aureus* was mixed with purified *M. luteus* or *S. aureus* peptidoglycan instead. This increased killing allowed the infective dose, in the mouse sepsis model, to significantly drop from 10^7 to 10^4 CFU, thanks to the added peptidoglycan.

Furthermore, a few other studies have described similar effects, where for instance different prospective adjuvants like starch were tested (James and MacLeod, 1961). Starch, being found in surgical glove powder and suture materials, was stated to have an augmenting effect to an *S. aureus* wound infection. This led to the dose to be lowered from 10^7 to 10^3 . Another study indicated that depending on the timing of injection of *E. coli*, it can confer protection against infection or increased susceptibility (Rowley, 1956).

1.9 Aims of the project

The primary aim of this project was to establish the *S. pyogenes* infection model in the zebrafish embryo (larvae). The next step was to use established tools, such as morpholino genetic manipulation and fluorescence microscopy, to interrogate the validity of this model, and whether it resembles appropriate host-pathogen interactions. Finally, the last step was to examine population dynamics during *S. pyogenes* infection.

Chapter 2: Materials and Methods

2.1 Bacterial media

Bacterial media were all prepared using distilled water (dH₂O), and were sterilised by autoclaving for 20 minutes at 121 °C and 15 psi.

2.1.1 Todd-Hewitt 0.2% w/v yeast (THY) broth

Todd-Hewitt Broth (Oxoid)	36.4 g L ⁻¹
Yeast extract (Oxoid)	2.0 g L ⁻¹

THY agar contained 0.7% Oxoid No.1 agar.

2.1.2 Columbia horse Blood Agar (CBA)

Special peptone	23.0 g L ⁻¹
Starch	1.0 g L ⁻¹
Sodium chloride	5.0 g L ⁻¹
Agar	10.0 g L ⁻¹

pH 7.3 ± 0.2 at 25 °C

CBA plates were purchased from Thermo Scientific (CM0331), and stored at 4 °C.

2.1.3 Luria-Bertani (LB) broth

Tryptone (Oxoid)	10 g L ⁻¹
Yeast extract (Oxoid)	5 g L ⁻¹
NaCl	5 g L ⁻¹

1.5% (w/v) Oxoid No. 1 agar was added to make LB agar.

This media was used for cultivating *E. coli*.

2.1.4 Brain Heart Infusion (BHI) broth

Brain Heart Infusion (Oxoid)	37 g L ⁻¹
------------------------------	----------------------

1.5% (w/v) Oxoid No. 1 agar was used for BHI agar.

2.1.5 Electroporation medium

MgCl ₂	1 mM pH 6.5
Glucose	272 mM

2.2 Antibiotics

Tetracycline (Tet) was used in this study. The *S. pyogenes* working concentration was 5 µg mL⁻¹. The antibiotic stock solutions were prepared by dissolving the antibiotics in appropriate solvent, filter-sterilised (0.22 µm pore size) and stored at -20 °C. For use in agar plates, the antibiotic stock solutions were added to the media once they had cooled to below 55 °C. For use in liquid media, the antibiotic stock solutions were added prior to usage.

2.3 Bacterial strains

2.3.1 *Streptococcus pyogenes* strains

The *S. pyogenes* strains used in this study are listed in Table 2.1. Strains were grown from -80 °C Microbank beads (Pro Lab Diagnostics) and cultured onto CBA plates with antibiotics incorporated if necessary, to maintain resistance markers. For short-term storage, strains were kept on CBA plates at 4 °C. For long-term storage, a single colony was mixed with Microbank bead stocks and kept at -80 °C.

For bacterial growth in liquid media, strains were grown at 5% v/v CO₂ at 37 °C. Three colonies were used to inoculate 10 mL THY broth, in a 15 mL tube, and incubated overnight at 37 °C. 50 mL of THY broth, in a 50 mL tube, were inoculated

with the necessary volume so the OD₆₀₀ was close to 0.05, and re-incubated at 37 °C at 5% v/v CO₂ until 0.3 OD₆₀₀.

Table 2.1 List of *S. pyogenes* strains used in this study

Strain	Genotype or description	Reference
H305	<i>emm1</i> type	(Sriskandan et al., 2002)
HSC5	<i>emm14</i> type	(Port et al., 2013)
H293	<i>emm89</i> type	(Turner et al., 2015)
H293-GFP	H293 carrying pMV158- <i>gfp</i> , Tet ^R	This study
H293-mCherry	H293 carrying pMV158- <i>mCherry</i> , Tet ^R	This study

Tet^R – tetracycline resistant

2.3.2 *Escherichia coli* strains

E. coli strain TOP10 from Invitrogen was used in this study. Strains were grown from -80 °C Microbank beads (Pro Lab Diagnostics) and cultured onto LB agar plates. For short-term storage, strains were kept on LB agar plates at 4 °C. For long-term storage, a single colony was inoculated into Microbank bead stocks and kept at -80 °C.

For bacterial growth in liquid media, strains were grown aerobically at 37 °C. Three colonies were used to inoculate 5 mL LB and incubated overnight at 37 °C on a rotary shaker at 250 rpm. 0.5 mL of overnight culture was used to inoculate 50 mL LB in a 250 mL conical flask and re-incubated at 37 °C and 250 rpm on a rotary shaker until exponential phase growth was reached.

2.3.3 *Staphylococcus aureus* strains

Strain SH1000 was used in order to retrieve the pMV158-*gfp* and pMV158-*mCherry* plasmids (Prajsnar et al., 2008). Growth and storage methods were the same as for *E. coli* but using BHI.

2.3.4 *Micrococcus luteus* strains

M. luteus SJF256 (ATCC4698, Sigma Lysophilised cells) was used in this study. For this study, frozen inocula prepared and provided by Dr Josie Gibson (University of Sheffield) were used. They were grown aerobically at 30 °C in BHI, and stored similarly to the *E. coli* strains.

2.4 Plasmids

Plasmids used in this study were the pMV158 ones carrying *gfp* and *mCherry* (Nieto and Espinosa, 2003). All plasmids were purified from *S. aureus* SH1000 strains using a QIAGEN kit, and eluted into dH₂O, and stored at -20 °C.

2.5 Buffers and solutions

All buffers and solutions were prepared using dH₂O, sterilised by autoclaving, if necessary, and stored at room temperature.

2.5.1 Phosphate buffered saline (PBS)

NaCl	8.0 g L ⁻¹
Na ₂ HPO ₄	1.4 g L ⁻¹
KCl	0.2 g L ⁻¹
KH ₂ PO ₄	0.2 g L ⁻¹

2.5.2 QIAGEN buffers

2.5.2.1 QIAGEN Buffer P1

Tris-HCl, pH 8.0	50 mM
EDTA	10 mM
RNase A	100 µg mL ⁻¹

2.5.2.2 QIAGEN Buffer P2

NaOH	200 mM
SDS	1% (w/v)

2.5.2.3 QIAGEN Buffer P3

Potassium acetate, pH 5.5	3.0 M
---------------------------	-------

2.5.2.4 QIAGEN Buffer EB

Tris-HCl, pH 8.5	10 mM
------------------	-------

2.5.2.5 QIAGEN Buffer TE

Tris-HCl, pH 8.0	10 mM
------------------	-------

EDTA	1 mM
------	------

2.5.2.6 QIAGEN Buffer QBT

NaCl	750 mM
------	--------

MOPS	50 mM, adjusted to pH 7.0 with NaOH
------	-------------------------------------

Isopropanol	15% (v/v)
-------------	-----------

Triton X-100	0.15% (v/v)
--------------	-------------

2.5.2.7 QIAGEN Buffer QC

NaCl	1 M
MOPS	50 mM, adjusted to pH 7.0 with NaOH
Isopropanol	15% (v/v)

2.5.2.8 QIAGEN Buffer QF

NaCl	1.25 M
Tris-HCl pH 8.5	50 mM
Isopropanol	15% (v/v)

2.5.2.9 QIAGEN Buffer N3, PB, PE

Supplied in QIAprep Spin Miniprep Kits, details not given.

2.6 Chemical dyes

All dyes were purchased from Fisher Scientific.

Table 2.2 Chemical dyes used in this study

Stock solution	Stock concentration	Solvent Storage
AlexaFluor405	10 mM DMSO	-20 °C in dark
AlexaFluor647	10 mM DMSO	-20 °C in dark
pHrodo Red	10 mM DMSO	-20 °C in dark

2.7 Determination of bacterial cell density

2.7.1 Spectrophotometric measurement (OD₆₀₀)

To quantify the bacterial yield of a liquid culture, spectrophotometric measurements at 600 nm (OD₆₀₀), were carried out. These measurements were taken using a Jenway 6100 spectrophotometer. At OD₆₀₀ over 1, samples were diluted 1:10 in the appropriate sterile culture medium.

2.7.2 Cell counts (CFU mL⁻¹)

To determine viable cell numbers, cell counts were performed. Bacterial samples were serially diluted 1:10 in THY and plated in triplicates or quadruplicates. 10 µL samples of each dilution were spotted onto THY agar or CBA plates containing

antibiotics where appropriate. After overnight incubation at 37 °C, and at 5% v/v CO₂, the number of colony forming units (CFU) was determined.

2.8 DNA Purification techniques

2.8.1 Plasmid preparation from *S. aureus*

Plasmid purification from *S. aureus* was performed using the QIAGEN QIAprep™ Spin column kit. A 3 mL overnight culture of *S. aureus* was first mixed and incubated with 10 µL of lysostaphin (Sigma-Aldrich). This digests the cell wall which exposes the plasmids for purification. The cell content was then recovered by centrifugation in a microcentrifuge at 10,000 rpm for 1 min. The pellet was then resuspended in 250 µL of buffer P1 with RNase A. For lysis, 250 µL buffer P2 were added and the 1.5 mL Eppendorf tube was gently inverted 10 times; the lysis reaction was not allowed to proceed for more than 5 min. 350 µL of neutralising buffer N3 was added and the tube immediately inverted gently 10 times to prevent localised precipitation. The cloudy suspension was then centrifuged for 10 min at 13,000 rpm to remove precipitated proteins, chromosomal DNA, cellular debris and SDS. The supernatant was transferred into a QIAprep spin column and centrifuged for 1 min at 13,000 rpm. The flow-through was discarded. The column was washed with 750 µL of buffer PE and centrifuged for 1 min at 13,000 rpm. To remove residual wash buffer that may inhibit further reactions, the flow-through was discarded and the tube centrifuged again for 1 min. The column was then placed in a clean microcentrifuge tube and

the DNA eluted by pipetting 50 μL of dH_2O directly to the centre of the column. The column was left to stand for 1 min before centrifugation at 13,000 rpm for 1 min. The eluted plasmid DNA was stored at $-20\text{ }^\circ\text{C}$.

2.9 Transformation of *S. pyogenes*

2.9.1 Preparing electro-competent *S. pyogenes* cells

10 mL of a *S. pyogenes* overnight culture was used to inoculate 90 mL of preheated THY. The solution was left to incubate with 30 μL of hyaluronidase (30 $\mu\text{g}/\text{mL}$) for at least 30 min. At an OD_{600} of 0.150 - 0.175, the culture was centrifuged at 4500 rpm at $4\text{ }^\circ\text{C}$ for 10 min. The supernatant was discarded, and the cells were washed twice with ice-cold electroporation medium at 4500 rpm at $4\text{ }^\circ\text{C}$. After the last wash, the cells were resuspended in 750 μL of electroporation medium, kept on ice, and used for transformations immediately.

2.9.2 Electroporation of DNA into competent *S. pyogenes* cells

A mixture of 75 μL of competent cells with 5 μL of DNA was placed within 1.5 mL Eppendorf tubes. At least 0.1 μg of purified plasmid was used. This solution was then transferred into sterile electroporation cuvettes (1 mm).

Electroporation was conducted with a Gene Pulser system set at 1 kV, 129 Ω , and 50 μF . Post-electroporation, 1 mL of fresh THY was added into the cuvette, and the

entire suspension was placed in a 15 mL tube with 9 mL of preheated THY. The tubes were left to incubate at 37 °C for 2.5 - 3 hours. The cells were then harvested by centrifuging at 2000 rpm for 10 min, and plated onto CBA or THY-tet plates.

2.10 Zebrafish lines

The London Wild Type (LWT) zebrafish line was used for most of the experiments involving zebrafish. For microscopy experiments, the following lines were used:

Table 2.3 Transgenic zebrafish lines used in this study

Name	Features	Reference
<i>Tg(mpeg1:mCherry-CAAX)sh378</i>	mCherry macrophages	(Loynes et al., 2018)
<i>Tg(mpx:GFP)i114</i>	GFP neutrophils	(Boucontet et al.,2018)
<i>Tg(fms:GAL4);Tg(UAS:nfsB.mCherry);Tg(mpx:GFP)</i>	mCherry macrophages- GFP neutrophils	(Prajsnar et al., 2012)
<i>Tg(lyz:nfsB-mCherry)sh260</i>	NTR neutrophils, for Mtz	(Buchan et al., 2018)

2.11 Zebrafish husbandry

Adult zebrafish were housed in a continuous re-circulating closed aquarium system with light day/night cycle of 14/10 hours, respectively, at 28 °C. All embryos collected were kept in E3 1x medium at 28.5 °C.

Transgenic adult fish were handled under a Project Licence awarded by the UK Home Office to the University of Sheffield. All zebrafish experiments were carried

out using younger than 5 dpf embryos, hence not protected under the Animals (Scientific Procedures) Act.

2.12 Zebrafish media

2.12.1 E3 (x10)

NaCl	50 mM
KCl	1.7 mM
CaCl ₂	3.3 mM
MgSO ₄	3.3 mM

A 1x solution was used for experiments which was derived from a 10x stock in distilled water. Methylene blue was also added (approximately 5×10^{-5} % final concentration) for fungal growth prevention (Nusslein-Volhard C, 2002), and autoclaved.

2.12.2 Methylcellulose

Methylcellulose was prepared at a 3.0% (w/v) concentration in E3. As solubilisation is critical, it was partially frozen, mixed and defrosted several times (Nusslein-Volhard and Dahm, 2002). The resulting solution was subsequently aliquoted into 20 mL syringes and frozen for long-term storage. Syringes were also kept at 28.5 °C for short-term use.

2.13 Zebrafish anaesthesia

A stock solution of 0.4% (w/v) 3-amino benzoic acid ester (tricaine or MS322, Sigma) was prepared in 20mM Tris-HCl (pH adjusted to 7) and stored at -20 °C. A working stock was kept at 4 °C in the dark. Before any injections or microscopy experiments were carried out, embryos were anaesthetised in a 0.02% (w/v) tricaine.

2.14 Microinjections of *S. pyogenes* into zebrafish embryos

A 50 mL tube, with 50 mL prewarmed THY, was inoculated from an overnight culture of *S. pyogenes*. Following that, 40 mL were collected to adjust for the same OD₆₀₀ as well as to make up for any volume discrepancies due to additional OD₆₀₀ measurements of any specific culture. These 40 mL were grown until the OD₆₀₀ was approximately 0.3, and the cells were harvested by centrifugation (4500x g, 10 min, 4 °C). The cells were resuspended in fresh THY media to the set concentration for the experiment, and kept on ice throughout the injections. The volume of fresh THY added, was appropriate for each experiment and strain, and doses were quantified before and after injections. This was done by a 10⁻⁴ dilution of the dose in sterile THY, and 4 spots of 10 µL, were plated on CBA plates, and incubated at 37 °C at 5% v/v CO₂ overnight. The CFUs were counted the next day. *M. luteus* frozen aliquots were provided by Dr Josie Gibson, were thawed, washed once with PBS, and injected into fish.

The larvae were naturally dechorionated, as they were at 2 dpf, and injected with 1 nL of the bacterial suspension, after being anaesthetised and immobilised onto 3.0% (w/v) methylcellulose. An electrode puller was used to create a fine injection tip on non-filament glass capillaries, in which the bacteria were then loaded. The injection volume was calibrated with the use of a graticule slide. For injections, a pneumatic micropump (WPI, PV820), a micromanipulator (WPI), and a dissecting light microscope (Leica) were used.

Following injections, embryos were incubated in Petri dishes with E3 at 28.5 °C for about 1 hour, allowing for the methylcellulose to dissolve. The fish were then transferred individually into 96-well plates.

2.15 Determination of zebrafish embryo mortality following infection

Fish groups of 25-30 embryos were injected with *S. pyogenes*. Post injections, the embryos were visually inspected, using a dissecting light microscope (Leica), once a day. Heartbeat cessation was used as evidence of mortality.

2.16 Determination of *S. pyogenes* growth *in vivo*

In order to measure *S. pyogenes in vivo* growth, the appropriate number of fish were individually collected at each time-point, and placed into ceramic bead-containing 2 mL cap containers (Peqlab) with 200 µL of E3. The embryos were then mechanically homogenised with a PreCellys 24-dual. The homogenates were serially diluted in

THY, plated onto CBA plates or Omni trays, and left at 37 °C overnight. The CFUs were determined the next day.

2.17 Fixation of embryos

For fixing embryos, Paraformaldehyde 4% (w/v) (PFA) dissolved in PBS, was used. Embryos were anaesthetised and transferred into ice-cold PFA, and left to incubate overnight at 4 °C.

2.18 Microscopy

2.18.1 Mounting of zebrafish

Embryos were anaesthetised, and placed on a coverslip (number 0) mounted over a 10 mm puncture in a 50 mm plastic Petri dish. They were then immersed in a 1% (w/v) low melting point agarose (Sigma) E3 solution, and left for about 8 min, until the agarose solidified.

2.18.2 Imaging of zebrafish

In this study, the following three microscopes were used:

1. UltraVIEW VoX (Perkin Elmer): This spinning disc confocal microscope was used for the majority of the microscopy experiments in this study. GFP,

mCherry, AlexaFluor647, and AlexaFluor405 were excited by a 457-514 nm argon laser, a 561 nm sapphire laser, a 642 nm diode laser, and a 407 nm laser. Images were acquired using its bright field, GFP, TxRed, and far red emission settings using a Hamamatsu C9100-50 EM-CCD camera. Volocity software was used for image acquisition and processing. The 4x Nikon Plan Fluor NA 0.13, and the 20x Nikon Plan Fluor NA 0.45 objectives were used. GFP was excited with 488 nm.

2. Nikon TE-2000 U: This microscope uses a Hamamatsu Orca-AG camera, and NIS Elements for both image acquisition and processing.

3. Nikon custom widefield: This microscope was used for the strain population dynamics experiments of Chapter 5. The objective used was 10x NA 0.45. NIS Elements was used for both image acquisition and processing.

Its features include: a Nikon Ti-E, a CFI Plan Apochromat λ , a custom-built 500 μm Piezo Z-stage, and ET/sputtered series fluorescent filters 49002 and 49008.

2.19 Chemical staining of *S. pyogenes*

The same protocol was followed for pHrodo and AlexaFluor405 staining of *S. pyogenes*, as well as for AlexaFluor647 labelling of peptidoglycan (PG). For PG, frozen aliquots were resuspended, and directly mixed with the dye. Bacteria were prepared as described before (Section 2.14), but the last resuspension of the cells

was instead carried out in PBS pH9, and not THY. 200 μ L of that culture was subsequently mixed with 0.5 μ L of 2.5 mM pHrodo. This mixture was left to incubate for 30 min on a 100 rpm rotary shaker at 37 °C. To remove excess dye, three washes followed. The tube was taken from the shaker, and 1 mL PBS pH 8 was added to it, it was vortexed, and centrifuged (13,400 rpm, 3 min, RT). Two more washes followed with 1 mL 25 mM Tris pH 8.5, and 1 mL PBS pH 8, respectively. After the final supernatant was removed, *S. pyogenes* was resuspended in 200 μ l of PBS pH 7.4, and kept on ice.

2.20 Microinjections of morpholino oligonucleotides into zebrafish embryos

2.20.1 Morpholinos

Morpholino-modified antisense oligonucleotides were acquired from Gene Tools, LLC. In this study, morpholinos targeted the mRNA AUG codon in order to knock-down the translation of the gene of interest, and were used at a concentration of 0.5 pmole per embryo.

Table 2.4 Morpholinos used in this study

MO target	Sequence (5' - 3')	Reference
<i>pu.1</i>	GATATACTGATACTCCATTGGTGGT	(Rhodes et al., 2005)
<i>irf8</i>	TCAGTCTGCGACCGCCCGAGTTCAT	(Li et al., 2011)
Standard Control	CCTCTTACCTCAGTTACAATTTATA	Gene Tools, LLC

2.20.2 Morpholino injections into zebrafish eggs

Morpholinos were kept in 2 mM stocks in dH₂O, but injected at 1 mM into the yolk sac of 1-4 cell embryos as described in 2.14.

2.21 Neutrophil ablation via Metronidazole treatment

Tg(lyz:nfsB-mCherry)sh260 embryos carrying NTR-expressing neutrophils were collected (Table 2.3). At 34 hpf, the larvae were treated with 10 mM dissolved in E3 for 18 h. The plates were additionally wrapped loosely with foil to protect Mtz from light. The embryos were inoculated with *S. pyogenes* at 54 hpf.

2.22 Macrophage ablation via Metronidazole treatment

LWT embryos were mechanically dechorionated at 24 hpf, and subsequently injected with liposome-encapsulated clodronate or liposome-encapsulated PBS as the control. The fish were left to incubate overnight, and they were injected with *S. pyogenes* at 54 hpf.

2.22 Statistical analysis

All statistical analysis was performed in GraphPad Prism version 7.04. Zebrafish groups had always n=25-30. A representative graph is shown from three replicates of each experiment. Zebrafish data was not combined as embryo batches vary.

Survival analysis: Comparisons between survival curves of different groups were assessed using the log-rank Mantel-Cox test.

Linear regression: Line of best fit for all data points within an experiment. $R^2=1$ represents 100% of the points lie on the line.

Chapter 3: Developing the zebrafish embryo infection model for *S. pyogenes*

3.1 Introduction

3.1.1 Choosing an embryo age

For my infection study, 1-day post fertilisation (dpf) or 2 dpf zebrafish embryos were explored. The first model has been widely used before for infection studies, while the latter allows for a more robust immune system (Prajsnar et al., 2008). Both ages are at a developmental stage that enables the isolation and the investigation of the innate immune system without any complications from the adaptive immune system, that becomes functional 4-6 weeks later (Sullivan et al., 2017). At 2 dpf, fish have both mature macrophages and neutrophils, as functional macrophages have been detected at about 1 dpf (Herbomel et al., 1999), and mature neutrophils emerge at 2 dpf (Lieschke et al., 2001). Exploring host-pathogen interactions between *S. pyogenes* and zebrafish is the aim of this study. Hence, to that end, this chapter sought to establish the model that was subsequently used as a platform to ask the questions of the next two following chapters. Technically, at roughly 2 dpf, the fish are called pro-larvae, however, going forward they will be called “embryos”. Finally, after injections, the embryos are monitored only until they become protected under the Animals Scientific Procedures Act (1986), which is before 5 dpf (120 hours).

3.1.2 Choosing an *S. pyogenes* strain

HSC5 (*emm14*)

The HSC5 strain is an *emm14* type that has been the preferred strain for the few adult zebrafish models that have been developed, and the only one of the three strains in this study that has been used in zebrafish (Neely et al., 2003, Fisher et al., 2008). The origin of this strain is not known. It is an encapsulated strain that has been reported to have a strong production of the SpeB cysteine protease, but no NAD-glycohydrolase activity (Meehl et al., 2005).

H293 (*emm89*)

H293 (*emm89*, PT4245 type- Central Public Health Laboratory of London) was acquired from thigh muscle tissue of a patient who survived necrotizing fasciitis and STSS (Sriskandan et al., 2000, Turner et al., 2009, Turner et al., 2015, Reglinski et al., 2016). This *emm89* strain has high expression levels of SpeB, a cysteine proteinase that contributes to evasion of the immune system. Additionally, it is capsular (HA) and has low NADase and Streptolysin O (SLO) activity.

H293 has been fully genome sequenced and annotated (GenBank accession no. HG316453.2), and is genetically transformable (personal communication with Dr Claire Turner, University of Sheffield). Finally, it is well-characterised both *in vitro* and *in vivo* (Sriskandan et al., 2000, Turner et al., 2012, Reglinski et al., 2015, Lamb et al., 2018).

H305 (*emm1*)

H305 is an *emm1* strain (NCTC 8198) that was isolated from the throat of a patient with scarlet fever (Reglinski et al., 2015, Reglinski et al., 2016). *emm1* is the single most prevalent type that has dominated Europe, the US and Canada (Gherardi et al., 2018). H305 produces SpeB at high levels (Unnikrishnan et al., 1999). This strain also carries a single-base insertion mutation in *covS* that truncates the protein and disrupts the CovR/S regulon (Turner et al., 2009). H305 is additionally well-characterised in murine models (Alam et al., 2013).

3.2 Aims of this chapter

- i. To establish a systemic model of infection in zebrafish embryos.
- ii. Assess the suitability of a range of *S. pyogenes emm* type strains for zebrafish infection studies.

3.3 Results

3.3.1 Determination of optimal infection point post-fertilisation

The first question to be addressed was whether injection of 1 dpf (30 hours post fertilisation- hpf) embryos is suitable to establish the *S. pyogenes* infection model. This model has been used for several other pathogens, such as *Staphylococcus aureus* (Prajsnar et al, 2008). In the case of 1 dpf embryos proving too susceptible to *S. pyogenes* to study, 2 dpf (54 hpf) fish were also used as they have a more robust immune system. Hence, in order to determine the optimal infection point post-fertilisation, a pilot study was run comprised of four dose titration experiments.

Two dose titration experiments were carried out using 1 dpf embryos (Figure 3.1). The experiments were carried out by injecting into the bloodstream via the ventral aspect of the yolk sac circulation valley of the embryos. They were then placed into individual wells of a 96-well plate and monitored at 28.5 °C for 3 days. The first strain to be examined was the *emm14* type HSC5 as it has been studied in zebrafish in the past (Miller and Neely, 2004, Neely et al., 2002), with the second one being a more clinically relevant one; the *emm89* type H293. Using HSC5 (*emm14*), a dose as low as 50 CFU caused 6% survival as early as 24 hours post infection (hpi), which remained the same until 66 hpi (Figure 3.1A). On the other hand, H293 (*emm89*) was not as virulent with the lower doses 34 and 103 CFU yielding 81% and 88% survival respectively by 66 hpi, whereas the high dose of 3748 CFU had 30%

survival (Figure 3.1B). Due to the high mortality caused by HSC5, the 2 dpf model was also tested.

The two *S. pyogenes* strains were tested in 2 dpf embryos to assess pathogenesis. For both strains, embryo survival demonstrated a dose-dependent increase in mortality. HSC5 was observed to be still more virulent than H293. In this model, an HCS5 dose of 57 CFU yielded a 67% survival by 66 hpi, whereas a dose of 1413 CFU gave 0% survival (Figure 3.1C). In the case of H293, the low dose of 253 CFU caused 73% survival by 66 hpi (Figure 3.1D). These pilot experiments demonstrated that using the 2 dpf model, infection could be monitored in a timescale amenable to investigation, and was used forthwith.

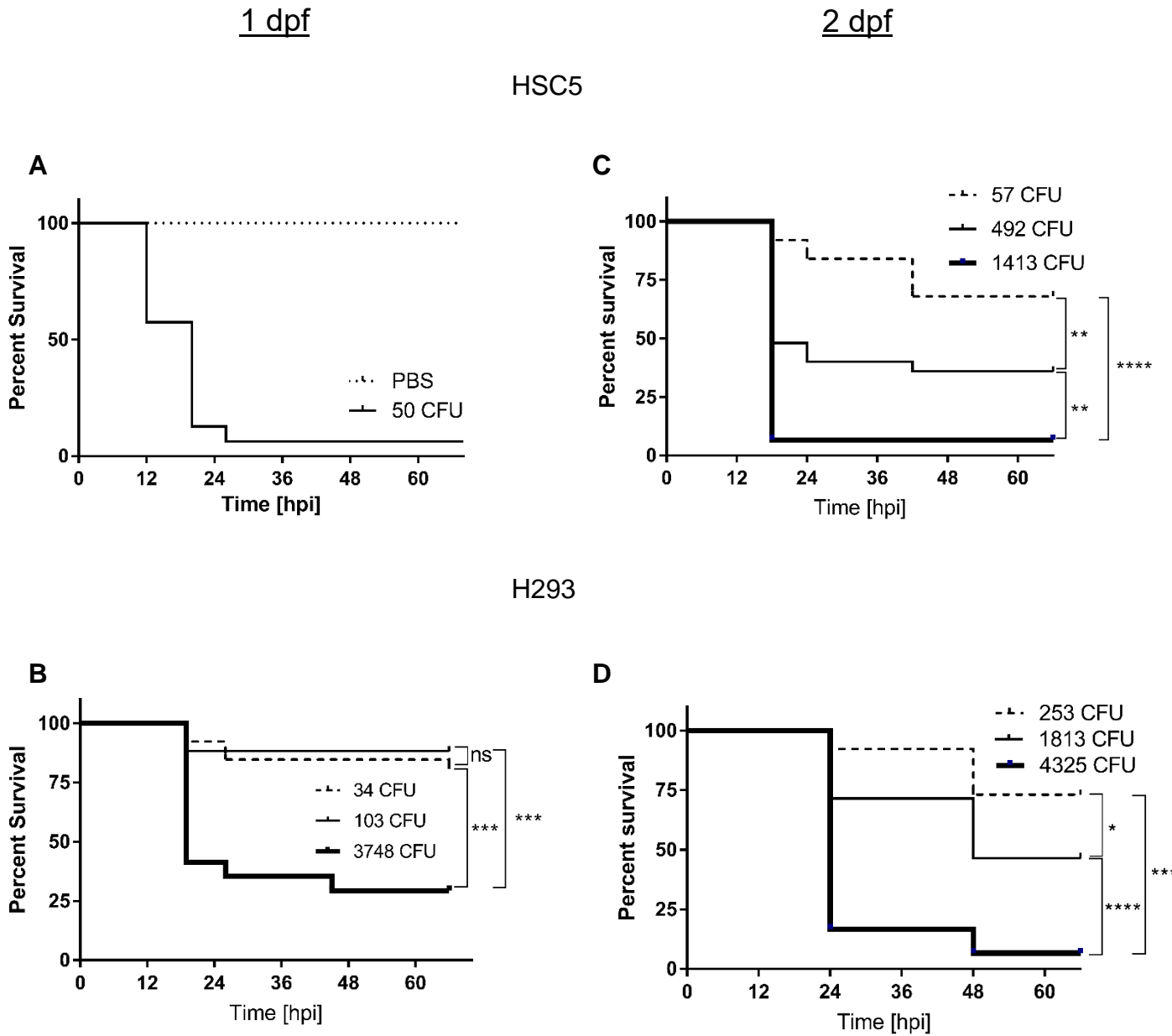


Figure 3.1 Effect of embryo age on the *S. pyogenes* zebrafish infection model

Survival of 1 dpf (**A,C**) and 2 dpf (**B,D**) embryos injected with *S. pyogenes* HSC5 and H293 with doses as indicated. For each group $n=25-30$. Negative controls shown here were taken from another experiment and were performed using PBS ($n=10$). *S. pyogenes* supernatant was also tested, and no mortality was observed (data not shown). (**B**) $p=0.0089$ (**), $p=0.0028$ (**), $p<0.0001$, (**C**) $p=0.0009$ (***), $p=0.0003$ (***), (**D**) $p=0.0304$ (*), $p<0.0001$ (****).

3.3.2 Investigation of HSC5 virulence in the zebrafish embryo model

The zebrafish embryo infection model was then further characterised using strain HSC5. Dose titration experiments were performed in order to characterise the parameters of the model. Independent dose titration experiments were performed, and a representative of three is shown in Figure 3.2A. The three groups in Figure 3.2A show a dose-dependent survival with 57 CFU yielding about 70% survival, 429 CFU 36%, and 1413 CFU 6%. Linear regression further confirmed this dose dependency (Figure 3.2B).

3.3.3 HSC5 population dynamics *in vivo*

In this experiment, 40 CFU yielded approximately 50% survival (Figure 3.2C). No host death was noted until 17 hpi, after which additional mortality was only seen up to 43 hpi (Figure 3.2D). For each time-point, 5 live and all succumbed larvae were collected, homogenised, and plated on media. Bacterial numbers had already begun increasing by as early as 2 hpi (Figure 3.2D). At 8 hpi, the data suggests a bifurcation of populations, one population having high bacterial numbers of 10^4 - 10^5 CFU, and the other population low bacterial numbers of undetectable to 10^2 CFU. At 17 hpi, the first mortality was noted, with overwhelmed hosts revealing $>10^4$ CFU. Despite few live fish after 17 hpi having $<10^2$ CFU, there were a few live embryos carrying $>10^5$ CFU. Figure 3.2D demonstrates that that HSC5 virulence is associated with bacterial growth, and *S. pyogenes* started growing by the first time-point (2 h).

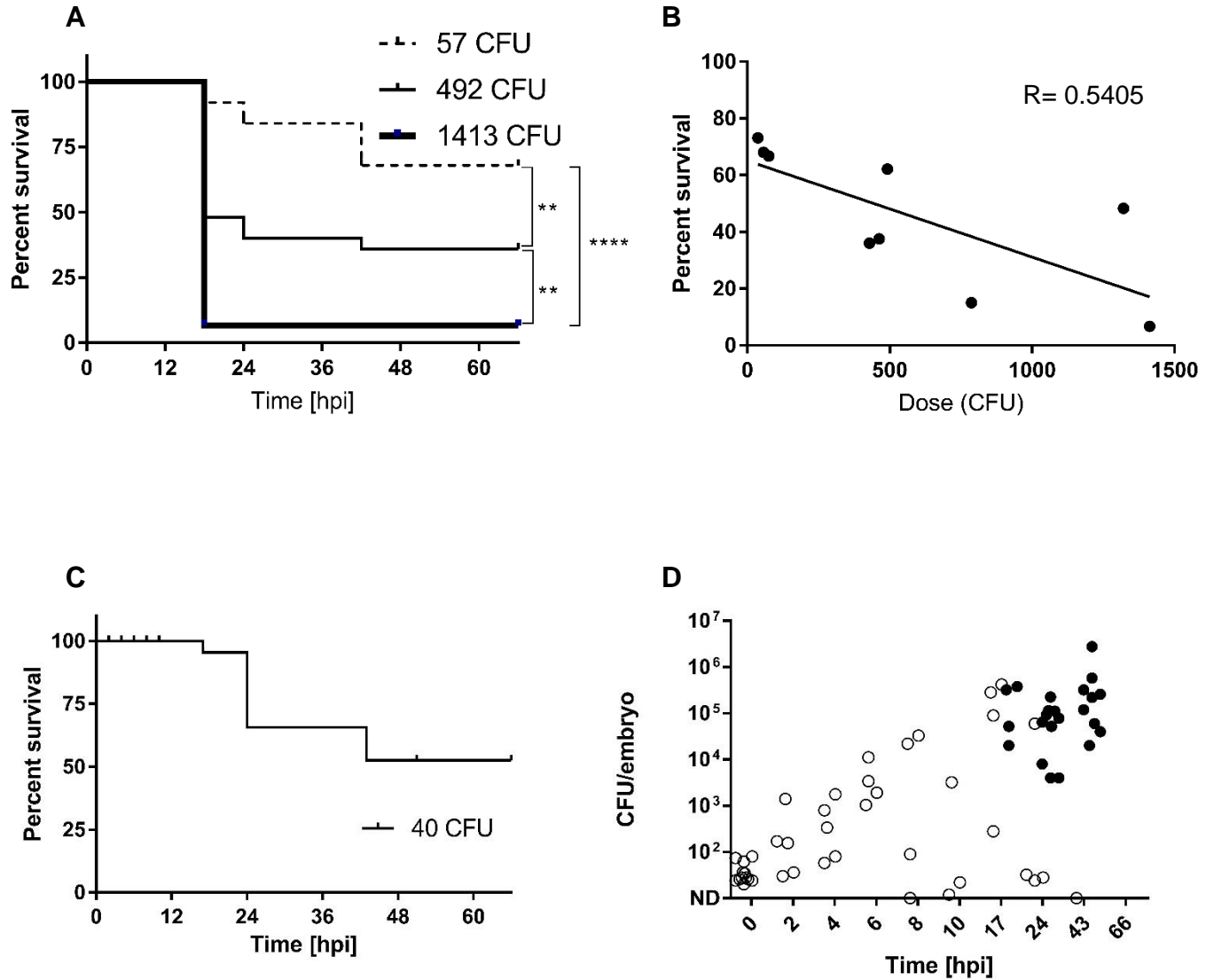


Figure 3.2 Host-pathogen dynamics during zebrafish embryo infection with HSC5

A,B) LWT larvae were inoculated with HSC5 *S. pyogenes* with doses as indicated (n=25-30) **(A)**. $p = 0.0089$ (**), $p = 0.0028$ (**), $p < 0.0001$ (****). All dose titration experiments (n=9) at 66 hpf were combined into one figure, and a linear regression line was drawn **(B)**.

C,D) *In vivo* growth of *S. pyogenes* HSC5 in zebrafish embryos. Fish were injected with 40 CFU. At each time point, 3-5 live embryos and all dead ones were collected, homogenised, and 100 μ L were plated on THY plates. Live embryos are marked with open circles, and dead with filled circles. CFU below 10 are not detectable (ND).

3.3.4 Investigation of H293 virulence in the zebrafish embryo model

The same protocol was followed to carry out dose titrations with the H293 *emm89* strain. Three independent experiments were run, a representative of which is presented in Figure 3.3A. The model shows a clear dose dependence between 250 to 4000 CFU inoculum. Linear regression supported this assertion (Figure 3.3B). Approximately 1800 CFU gave a dose of 50% embryo survival after 66 hpi. This provided a convenient dose for future experiments.

3.3.5 H293 population dynamics *in vivo*

Using the dosing experiment as a guide, embryos were injected with 1400 CFU H293 at 54 hpf. This led to approximately 50% embryo survival after 66 hpi (Figure 3.3C). No hosts had succumbed until 21 hpi, and of those embryos that did, most had done so by 44 hpi. 5 live embryos and all dead ones were collected at each time-point, homogenised, and evaluated for total CFU. After injection, bacterial numbers began to alter within individual embryos. After 10 hpi, succumbed embryos began to appear. All overwhelmed hosts had a bacterial load of $>10^5$ CFU, whereas this was never observed in live hosts. In fact, all live larvae showed a reduction in bacterial numbers from the original dose injected, often to the limit of detection. These results confirm that H293 virulence is linked to bacterial growth, and although bacterial proliferation is restricted for about 8 hours, in some fish, *S. pyogenes* can then grow and overwhelm the host. This shows that this chosen infectious dose provides a good model of host-pathogen interactions.

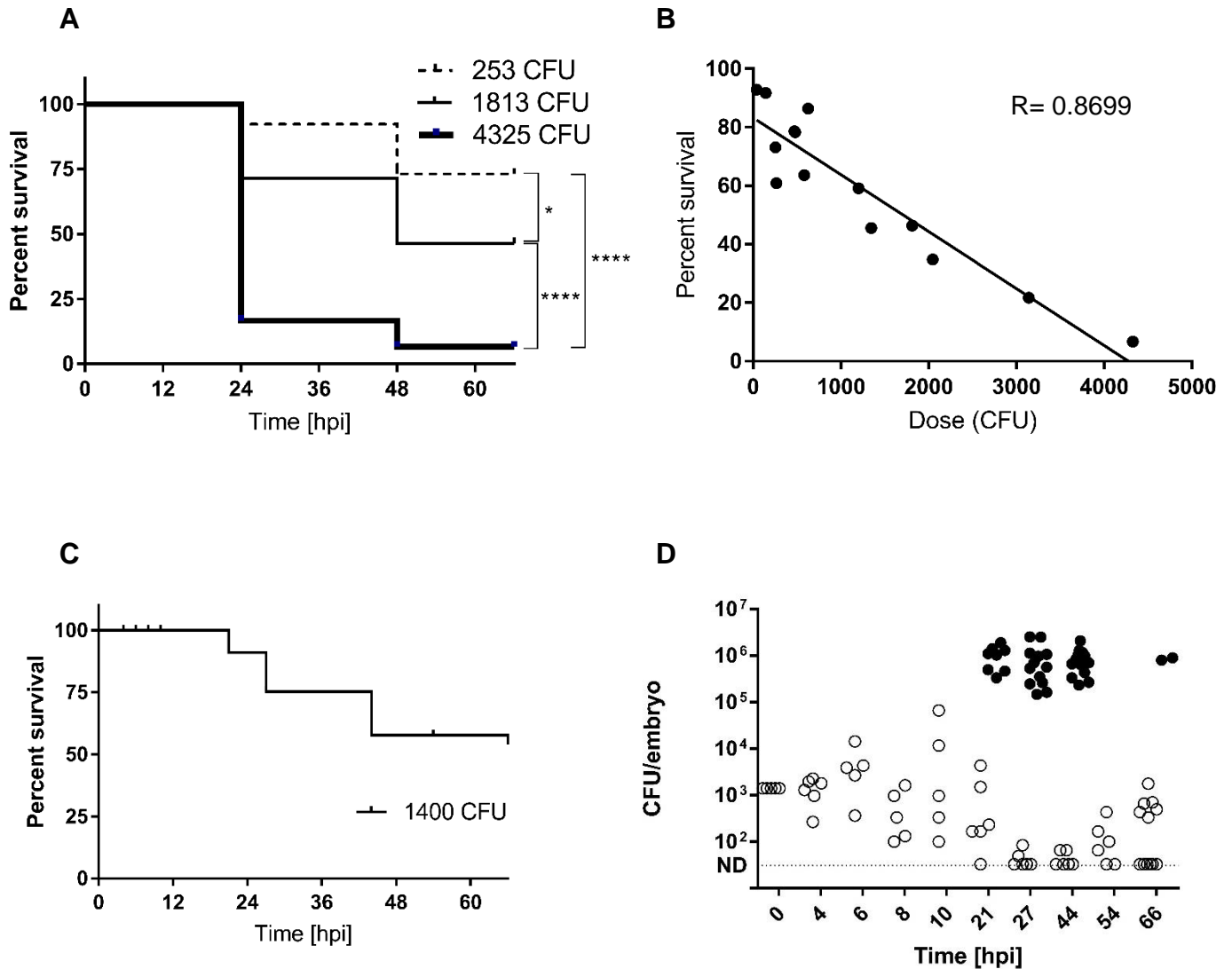


Figure 3.3 Host-pathogen dynamics during zebrafish embryo infection with H293

A,B) Survival of 2 dpf LWT fish injected with H293 *S. pyogenes* with doses as shown (n=25-30) **(A)**. $p= 0.0304$ (*), $p<0.0001$ (****). All dose titration experiments (13) at 66 hpf were combined into one figure, and a linear regression line was drawn **(B)**.

C,D) *In vivo* growth of *S. pyogenes* H293 in zebrafish embryos. The infectious dose was 1400 CFU. At each time point, 5-6 live embryos and all dead ones were collected, homogenised, and 10 μ L were plated on THY omni trays. Live embryos are marked with open circles, and dead with filled circles. CFU below 40 was not detectable (ND).

3.3.6 Investigation of H305 virulence in the zebrafish embryo model

The last *S. pyogenes* strain to be examined was H305. This *emm1* type, displayed the highest virulence with 91 CFU producing 28.5% host survival, 858 CFU 15%, and 1888 CFU 5% (Figure 3.4A). This figure is a representative of three independent experiments, each group having n=25-30. The linear regression line in Figure 3.4B illustrates both a dose-dependency and the very high virulence of H305 compared to the other two strains used here.

3.3.7 H305 population dynamics *in vivo*

An infectious dose of 28 CFU resulted in about 50% survival. 5 live zebrafish embryos were then collected along any embryos that had succumbed at every time-point, homogenised, and examined for their bacterial load. Similar to the other two strains, no fish had succumbed up until 17 hpi, when the first mortality was seen (Figure 3.4D). The two distinct populations were very apparent in the case of this strain. *S. pyogenes* started growing by the first time-point at 2 hpi and can be seen growing steadily between 2-8 hpi with CFU numbers being between $\sim 10^2$ and 10^4 . Between those two time-points a second population of hosts was noted, that was able to successfully restrict *S. pyogenes*, with CFU numbers remaining $< 10^2$ with few live embryos going up to $< 10^3$ at 66 hpi. The first fish that succumbed at 19 hpi, carried 10^6 , with all of the subsequent overwhelmed hosts having 10^6 - 10^7 CFUs. In spite of their bacterial load being as high as 10^5 - 10^6 , there were four fish that were alive.

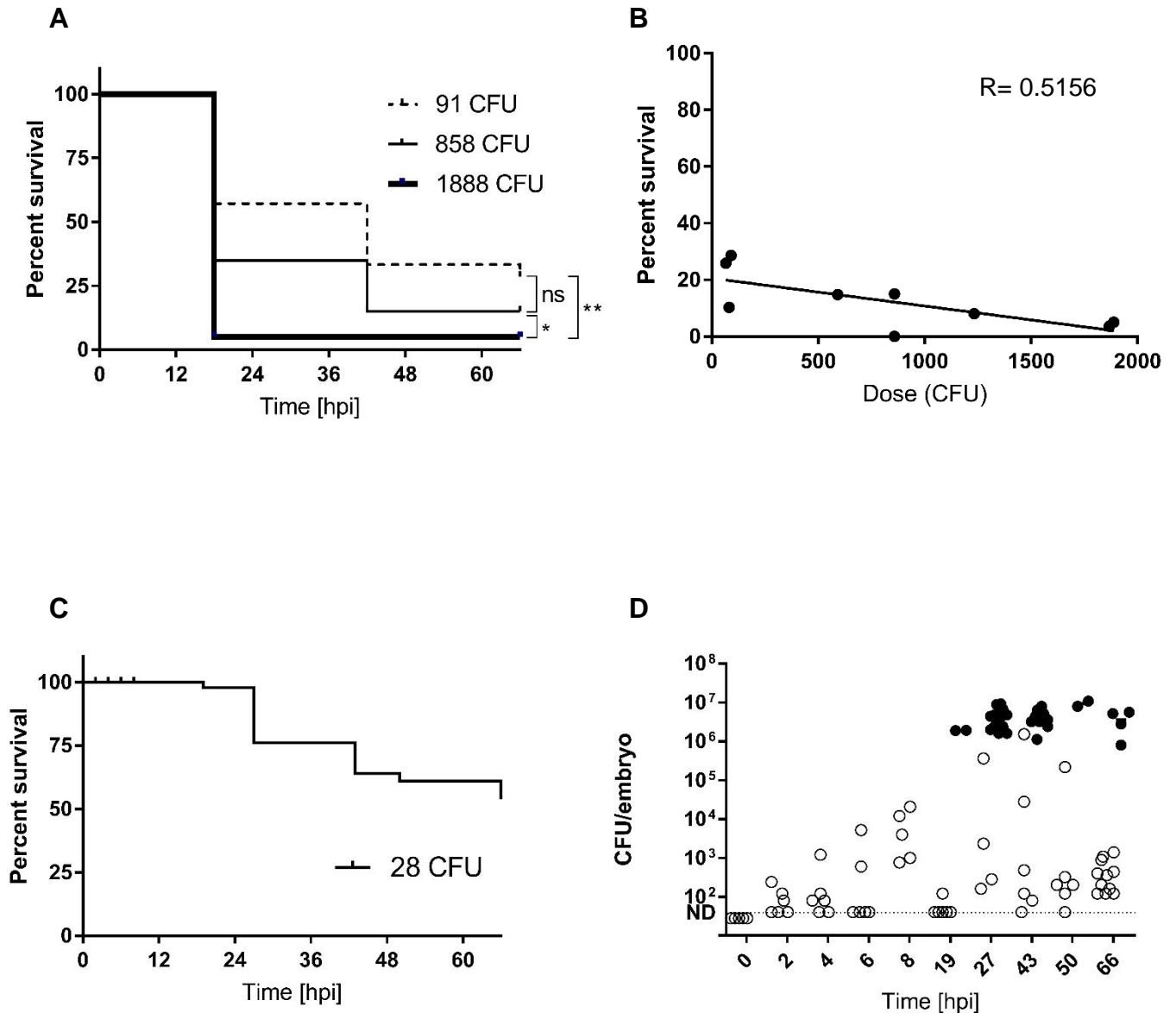


Figure 3.4 Host-pathogen dynamics during zebrafish embryo infection with H305

A,B) Survival of 2 dpf LWT larvae challenged with H305 *S. pyogenes* (doses as shown) (n=25-30). **(A)**. $p= 0.0240$ (*), $p= 0.0028$ (**). All dose titration experiments (9) at 66 hpf were combined into one figure, and a linear regression line was drawn **(B)**.

C,D) *In vivo* growth of *S. pyogenes* H305 in zebrafish embryos. The infectious dose was 28 CFU. At each time point, at least 5 live embryos and all dead ones were collected, homogenised, and 10 μ L were plated on THY omni trays. Live embryos are marked with open circles, and dead with filled circles. CFU below 40 were not detectable (ND).

3.8 Discussion

3.8.1 Choosing the systemic model of infection

The site of infection chosen was into the circulation valley resulting in systemic disease. Within the zebrafish embryo, there are several infection sites to select from, the circulation valley (systemic), the otic vesicle, somites (tail muscle) and yolk, to name a few (Prajsnar et al., 2008, Harvie and Huttenlocher, 2015, Benard et al., 2012). Apart from asymptotically colonising the nasopharynx, *S. pyogenes*, can also become invasive and cause lethal infection, which leads to its notoriety as an agent of necrotising fasciitis and streptococcal toxic shock syndrome (STSS) (Stevens, 2000). Introducing *S. pyogenes* into the bloodstream creates a potential interaction between the pathogen and the host immune phagocytes. This provides an excellent opportunity to examine the role of phagocytes in the control of *S. pyogenes* disease. Furthermore, the model is versatile to allow the potential of the newly described phenomenon of pathogenesis augmentation to be examined (Boldock et al., 2018).

3.8.2 2-dpf embryos offer an amenable model to study *S. pyogenes* infection

Previously, 1 dpf embryos have been used to establish models for *S. aureus* and *E. faecalis* disease (Prajsnar et al., 2008, Prajsnar et al., 2013). For that reason, the 1 dpf model was tested first (Figure 3.1 A, B). This development stage of the zebrafish

embryos was appropriate for the H293 strain, but not for HSC5, as a dose of 50 CFU led to an almost 50% mortality in the first 12 hpi with that increasing up to 94% by 24 hpi. This was too rapid for amenable experimentation.

Consequently, the 2 dpf model was examined, which resulted in both strains yielding a wider range of dose-dependent mortalities, likely as the immune system had more time to develop. Giving a long window for infection to progress provides the opportunity to observe pathogen dynamics within the context of a host, for which the immune system has not been overwhelmed. It is also important to be able to use an infectious dose that is high enough to allow reproducible infection but not so large that the material infected *per se* has an undue deleterious effect on the host. For these reasons, the 2 dpf model was used henceforth.

3.8.3 H293 *S. pyogenes* strain allows for examination of the infection bottleneck

All three *S. pyogenes* strains used here, yielded dose-dependent survival, with virulence going H305>HSC5>H293. *In vivo* growth experiments showed that virulence was linked to bacterial growth for all strains. For H293, growth was restricted between 2-8 hpi. This bottleneck was followed by a bifurcation of zebrafish hosts; ones carrying about 10^6 CFU, and the others 10^1 - 10^3 . This bottleneck was not found in the other two strains. Instead, *S. pyogenes* CFU numbers were found to increase as early as the 2 hpi. The dichotomy of the zebrafish populations was

also observed, with H305 showing it as early as the first couple of time-points. Given that HSC5 and H305 produced a much higher fish mortality than H293, their bottleneck had likely been resolved by 2 hpi, thus not being detected by the time-points chosen for the experiment. The resolution of this bottleneck reveals the fate of the host; either being overwhelmed or having seemingly cleared the infection. It is therefore important to interrogate this bottleneck further to elucidate *S. pyogenes* disease.

Chapter 4: Investigating host-pathogen interactions in the zebrafish embryo model of *S. pyogenes* infection

4.1 Introduction

Zebrafish embryos show no markers of adaptive immunity in their first four days, after which T and B cells start developing to eventually establish the adaptive system. The adaptive immune response, however, is only functional four to six weeks later (Sullivan et al., 2017). Conversely, functional macrophages and mature neutrophils have been reported to be present within 25 hpf (Herbomel et al., 1999) and 48 hpf (Lieschke et al., 2001) respectively. This isolation of the innate immune system reactions, allows for studying the innate responses without complications by the adaptive response. In order to study host-pathogen interactions during infection, specific tools for spatial and temporal imaging in a living fish need to be used. Several transgenic fish lines that have fluorescent tags on professional phagocytes have been created and used in previous studies (Renshaw et al., 2006, Hall et al., 2007, Prajsnar et al., 2012). In the same manner, fluorescent labels can be created for the bacterial strains in use. Together, visualisation of both leukocytes and bacteria is possible, elucidating their interactions within the host.

Another way of interrogating the role of the innate immune system in fighting *S. pyogenes*, is by knocking-down individual elements of the system itself to identify their role. One of the knock-down technologies are the antisense, morpholino-modified oligonucleotides (morpholinos). Morpholinos block specific gene expression by targeting mRNA transcripts at translation (Nasevicius and Ekker, 2000). For instance, a morpholino against *pu.1* can be used to block the expression of this myeloid cell transcriptional activator in 1-4 cell embryos (Rhodes et al., 2005, Prajsnar et al., 2008). This, yields both phagocyte cell types being depleted, with macrophages not developing until 48 h, and neutrophils being retarded by 36 h. This knock-down effect is only transient, and eventually gene expression resumes. Another knock-down technique that will be used in this Chapter, is chemical ablation of specific phagocyte types. For example, the injection of liposome-encapsulated clodronate in 1 dpf fish, results in the neutralisation of macrophages by 2 dpf (van Rooijen and Hendrikx, 2010, Nguyen-Chi et al., 2017).

4.2 Aims of this chapter

1. Visualise spatial and temporal interactions between *S. pyogenes* and professional phagocytes.
2. Genetically disrupt the myeloid cell lines in order to elucidate the role of phagocytes in infection.

4.3 Results

4.3.1 pHrodo staining of *S. pyogenes* injected in zebrafish embryos.

In order to investigate host-pathogen interactions, the first question to be addressed was whether or not *S. pyogenes* is phagocytosed. To that end, *S. pyogenes* H293 was stained using red pHrodo (ThermoFisher Scientific). pHrodo is a fluorescent dye that binds to the cell wall of bacteria. It remains almost non-fluorescent at neutral pH, but at a pH below 5, it fluoresces brightly. As a consequence, in the case that *S. pyogenes* is phagocytosed and ends up in a phagolysosome, this event would be detected by the microscope as increased fluorescence in that acidified environment (Zhu et al., 2015). *S. pyogenes* H293 was prepared by incubation with pHrodo as described in Section 2.19.

A group of larvae was injected with 800 CFU of *S. pyogenes* H293 stained with pHrodo, and after 1-2 hours, three live embryos were chosen to be imaged by confocal microscopy. Figure 4.1 is a representative picture from the three embryos, and it shows the stained bacteria fluorescing inside what are presumably phagocytes, suggesting that *S. pyogenes* was phagocytosed. These cells were situated at the outer surface of the embryo yolk sac, where phagocytes stay attached to the plasma membrane of the sac, unlike the evermoving red blood cells (Herbomel et al., 1999).

4.3.2 Creating fluorescently-labelled *S. pyogenes*

In order to be able to monitor host-pathogen interactions in real-time, a permanent label is needed for *S. pyogenes*. The pHrodo dye only provided a temporary solution, as the dye binds to the cell wall and gets subsequently diluted as bacteria grow. For this reason, the pMV158-mCherry and pMV158-GFP plasmids were introduced into *S. pyogenes* H293 via electroporation (Boldock et al., 2018 (Figure 4.2)).

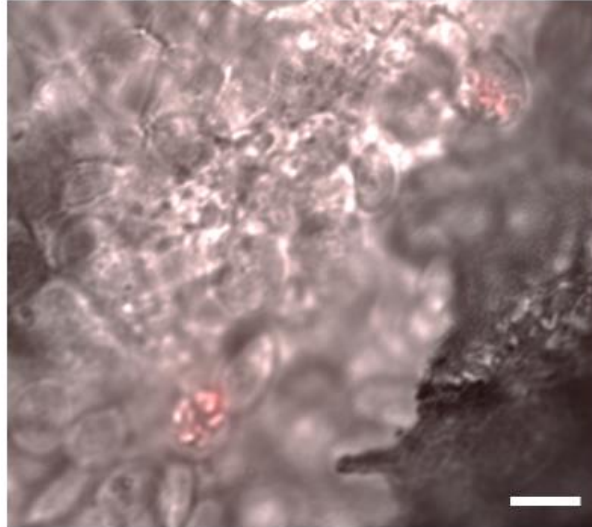


Figure 4.1 pHrodo stained *S. pyogenes* was internalised by likely embryo phagocytes

Zebrafish embryos were injected with 800 CFU *S. pyogenes* stained with pHrodo™, and imaged after 1-2 hours using a confocal microscope. Three embryos were picked to be imaged, and a representative image was chosen to be presented here. These cells were situated in the circulation over the yolk of the fish, and were captured at 60x magnification. Scale bar represents 10 μ m.

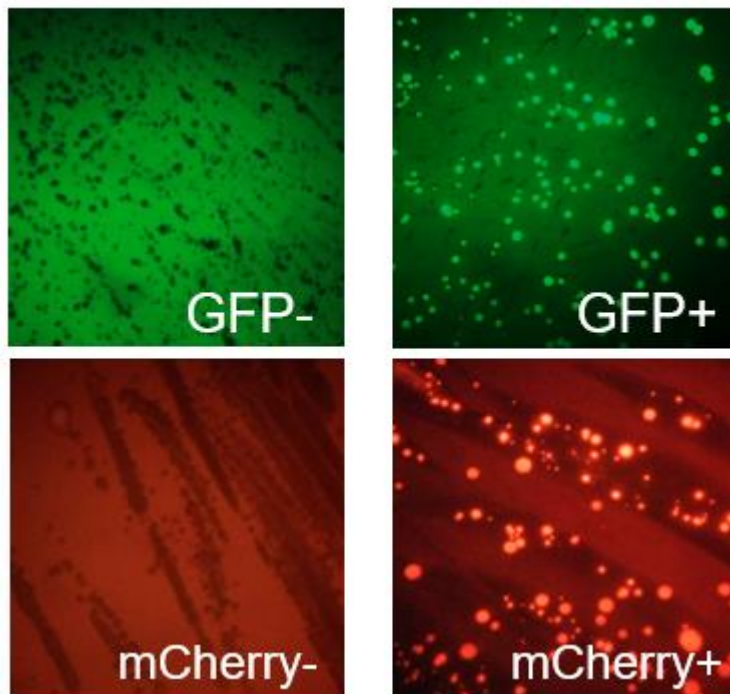


Figure 4.2 Transformation confirmation of pMV158-GFP and pMV158m-Cherry in H293

S. pyogenes H293, was transformed with either pMV158-GFP or pMV158-mCherry via electroporation. After the recovery step, the resuspended cells were plated on Columbia horse Blood Agar (CBA), with no antibiotics. This figure presents four different CBA plates, viewed under a stereomicroscope. The strains also grew on THY-tet plates, but with a significantly reduced colony size than shown here on CBA.

4.3.3 Whole fish microscopy of *S. pyogenes* during the initial and terminal stages of infection

Zebrafish embryos were challenged with 500 CFU of H293 carrying pMV158-GFP. Following, 1 hour of incubation at 28°C, three live fish were imaged via confocal microscopy (Figure 4.3). At 2x magnification, all three fish had the same two areas where bacterial foci were mainly aggregated; the area below the circulation valley, and the end of the tail (Figure 4.3A). In order to visualise the host-pathogen interactions at the cellular level, the tail region was chosen to be looked at, at 60x magnification (Figure 4.3B). It could be observed that most labelled bacteria had already been phagocytosed, as most of them could be seen inside cells. *S. pyogenes* was observed to be successfully phagocytosed as early as 0.5 hpi (data not shown). Here, colocalization of bacteria with phagocytic cells is considered as phagocytosis. These cells could be either macrophages or neutrophils, as both types are present at this development stage.

At 20 and 26 hpi, six more larvae were collected in random, three per time-point, and imaged (Figure 4.4). Figure 4.4A shows a fish that was collected very shortly after its terminal stage, which was determined by loss of heartbeat but no decomposition. The bacteria could be seen concentrated mainly around the circulation valley and the yolk sac, either above or below. Collectively these areas are the upper part of the circulation system of the zebrafish, and bacteria were found where blood vessels have been reported to be. No bacteria were seen in the yolk. Fish 4.4B, was collected after the terminal stage, as can be seen from its decomposing state. Having less of a structure, the bacteria could still be mainly found around the yolk. No fluorescent *S. pyogenes* was detected in fish 4.4C, which suggests clearance of the infection.

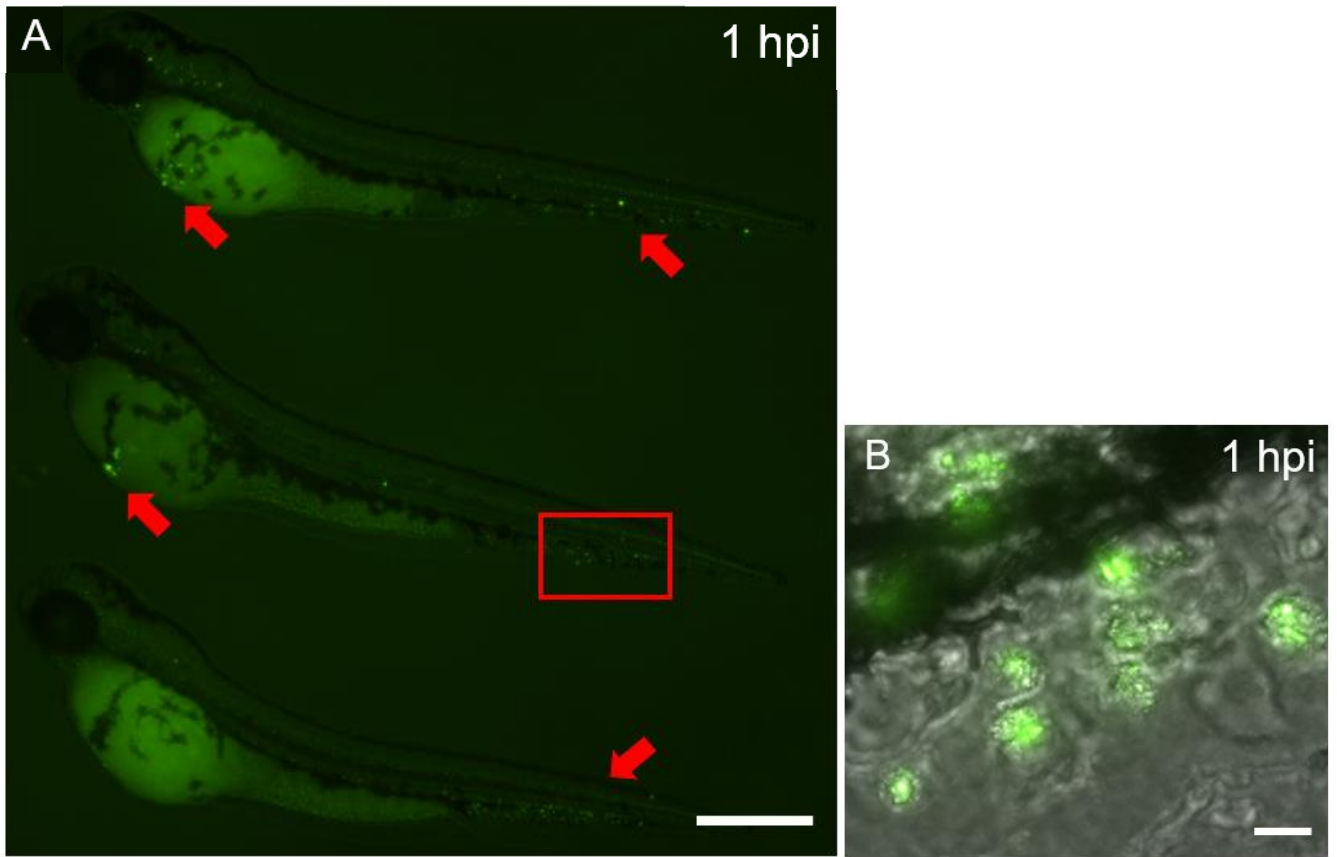


Figure 4.3 Imaging of disseminated bacterial foci at 1 hpi after systemically challenging embryos with GFP-tagged *S. pyogenes*

Zebrafish larvae were inoculated with 800 CFU of *S. pyogenes* H293 carrying pMV158-GFP. At 1 hpi, three embryos were chosen to be imaged (**A**). The red arrows show the two major aggregation zones, which were just below the circulation valley, and the tail. The three embryos were imaged using a 2x magnification (**A**), whereas a 60x was used to zoom in on the tail of one of the embryos (**B**). The zoomed in area is indicated by the red box outline. Scale bars represent 750 μm (**A**), and 10 μm (**B**).

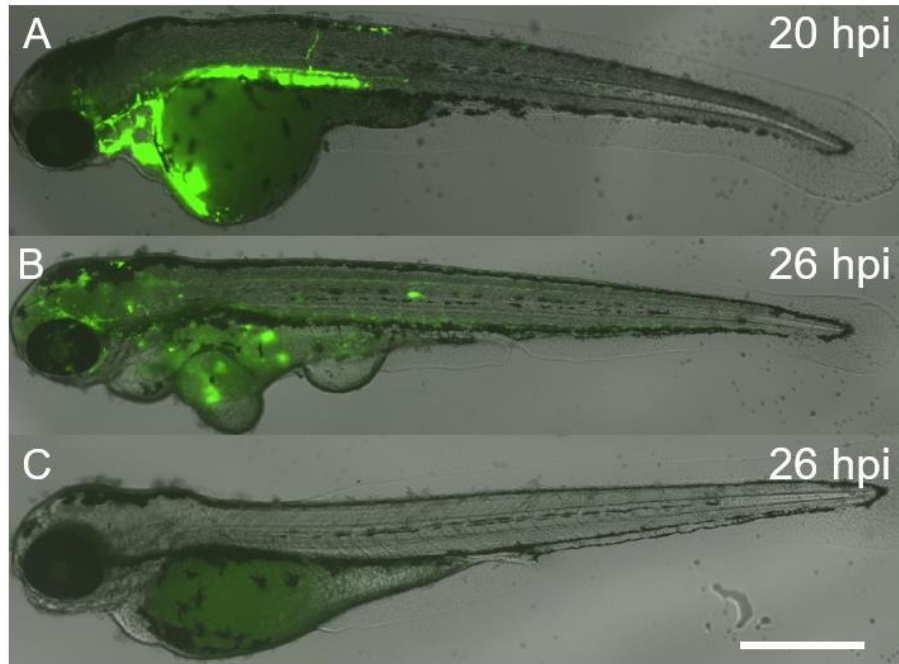


Figure 4.4 Visualisation of *S. pyogenes* localisation at the terminal stage of infection versus a cleared infection

Embryos were injected with 800 CFU *S. pyogenes* H293-GFP, and three were picked to be imaged after 20 (**A**) and 26 hpi (**B, C**). No heartbeat could be seen for fish **A** and **B**, whereas **C** had no fluorescent *S. pyogenes* detected, and had a strong heartbeat. Magnification was at 2x. Scale bar represents 750 μm .

4.3.4 Elucidating the involvement of macrophages and neutrophils during infection

Having mapped the spatial arrangement of *S. pyogenes*, at the beginning and the end of the infection, the next goal of this Chapter was to carry out more detailed microscopy, defining the role of specific phagocyte types in *S. pyogenes* infection. Therefore, transgenic zebrafish lines were employed, and used in combination with the fluorescently-tagged bacteria. *S. pyogenes* H293 carrying pMV158-GFP was injected intravenously into *Tg(mpeg1:mCherry-CAAX)sh378* embryos at a dose of 1850 CFU (Loynes et al., 2018). This line has mCherry labelled macrophages. At 3 hpi, five fish were chosen to be fixed and imaged. By this time-point, GFP-labelled bacteria had been colocalised with macrophages (Figure 4.5A). The tail region of the fish was chosen to be imaged, (red box in Figure 4.5A), due to its flat surface which made visualisation more optimal.

In order to determine the action of neutrophils against *S. pyogenes*, *Tg(mpx:GFP)i114* embryos were infected with 1780 CFU H293-mCherry (Boucontet et al., 2018). After 3 hours of incubation, five larvae were chosen randomly and fixed to be imaged the next day (Figure 4.5 B). Although, most bacteria were found in clusters, which suggests phagocytosis, many of those mCherry aggregates were found to colocalise with what might be unlabelled phagocytes (indicated by white arrows). Regardless, unlike with tagged-macrophages, in the case of these GFP-neutrophils, bacteria could be seen within distinct phagosomes.

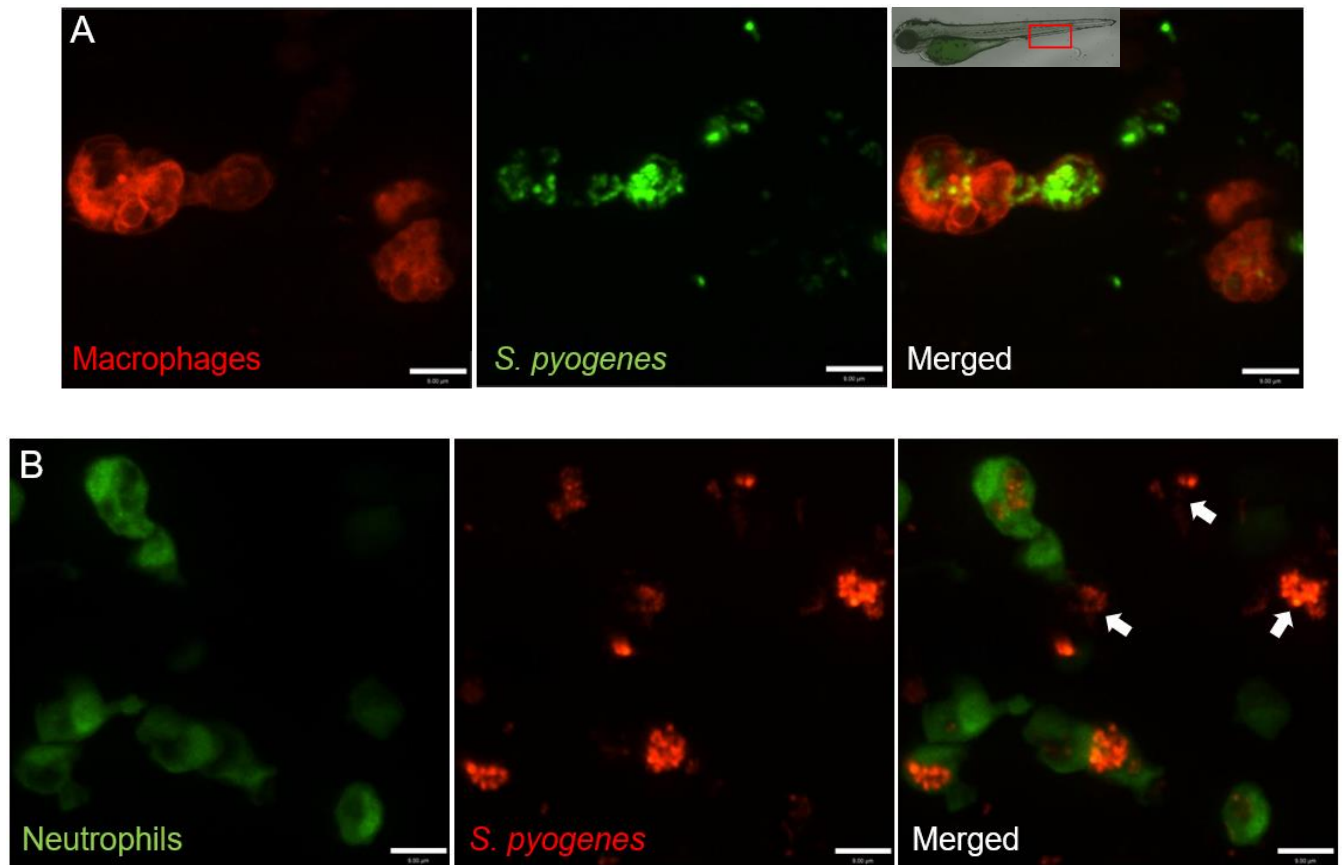


Figure 4.5 *S. pyogenes* colocalised with both embryo macrophages and neutrophils

Confocal microscopy of individual mCherry-macrophages showing GFP puncta (**A**), and GFP-neutrophils showing mCherry puncta (**B**). *S. pyogenes* carrying either pMV158-GFP (**A**) or pMV158-mCherry (**B**) was injected into *Tg(mpeg1:mCherry-CAAX)sh378* fish (**A**), and *Tg(mpx:GFP)i114* (**B**) fish respectively. At 3 hpi, five larvae were fixed, and imaged the next day. A representative image from the five larvae was chosen to be shown here. The 60x (**A**) and 40x (**B**) objectives were used from a confocal microscope. Scale bars represent 9 μm . The red box outline on the top, represents the tail area where the imaging took place. White arrows indicate mCherry labelled bacteria in clusters of unlabelled host cells.

There have been many reports suggesting that in the context of liquid environments, like the bloodstream in the case of a systemic model, macrophages are very efficient at taking up bacteria, whereas neutrophils are not (Le Guyader et al., 2008, Colucci-Guyon et al., 2011, Prajsnar et al., 2012). Neutrophils have been reported to demonstrate a “vacuum cleaner” phagocytic behaviour, making them very effective on tissue surfaces instead (Colucci-Guyon et al., 2011). This difference between macrophage and neutrophil phagocytosis efficiency was observed when *Tg(mpeg1:mCherry-CAAX)sh378* (mCherry macrophages), and *Tg(mpx:GFP)i114* (GFP neutrophils) zebrafish embryos were inoculated with their respective fluorescently labelled *S. pyogenes* H293 (Figure 4.6). Most of the mCherry-macrophages present had phagocytosed at least a few bacteria, whereas most of the GFP-neutrophils were empty.

To further explore this difference in colocalisation, a different fluorescent dye was used with a third colour in order to be able to detect all *S. pyogenes*, macrophages, and neutrophils separately. To that end, H293 was stained with AlexaFluor647, and was used to inoculate *Tg(fms:GAL4);Tg(UAS:nfsB.mCherry);Tg(mpx:GFP)* (mCherry macrophages-GFP neutrophils) fish at a dose of 1240 CFU (Prajsnar et al., 2012). At 1 hpi, five fish were chosen for live microscopy (Figure 4.7 A). Microscopy data from these fish was used for a quantitative assessment of the observations via manual counting of puncta within the labelled phagocytes (Figure 4.7 B).

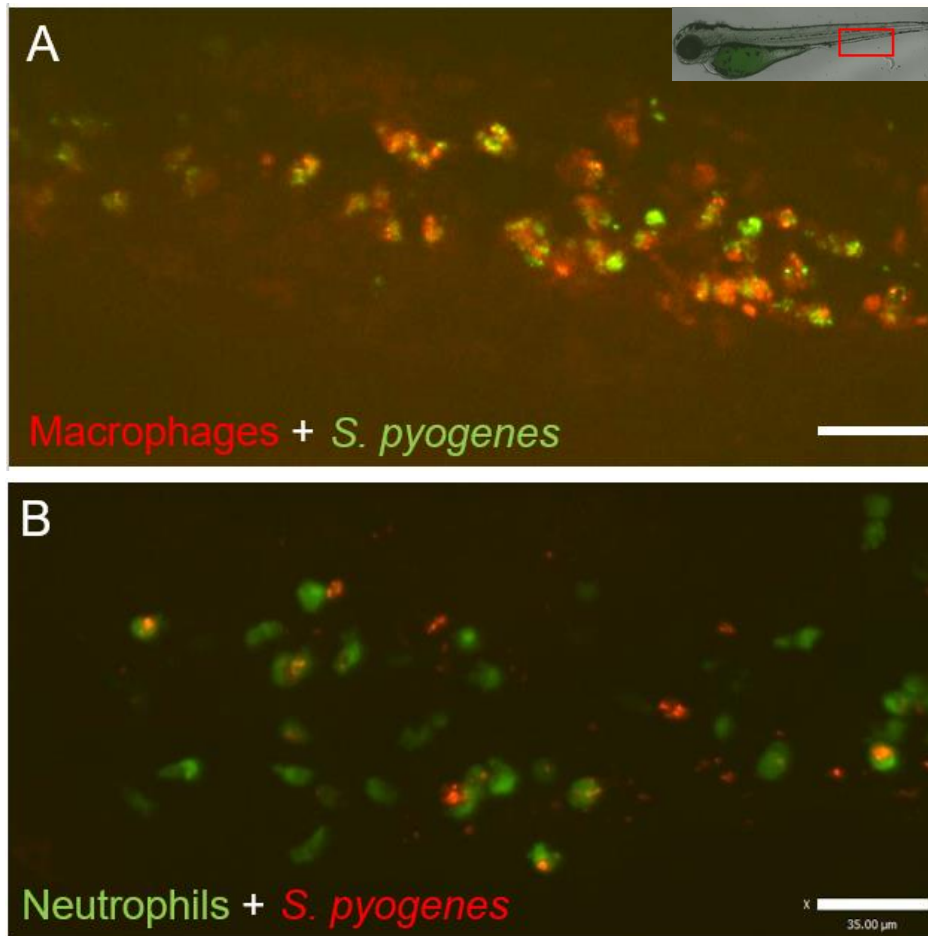
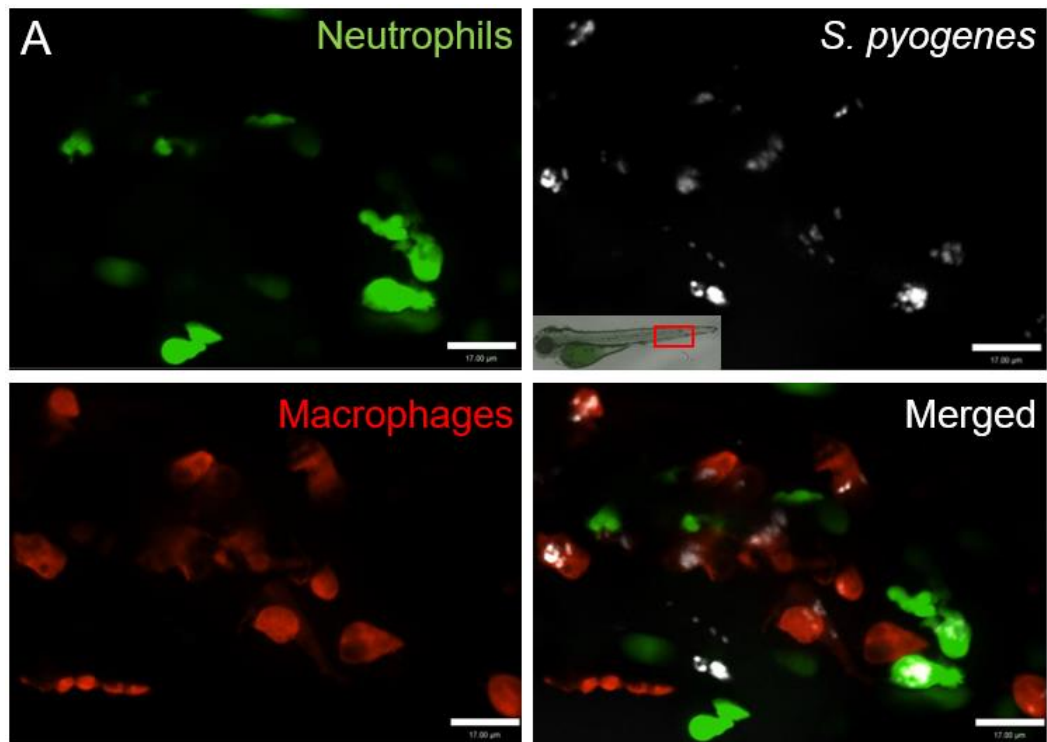


Figure 4.6 Phagocytosis of *S. pyogenes* by macrophages vs neutrophils

Tg(mpeg1:mCherry-CAAX)sh378 embryos were injected with 1850 CFU H293-GFP (A), and *Tg(mpx:GFP)i114* embryos were inoculated with 1780 CFU H293-mCherry (B). At 3 hpi, five fish per group were chemically fixed with 4% PFA in PBS as described in 2.17, and imaged the following day. The 10x objective was used. The scale bars represent 35 μm. The red box outline on the top, represents the tail area where the imaging took place.



B

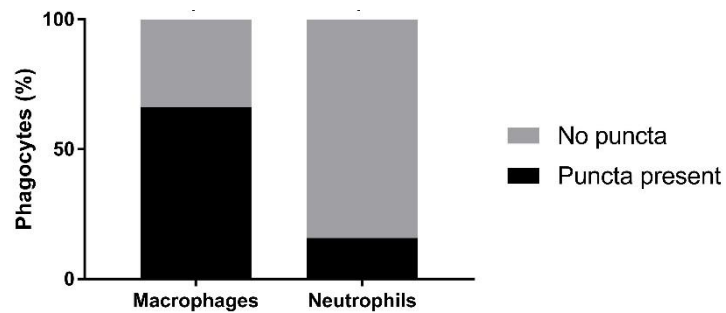


Figure 4.7 Macrophages are more efficient in phagocytosing *S. pyogenes* than neutrophils in the zebrafish systemic model of infection

S. pyogenes H293 was stained with Alexa647, and subsequently injected intravenously into a dually labelled GFP-neutrophils-mCherry-macrophages zebrafish line, at a dose of 1240 CFU. At 1 hpi, five embryos were chosen for live imaging (A). A confocal microscope was used with a 40x objective. The *S. pyogenes* colour was set to be represented as white for contrast. Scale bars represent 17 μ m. Images were manually quantified and the percentage of macrophages with puncta present over neutrophils is given (n=4 fish, 3 sections per fish, 92 macrophages and 135 neutrophils were counted in all 4 fish) (B).

A punctum was defined as a phagocytosis event, regardless of the actual number of bacteria inside the phagocyte. About 66% of observed macrophages were found to have phagocytosed bacteria (puncta), whereas only about 16% of observed neutrophils had phagocytosed *S. pyogenes*.

4.3.5 Imaging the infection progression over the first 8 hpi

It was established in Chapter 3 section 3.3.2., that by 8 hpi, the fate of the embryos had been determined with bacterial concentrations being either over 10^4 and on their way to overwhelm the host, or below 10^2 , and the host was clearing the infection. Since, the data above suggested that macrophages play a bigger role in phagocytosing *S. pyogenes*, than neutrophils do, visualisation of phagocytosis progression was chosen to be assessed by tracking macrophages. Hence, microscopy data from the previous experiment using the *Tg(mpeg1:mCherry-CAAX)sh378* line was used.

At three separate time-points, 2, 6, and 8 hpi, five fish were chosen, per time-point, and fixed to be imaged the following day (Figure 4.8). At 2 hpi, most of the GFP bacteria were found colocalised with macrophages, with a few clusters inside non-tagged phagocytes, as well as a very small number of bacteria being found outside cells (Figure 4.8 A). Such almost complete colocalisation was seen as early as

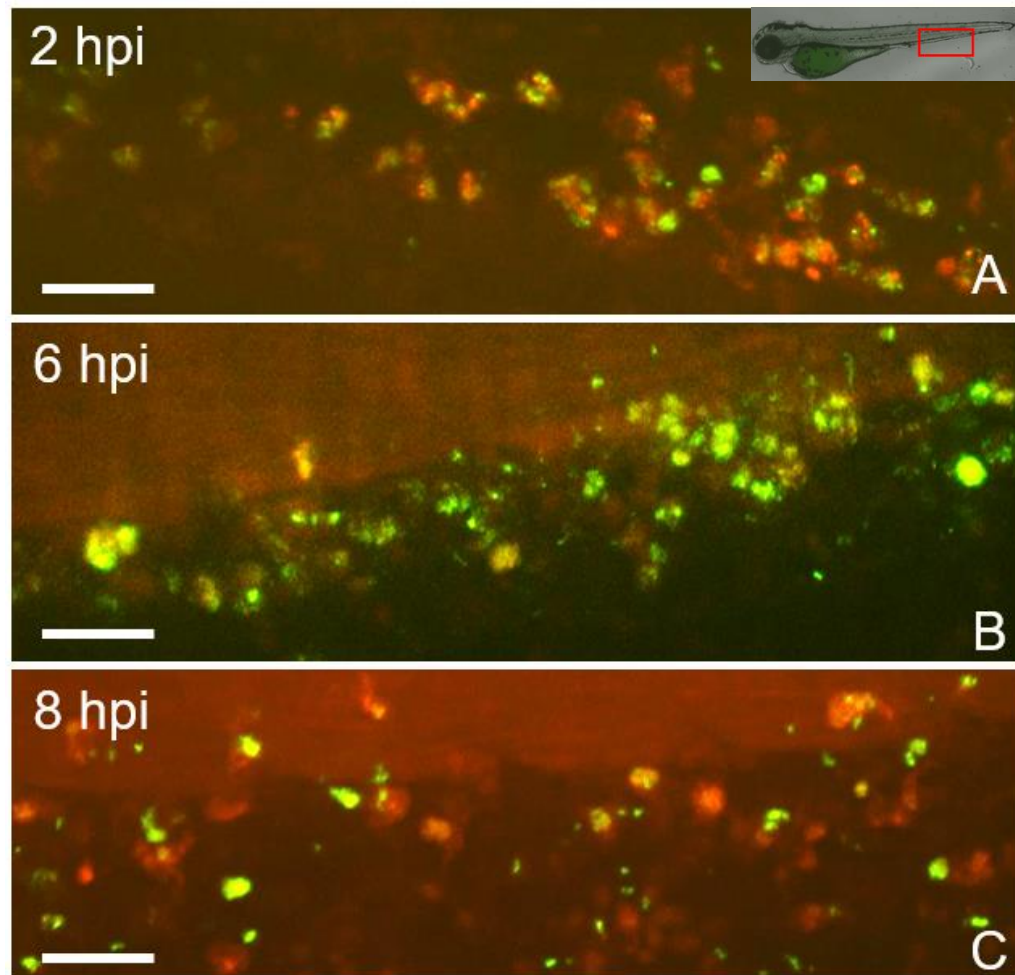


Figure 4.8 Visualising *S. pyogenes* progression of infection via macrophage phagocytosis over 8 hours

Tg(mpeg1:mCherry-CAAX)sh378 larvae were challenged systemically with 1850 CFU *S. pyogenes* H293 carrying pMV158-GFP, and imaged after 2, 4, and 6 hpi. The 10x objective was used. The scale bars represent 35 μ m. The red box outline on the top, represents the tail area where the imaging took place. At both 6 and 8 hpi the embryo heartbeat was very faint, suggesting the host being overwhelmed by the infection.

0.5 hpi (data not shown). At 6 hpi, *S. pyogenes* had started growing out of control, with a significant number of extracellular bacteria being observed as well as a few completely saturated macrophages (Figure 4.8 B). By 8 hpi, there were barely any macrophages still containing bacteria, and most of the bacteria were extracellular (Figure 4.8 C). The fish shown in Figure 4.8, represent hosts that had sufficient bacteria to allow for visualisation. No direct link could be drawn between the state of the host at the time-point, and its eventual fate. Five hosts were also imaged at 12 hpi, however the results were that the fish was either too damaged from infection or had no detectable bacteria.

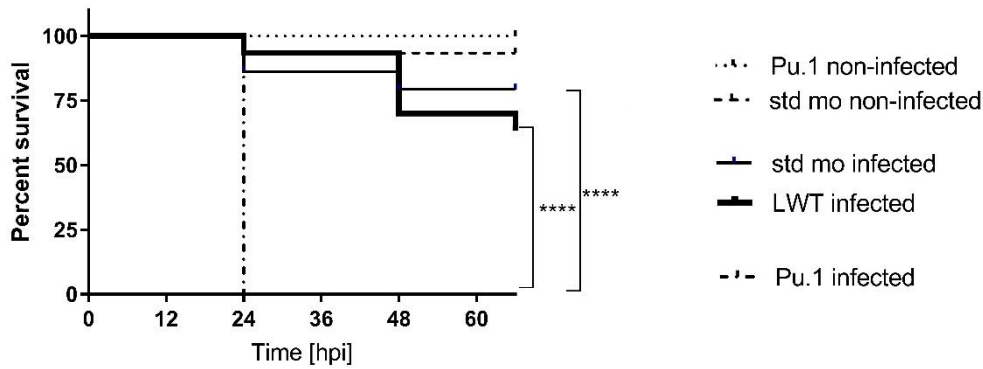
4.3.6 Myeloid depletion in zebrafish embryos via a *pu.1* morpholino

The microscopy data thus far suggested that both phagocytes were able to take up *S. pyogenes*, with neutrophils being less effective. Since, zebrafish embryos younger than 4 weeks only have the innate immune system for protection, the hypothesis is that the action of macrophages and neutrophils is the major limiting factor that prevents *S. pyogenes* from uncontrolled proliferation. In order to take a more quantitative approach after microscopy, and test this hypothesis, macrophages and neutrophils were knocked-down via different techniques, and embryo survival was monitored to observe the effect.

An antisense morpholino oligonucleotide (morpholino), against the PU.1 transcription factor, was used to knock-down myeloid cell development in LWT fish (Nasevicius and Ekker, 2000, Rhodes et al., 2005, Prajsnar et al., 2008). These knock-down embryos were then challenged at 2dpf, with 100 CFU of *S. pyogenes* H293, and a 100% mortality was seen at 24 hpi, compared to the 40% of WT embryos (Figure 4.9 A). The same striking drop in survival was observed with smaller inocula as small as 23 CFU (Figure 4.9 B).

An additional experiment was undertaken to illustrate the effect of the absence of the phagocytes on *S. pyogenes* localisation. A group of LWT embryos, and a group of *pu.1* knock-down larvae were injected with 1500 and 50 CFU, respectively, of H293-GFP (Figure 4.9 C, D). In LWT fish, at 19 hpi, the bacteria were restricted, in a very defined way, within the main vessels of the embryo vasculature that spans from the heart to the tail, with the biggest and most concentrated focus being the heart (Figure 4.9 C). In the morphants on the other hand, the bacteria had almost homogeneously dispersed across the entire fish, implying uncontrolled bacterial proliferation (Figure 4.9 D).

A



B

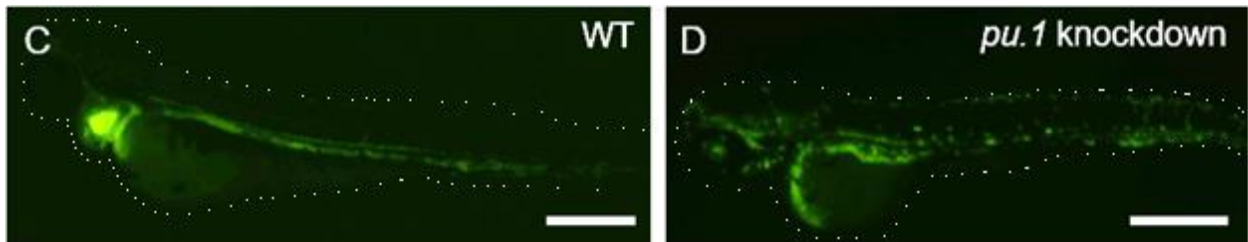
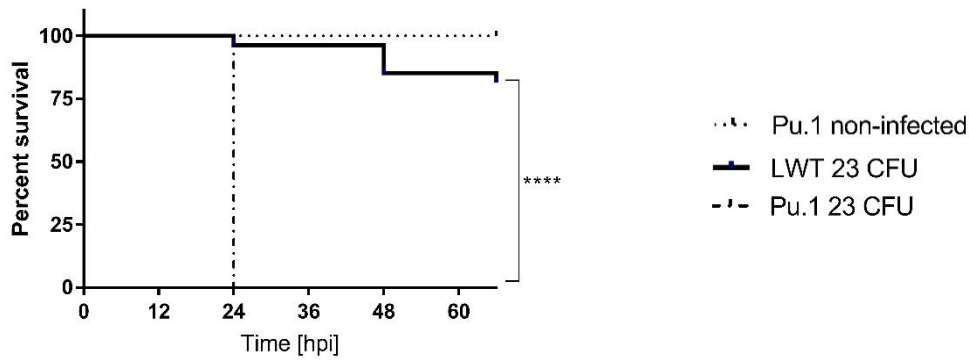


Figure 4.9 *pu.1* knock-down zebrafish larvae are significantly more susceptible to *S. pyogenes*

A,B) Survival rate curves of myeloid-depleted zebrafish larvae after injecting with *S. pyogenes* H293 intravenously at 100 **(A)** and 23 CFU **(B)**. $p < 0.0001$ (****) for *pu.1* knockdown compared to WT embryos. PBS was injected for the non-infected controls, and the standard morpholino (std mo) was used to control for the morpholino. $n = 26-30$.

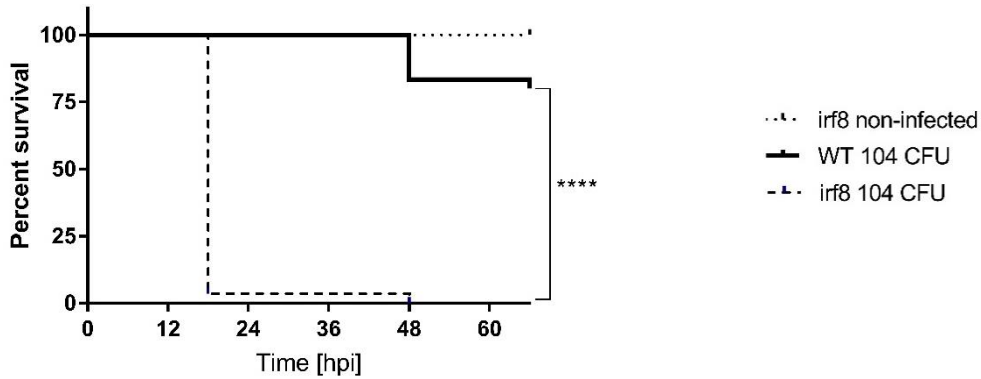
C,D) LWT larvae were injected with 1500 **(C)** and 50 CFU **(D)** *S. pyogenes* H293 carrying pMV158-GFP, and imaged after 19 hpi. Both embryos had no heartbeat. The 4x objective was used. The scale bars represent 750 μm .

4.3.7 *irf8* knock-down in zebrafish larvae

Interferon regulatory factor-8 (*irf8*) or interferon consensus sequence-binding protein, is mainly expressed in macrophages, lymphocytes, and dendritic cells (Li et al., 2011). It is required for myeloid cell progenitors to differentiate to macrophages however, it is not needed for differentiation into neutrophils. As a result, a knock-down of *irf8* replaces all host macrophages with neutrophils as the progenitors are pushed towards developing almost solely into neutrophils (Li et al., 2011, Nguyen-Chi et al., 2017). Despite the fact that macrophages are depleted, the total number of phagocyte population remains the same.

The *irf8* MO^{atg} morpholino was used in order to remove macrophages from *Tg(mpx:GFP)*i114** larvae. At 2 dpf, the embryos were then inoculated with 10⁴ CFU *S. pyogenes* H293. At 18 hpi, 96% mortality was observed in macrophage depleted hosts, as opposed to 20% mortality in WT embryos (Figure 4.10 A). A subsequent experiment used a 18 CFU dose, which yielded 25% mortality at 18 hpi, but a 96% mortality by 48 hpi (Figure 4.10 B). *irf8* knock-down and control LWT fish were injected with *S. pyogenes* carrying pMV158-GFP, to examine the effect of macrophage ablation on *S. pyogenes* localisation (Figure 4.10 C, D).

A



B

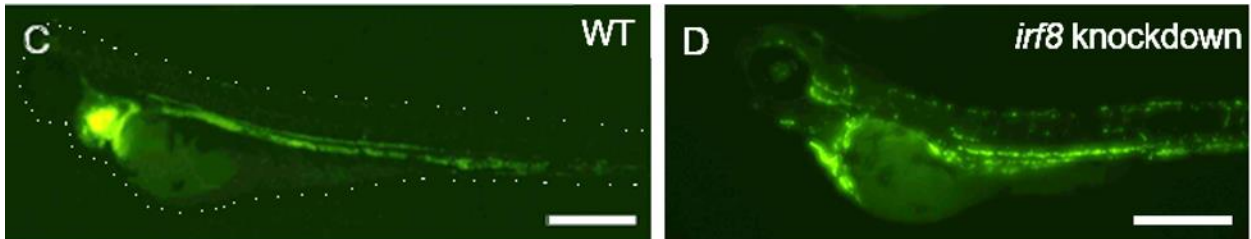
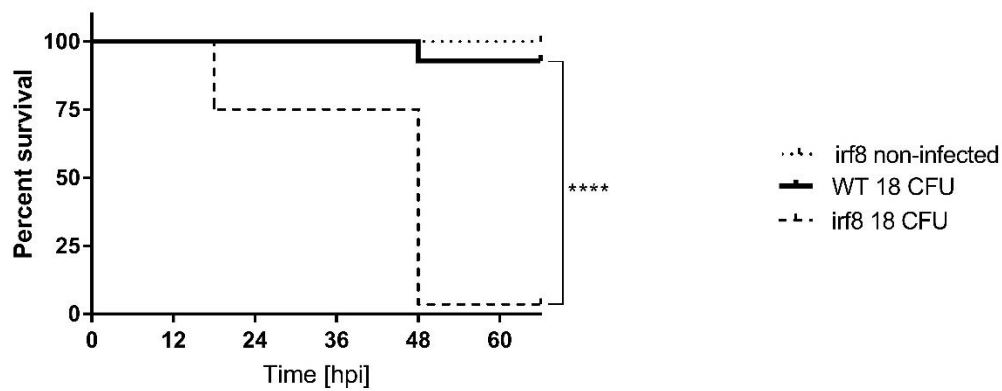


Figure 4.10 *irf8* knock-down zebrafish larvae are more susceptible to *S. pyogenes*

A,B) Survival rate curves of *irf8*-depleted *Tg(mpx:GFP)i114* larvae after injecting with *S. pyogenes* H293 intravenously at 104 (**A**) and 18 CFU (**B**). PBS was injected for the non-infected controls. $p < 0.0001$ (****).

C,D) LWT larvae were injected with 1500 (**C**) and 50 CFU (**D**) *S. pyogenes* H293 carrying pMV158-GFP, and imaged after 19 hpi. The 4x objective was used. The scale bars represent 750 μ m.

4.3.8 Use of clodronate liposomes for macrophage ablation

After having depleted the hosts of both phagocytes and seeing such a striking phenotype (Figure 4.9), the next step was to interrogate the role of macrophages specifically, by using liposome-encapsulated clodronate to neutralise them. This chemical approach comprises of injecting liposomes filled with clodronate (L-clodronate) intravenously into 1 dpf embryos, which reduces the number of macrophages efficiently after 24 h (van Rooijen and Hendrikx, 2010, Nguyen-Chi et al., 2017).

Biphosphonate dichloromethylene-biphosphonate (clodronate) is a small strongly hydrophilic molecule, that can be encapsulated within liposomes. Due to its hydrophilic properties, the leakage from liposomes is very low, as it cannot easily cross any phospholipid bilayers. This also means, that it cannot escape from the cytoplasm of any cell it is in. Once L-clodronate is administered to the fish via intravenous injections, it naturally ends up being phagocytosed mainly by macrophages. Within the macrophages, the phospholipid bilayer of L-clodronate gets lysed, releasing clodronate within the cell. As they cannot escape the cytoplasm, clodronate concentration will increase to a level that will eventually induce apoptosis (van Rooijen et al., 1996). Any free clodronate released following macrophage apoptosis, will be removed from the bloodstream since their circulation half-life is in the order of minutes (van Rooijen and Hendrikx, 2010).

A group of LWT embryos was injected at 1 dpf with L-clodronate to substantially reduce the number of macrophages. The fish were then injected with 128 CFU of *S. pyogenes* H293 at 2 dpf (Figure 4.11). At 24 hpi, there was a dramatic 100% mortality of macrophage depleted hosts, compared to 23% of immunocompetent hosts injected. Injection of L-PBS resulted in 14% mortality, however, the difference between L-clodronate injected and either L-PBS injected or just *S. pyogenes* was statistically significant with $p < 0.0001$ (Figure 4.11 A). A small group of *Tg(fms:GAL4);Tg(UAS:nfsB.mCherry);Tg(mpx:GFP)* (mCherry macrophages-GFP neutrophils) larvae were injected with either L-PBS or L-clodronate. At less than 1 hpi, 3 fish were chosen from each group, fixed, and imaged, to assess macrophage ablation (Figure 4.11 B). The number of mCherry-labelled macrophages was lower in L-clodronate injected fish (Figure 4.11 C) compared to L-PBS injected ones (Figure 4.11 B), being consistent with the survival curves (Figure 4.11 A). This was quantified manually, with the L-PBS image having 28 macrophages compared to the L-clodronate one having 12 (per field of vision shown in Figure 4.11B, C).

A

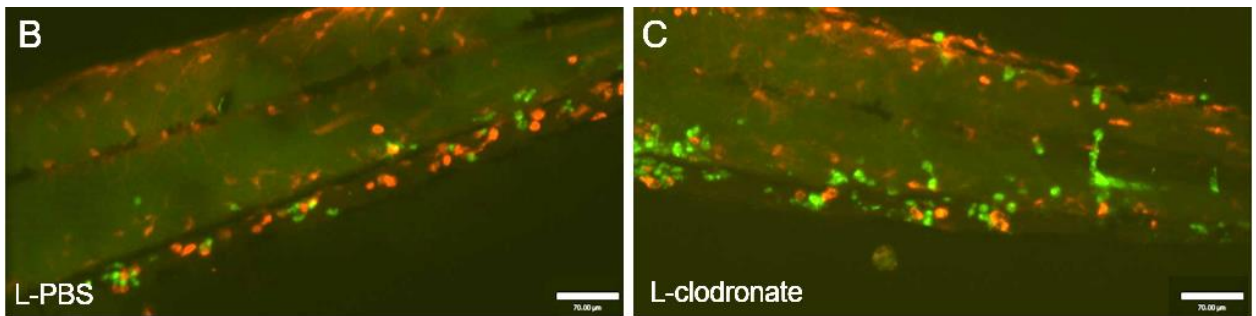
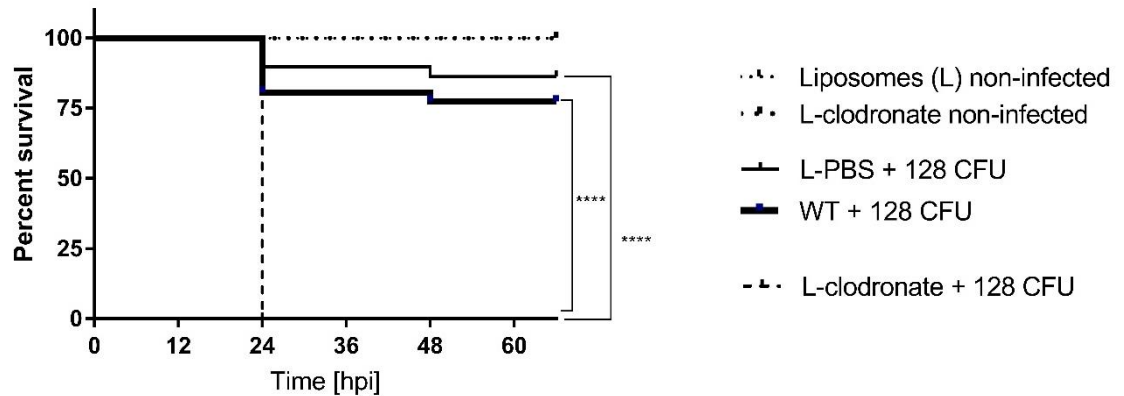


Figure 4.11 Macrophages are required for a successful defence against *S. pyogenes*

A) Survival of macrophage-ablated larvae after injecting with *S. pyogenes* H293 intravenously at 128 CFU. Macrophages of larvae were ablated using L-clodronate injections at 1 dpf. L-PBS and L-clodronate were used for negative controls. The two control lines overlap, showing 100% survival. This graph represents three repeats. $n=26-30$. $p < 0.0001$ (****).

B,C) *Tg(fms:GAL4);Tg(UAS:nfsB.mCherry);Tg(mpx:GFP)* embryos were injected with L-PBS (**B**) and L-clodronate (**C**). Embryos were then fixed and their lower tail section was imaged at 28 h post injection via confocal microscopy. This line carries mCherry-macrophages and GFP-neutrophils. The 20x objective was used. The scale bars represent 70 μ m.

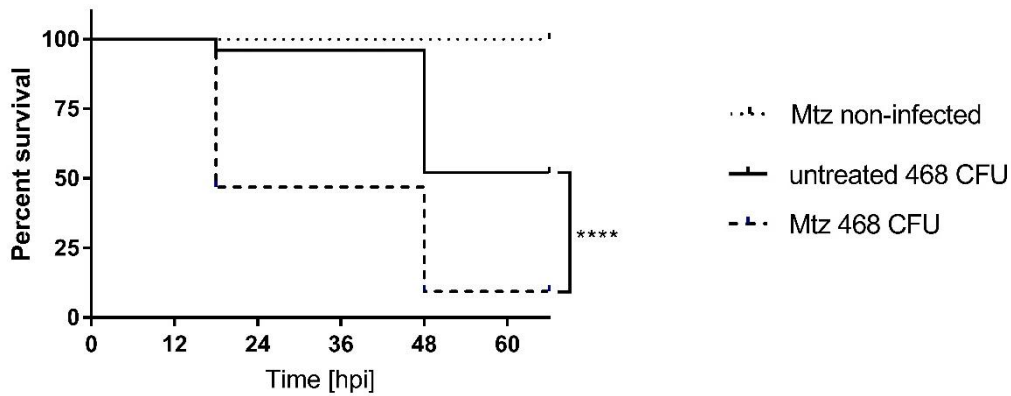
4.3.9 Metronidazole treatment for effective ablation of neutrophils

After having used macrophage ablation techniques, a different transgenic approach was employed to test for the effect of the absence of zebrafish neutrophils on *S. pyogenes* infection. There are zebrafish lines that express the nitroreductase (NTR) enzyme from *Escherichia coli*, that can be placed under the control of either neutrophil- or macrophage-specific promoters. NTR can reduce the non-toxic drug metronidazole (Mtz) into a cytotoxic DNA cross-linking agent inside the cells that express it, triggering cell death (Curado et al., 2007, Hall et al., 2009). This technique allows for a specific and inducible way to ablate either neutrophils or macrophages, and it was reported to have no effect on non-genetically labelled cell populations (Prajsnar et al., 2012).

At 34 hpf, *Tg(lyz:nfsB-mCherry)sh260* (NTR, mCherry neutrophils) embryos were treated with 10 mM Mtz overnight (Buchan et al., 2018). At 54 hpf, the neutrophil-depleted larvae were injected with 468 CFU of GFP-labelled *S. pyogenes*. A few fish were also fixed and imaged to assess ablation efficacy (Figure 4.12 C,D). There was a significant drop in survival for hosts that were treated with Mtz compared to the untreated group (Figure 4.12 A). The survival value for the untreated group was also relatively lower compared to when injecting LWT fish. In order to examine whether this change in mortality was due to the fish line, *Tg(lyz:nfsB-mCherry)sh260* fish were injected along with LWT fish (Figure 4.12 B). The observed mortality of 256 CFU *S. pyogenes* was within the expected range, however the *lyz:nfsB* hosts still

had a much lower survival, suggesting that the line was generally more susceptible to infection. Figure 4.12 B, also demonstrated that Mtz treatment can weaken the host regardless of NTR expression. For that reason, subsequent experiments sought to interrogate the effect of Mtz concentration to larvae susceptibility (Figure 4.13). It was shown that 157 CFU of *S. pyogenes* yield 23% mortality in untreated LWT fish, but as high as 49% mortality in 10 mM Mtz treated LWT fish. A worse effect was observed at 6.5 mM Mtz. This data implies that Mtz is harmful to the host, thus the proposed experiment to use Mtz to ablate neutrophils, could not be completed.

A



B

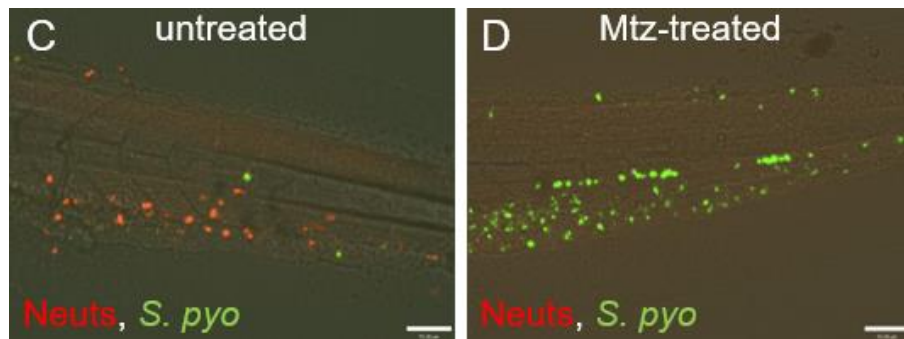
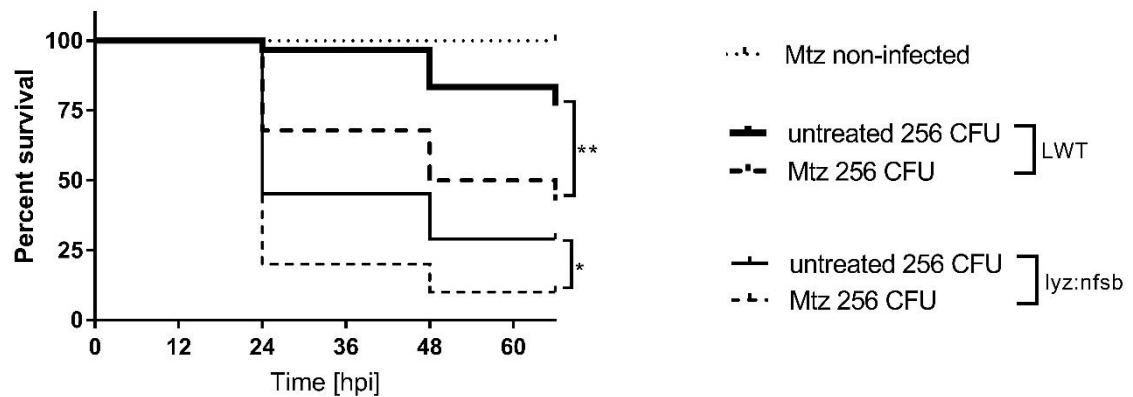


Figure 4.12 Metronidazole treatment effectively ablates neutrophils

A,B Survival of Mtz-treated *Tg(lyz:nfsB-mCherry)sh260* **(A)** and LWT and Nacre zebrafish **(B)** after being challenged with 468 CFU **(A)** and 256 CFU **(B)** *S. pyogenes* H293. **(A)** $p < 0.0001$ (****), **(B)** $p = 0.0029$ (**) (LWT) and $p = 0.0318$ (*) (*lyz:nfsb*). Larvae were bathed in Mtz without the presence of bacteria for the negative control.

C,D *Tg(lyz:nfsB-mCherry)sh260* larvae were injected with 468 CFU *S. pyogenes* H293 carrying pMV158-GFP. Hosts were imaged at 19 hpi with the 4x objective. The scale bars represent 70 μm .

A

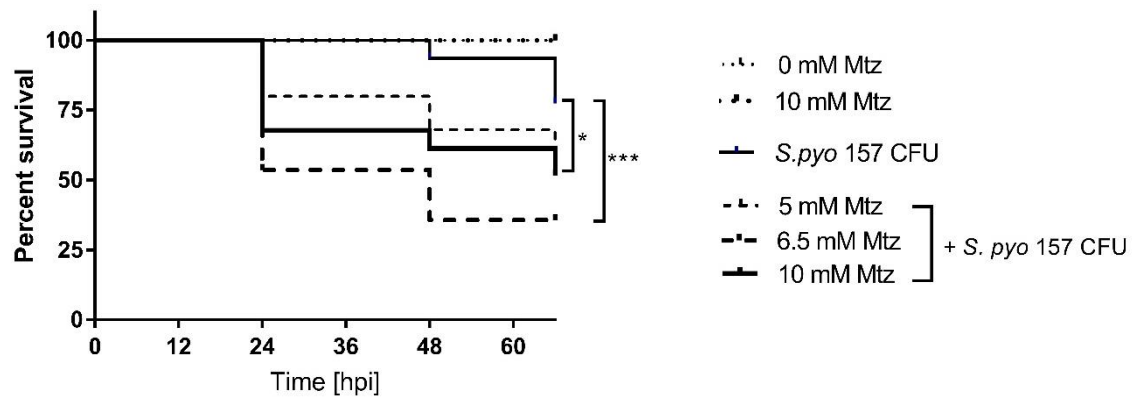


Figure 4.13 Metronidazole renders zebrafish embryos more susceptible to infection regardless of NTR expression

Survival rate curves of LWT larvae using various concentrations of Mtz, and injecting with 157 CFU of *S. pyogenes* H293. $p=0.0157$ (*) and $p<0.0001$ (***) . The 0 and 10 mM control lines overlap, showing 100% survival.

4.4 Discussion

Zebrafish up to 5 dpf, only have a functional innate immune response, and this isolation allows for an interrogation of the innate immune system without any adaptive response. A number of reports have suggested that the action of the innate immune system is more important than that of the adaptive for *S. pyogenes* infection. Macrophage ablation results in a significantly higher mortality as well as bacterial dissemination in hosts (Goldmann et al., 2004, Mishalian et al., 2011). On the other hand, *S. pyogenes* showed a similar mortality in mice with depleted B cells and T cells, when compared to their respective immunocompetent control (Medina et al., 2001). In order to examine if the same response occurs in the zebrafish embryos too, as well as to elucidate the role of specific phagocyte types during infection, microscopy and several knock-down techniques were employed in this chapter.

To begin with, the use of transgenic zebrafish lines, with fluorescently labelled macrophages or neutrophils, demonstrated that both macrophages and neutrophils are able to phagocytose *S. pyogenes* during infection. Fish injected with labelled bacteria and imaged at different time-points showed that as early as 0.5 hpi, most of the bacteria had been phagocytosed, but by 6-8 hpi, phagocytes had been saturated with bacteria, and there was a significant increase in extracellular *S. pyogenes*. By 12 hpi, the fish that would be overwhelmed, were already at a terminal stage. This data implies *S. pyogenes* intracellular growth or at least survival within phagocytes, provided that colocalisation is linked to successful phagocytosis.

S. pyogenes has been shown to survive in human macrophages (Thulin et al., 2006, O'Neil et al., 2016), epithelial cells (Marouni and Sela, 2004), and endothelial cells (Amelung et al., 2011). However, the majority of these studies were carried out using *emm1* strains. Specifically, O'Neil et al demonstrated intracellular replication of *S. pyogenes emm1* strains within macrophages (O'Neil et al., 2016). *S. pyogenes* has also been shown to persist in mouse neutrophils (Medina et al., 2003), and within epithelial cells for days (Kaplan et al., 2006). Regardless, many strains are unable to grow intracellularly, and it has been suggested that antibacterial autophagy could be a means to eradicate *S. pyogenes* from the host (Kaur et al., 2010; Sakurai et al., 2010; Amelung et al., 2011). Macrophages were additionally indicated as the primary reservoir of viable *S. pyogenes*, as a study found high bacterial numbers in spite of antibiotic treatment intravenously (Thulin et al., 2006). Further evidence implicated the *S. pyogenes* M1 surface protein in making *S. pyogenes* resistant against fusion with macrophage enzymolytic vesicles (Staali et al., 2006; Hertzén et al., 2010). The role of macrophages, potentially serving as a reservoir in *S. pyogenes* infection, is explored in the next Chapter.

In order to further analyse the role of specific phagocyte cell types, knock-down techniques have been employed in infection models, to look at the effect of phagocytes on host survival. In *S. aureus*, use of *pu.1* and *irf8* morpholinos, showed that phagocytes, and specifically macrophages (for *irf8*), are very important against the infection (Prajsnar et al., 2008, 2012). In this study, this was also observed. A *pu.1* morpholino was used to knock-down the entire myeloid cell lineage

(macrophages and neutrophils) (Nasevicius and Ekker, 2000, Rhodes et al., 2005). This yielded a rapid death of hosts, and at a significantly lower dose, when compared to immunocompetent embryos. Microscopy data also demonstrated that the bacteria had spread and grown at a much larger scale, than in the WT fish, at the same time-point. This data suggests that phagocytes are paramount in controlling invading pathogens in the bloodstream. However, this technique did not address whether or not a specific phagocyte type is more important in conferring a higher resistance against *S. pyogenes*. Using a dually-labelled mCherry-macrophage/GFP-neutrophils line, it was observed that, albeit both phagocytes being able to phagocytose bacteria, macrophages were more efficient at it, when examining the bloodstream.

irf8 knock-down fish, develop all of their potential macrophages into neutrophils, effectively depleting the host of any macrophages (Li et al., 2011, Nguyen-Chi et al., 2017). This resulted in a reduction in survival compared to WT hosts, but not as dramatic as the removal of *pu.1*. This suggested that the presence of macrophages is a major defence factor during infection. Additionally, it showed that neutrophils by themselves, are not able to mount an effective response, even when they are present in higher numbers than those in WT fish.

L-clodronate injections were used to achieve macrophage-specific ablation in embryos (van Rooijen and Hendrikx, 2010, Nguyen-Chi et al., 2017). These

liposomes were naturally phagocytosed by macrophages, broken down, and the clodronate initiates apoptosis. Microscopy data showed that ablation was effective. Macrophage-depleted embryos were hypersusceptible to *S. pyogenes*. This confirmed that macrophage action is very important during infection.

Using the prodrug metronidazole (Mtz) to treat neutrophil NTR-expressing zebrafish, produces a neutrophil depleted line (Curado et al., 2007, Hall et al., 2009). This experiment tested the importance of neutrophils. The results showed that despite the absence of neutrophils resulting in a significantly lower survival of hosts, it did not produce the observed 0% survival that PU.1 ablation yielded.

There are many studies that support this finding, suggesting that macrophages can engulf bacteria with significantly greater efficacy in fluid-filled environments, ie. the bloodstream, than neutrophils that barely do so (Le Guyader et al., 2008, Colucci-Guyon et al., 2011, Prajsnar et al., 2012). To take it a step further, Colucci-Guyon and colleagues, suggested that macrophages are very efficient phagocytes regardless of how the microbes are being presented, unlike neutrophils that are more effective against surface-associated bacteria.

Chapter 5: Elucidation of population dynamics during *S. pyogenes* infection and the role of augmenting material

5.1 Introduction

The work presented in this Chapter sought to interrogate the bottleneck phenomenon exerted by the zebrafish immune system in response to *S. pyogenes*, as well as investigate the potential effect commensals might have on infection. To that end, a co-infection of differently fluorescently tagged, but otherwise isogenic, *emm89* strains was carried out, monitored and documented. Different ratios of pathogenic and non-pathogenic bacteria or their cell wall components, were also injected in embryos in order to determine the impact of commensals on *S. pyogenes* infection. More specifically, *M. luteus*, and *M. luteus* and *S. aureus* peptidoglycan were examined.

5.2 Aims of this chapter

1. Assess the bottleneck effect on *S. pyogenes* infection.
2. Test the effect of live commensals or their cell wall peptidoglycan on *emm89* infection.

5.3 Results

5.3.1 Population dynamics during the *S. pyogenes* infection

The same two H293 strains, containing pMV158-GFP and pMV158-mCherry, used for microscopy in Chapter 4 were also used here. This ensured that genetic background would not be one of the contributing factors during the bottleneck. LWT zebrafish embryos were injected with an initially designed 1:1 ratio of each of the two isogenic *emm89* strains (pMV158-GFP, pMV158-mCherry) in the circulation valley at a dose of 2717 CFU resulting in a 31% survival (Figure 5.1A). At 20 hpi, 9 fish were chosen, homogenised, and plated on THY plates. CFU counts permitted the quantification of the distribution of GFP and mCherry strains that comprised the final *S. pyogenes* population that overwhelmed the fish (Figure 5.1C). However, it was observed that a number of bacteria had lost their fluorescence in both the doses check stage and when plating the homogenised embryos.

As can be seen in Figure 5.1B, despite the fact that the GFP and mCherry *emm89* cultures were prepared to have a very similar OD₆₀₀, mCherry bacteria (1394 CFU) were almost three times the amount of GFP (516 CFU). Moreover, there were bacteria with no fluorescence (808 CFU), at a number 1.5 times greater than that of the GFP colonies. Both the original doses and the homogenised larvae were plated on THY media. The bacteria were distinguished from one another by checking for fluorescence under a stereomicroscope. At 20 hours after bacterial challenge, 9 fish

were picked, and their bacterial load and population ratios were analysed. In fish 1 to 3, no bacteria could be seen at 4x under the microscope, and the fish had a strong heartbeat as well as no signs of any lesions. These three fish had small bacterial loads: 160, 1600, 4200 CFU respectively. Fish 5 to 9 had no heartbeat, and clearly formed lesions, implying their terminal stage of infection. Fish 4 had CFU almost as high as fish 5 to 9, but instead had a strong heartbeat, and no lesions were visible (3×10^4 CFU).

Despite the mCherry:GFP ratio being almost 3:1 in the co-inoculum, in the four live fish (fish 1-4), the output population of *S. pyogenes* was not always symmetrically distributed (Figure 5.1C). Fish 1 had no unmarked colonies and the mCherry were almost twice the number of GFP colonies. On the contrary, fish 2, had no mCherry colonies, but instead was dominated by GFP bacteria. Fish 4 had no GFP colonies, and a close to 2:1 ratio of mCherry to unmarked colonies. For the hosts that had succumbed (fish 5-9), the three populations were evenly spread, with bacterial numbers being between 8.8×10^4 and 1.66×10^5 CFU.

Unfortunately, fish 1-4 had too low of a bacterial load to allow for direct observation *in vivo* via fluorescence. Fish 5-9 were imaged just before being homogenised (Figure 5.2). There were many lesions throughout the larvae indicating the late progression of the infection. In a few cases, there were lesions that were formed by only one strain (Figure 5.2C'), whereas in others, there were lesions that were

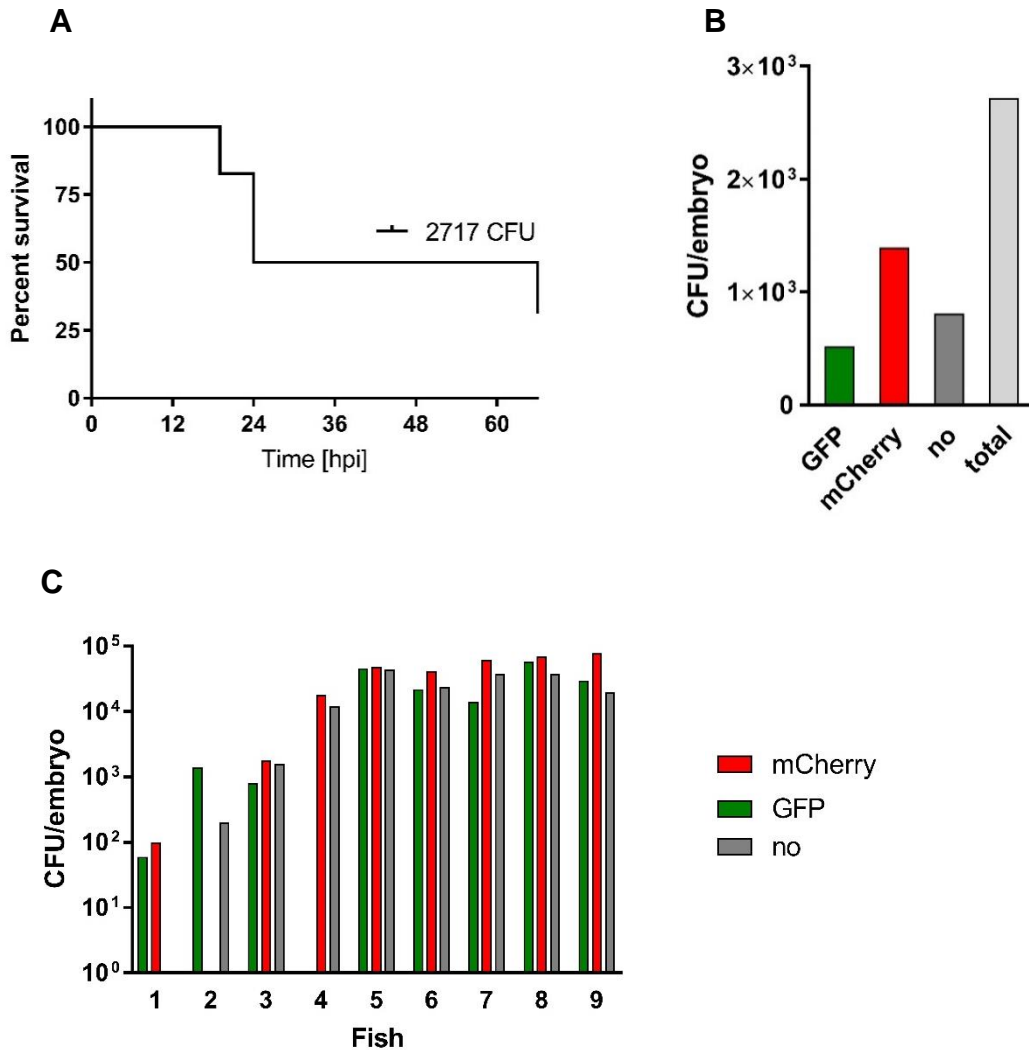


Figure 5.1 *S. pyogenes* population dynamics reveal polyclonality

A,B)Survival of LWT zebrafish upon infection with 2717 CFU of a mixture of pMV158-GFP and pMV158-mCherry *S. pyogenes emm89* (n=58) **(A)**, and their CFU dose ratios **(B)**.

C)Distribution of GFP, mCherry, and non-fluorescent bacteria counted after homogenising 9 collected embryos. The bacteria were plated on THY media and counted under a fluorescence stereomicroscope.

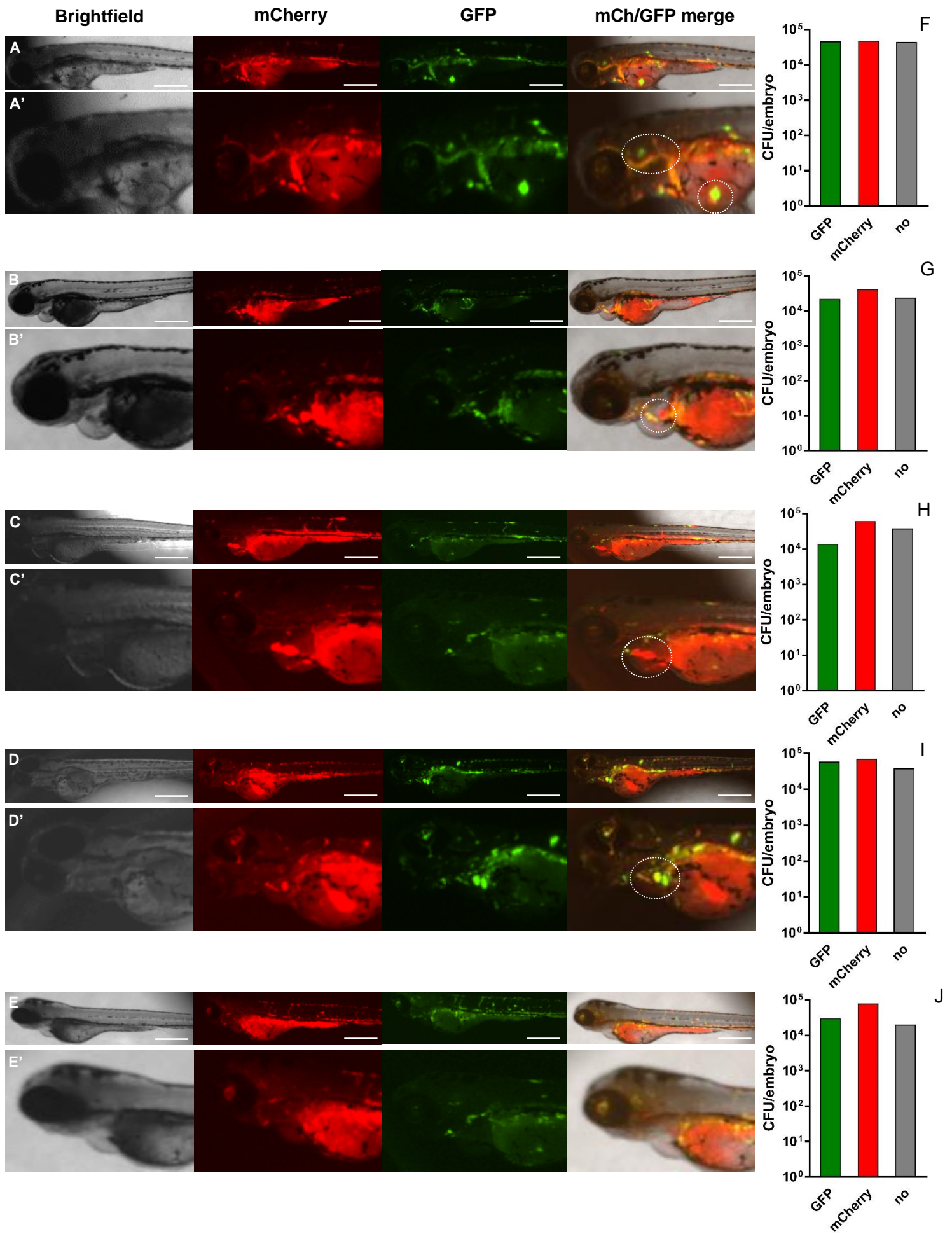


Figure 5.2 Visualisation of *S. pyogenes* population dynamics

A-E) *In vivo* images of fish 5-9 from Figure 5.1C that succumbed to infection (20 hpi), after being inoculated with 2717 CFU of a 3:1 mixture of mCherry- to GFP-labelled *S. pyogenes emm89*. Images were captured using a Nikon custom widefield microscope at 4x, with brightfield, mCherry, GFP, and merged views shown. Scale bars represent 500µm.

F-J) Bar charts showing CFU counts retrieved from the 5 selected fish.

were created by two strains that were colocalised (Figure 5.2A'), or a combination of the two within an individual host (Figure 5.2D').

5.3.2 Does the augmentation phenomenon occur during *S. pyogenes* infection?

5.3.2.1 The effect of the skin commensal *M. luteus* on *S. pyogenes* infection

As mentioned in the Chapter 1, previous work by Boldock and colleagues, established a phenomenon called augmentation in which the presence of a avirulent bacterium can enhance the virulence of a pathogen (Boldock et al., 2018). This presented an opportunity to explore the breadth of this phenomenon to other pathogens. One of the initial hypotheses of this observed enhanced virulence, was that by adding a second organism, the phagocytes would be pushed to their limit and be overwhelmed. This would exert less pressure on the pathogen, being at numbers smaller than the commensal, which would be free to colonise, grow and employ its virulence factors. This hypothesis was disproved by showing that the presence of latex beads, although being successfully phagocytosed, did not augment *S. aureus* pathogenesis, even with a dose as high as 9000 beads (Boldock et al., 2018).

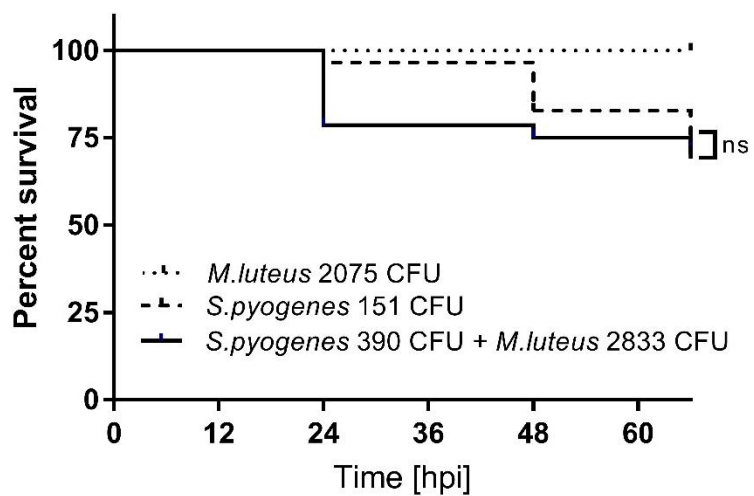


Figure 5.3 Skin commensal *M. luteus* has no effect on *S. pyogenes* infection.

Survival of LWT zebrafish larvae injected with *M. luteus* (2075 CFU), a low dose of *S. pyogenes* H293 (151 CFU) or a combination (2833 and 390 CFU respectively) (n=25-30). This figure is a representative of three repeats.

In order to assess whether this augmentation phenomenon can occur during an *S. pyogenes* infection, LWT zebrafish embryos were challenged with a combination of a low dose of *S. pyogenes* H293 and *M. luteus*. Given the fact that *S. pyogenes* can gain entry from skin breakage, *M. luteus* was used as it is a commensal that is part of the skin milieu (Davis C.P., 1996). *M. luteus* injected at 2075 CFU in zebrafish embryos yielded 100% survival (Figure 5.3). The low dose of *S. pyogenes* H293 at 151 CFU yielded 69% survival, whereas the co-inoculum of 390 CFU of H293 and 2833 CFU *M. luteus* resulted in 71% survival. There was no statistical significance between the two latter groups.

5.3.2.3 Elucidation of the role of cell wall peptidoglycan in augmentation of *S. pyogenes* infection

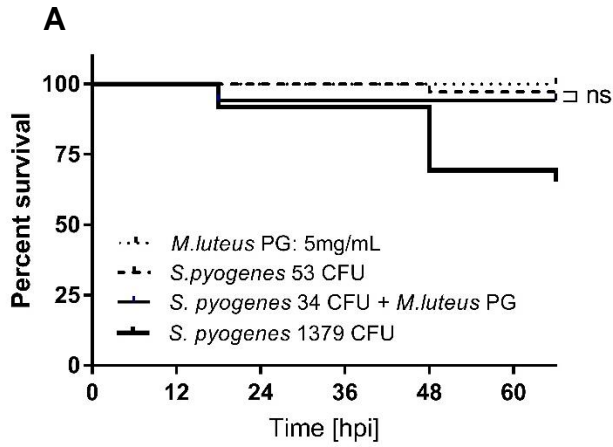
5.3.2.3.1 Effect of *M. luteus* peptidoglycan on *S. pyogenes* infection

Although, live *M. luteus* was unable to elicit the augmentation effect when co-injected with *S. pyogenes*, in order to further examine the potential for augmentation another approach was taken. Boldock et al (2018) showed that isolated cell wall peptidoglycan from a number of Gram-positive bacteria, including *M. luteus*, was able to augment *S. aureus* infection.

Peptidoglycan (PG) is the major component of the cell wall of Gram-positive bacteria. PG has been shown to provide a stimulus for the host immune system and is involved in *S. aureus* pathogenesis (McDonald et al., 2005). In order to explore the potential effect of PG on *S. pyogenes* infection, preparations of purified *M. luteus* and *S. aureus* cell wall peptidoglycan were individually co-inoculated with a number of doses of *S. pyogenes* H293. PG was first stripped of additional components that could also modulate a response of the host, and materials used in this study were provided by Dr Josie Gibson and Mr Josh Sutton. Amounts of PG injected were used as per Boldock et al (2018).

Injecting 25-30 individual zebrafish per group, 5 ng of *M. luteus* peptidoglycan alone, was found to cause no host mortality (Figure 5.4 A). In combination with a low dose of 34 CFU of *S. pyogenes*, it did not trigger a significant decrease in host survival. The same was observed when increasing the pathogen dose to 500 CFU (Figure 5.4 B). At 1200 CFU of *S. pyogenes* mixed with 5 ng *M. luteus* PG, a dramatic increase in host mortality was noted compared to 1200 CFU of the pathogen alone (Figure 5.4 C). Doubling the *M. luteus* PG concentration to 10 ng, was not toxic to the host. When co-injecting 10 ng of *M. luteus* PG with 363 CFU of *S. pyogenes* H293 systemically, a statistically significant drop in survival was seen (Figure 5.4 D). Challenging the hosts with 1260 CFU of *S. pyogenes* and 10 ng *M. luteus* PG, gave a statistically significant decrease in survival compared to bacteria alone.

[PG]= 5 ng



[PG]= 10 ng

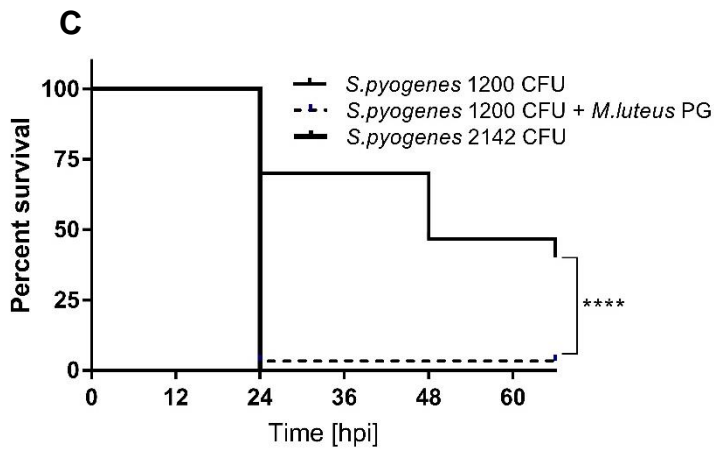
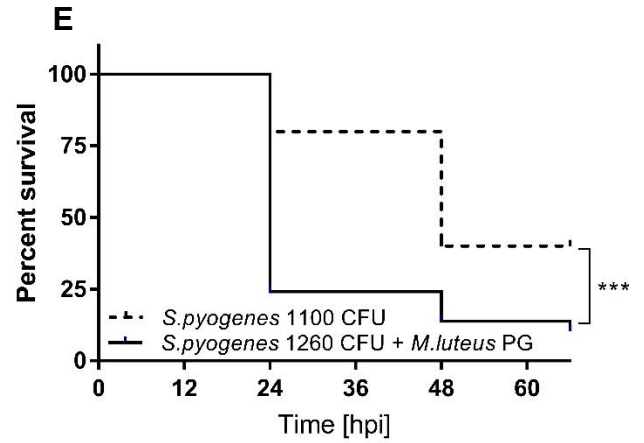
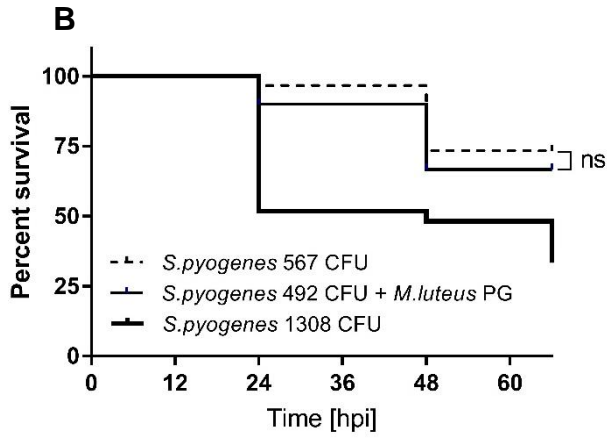
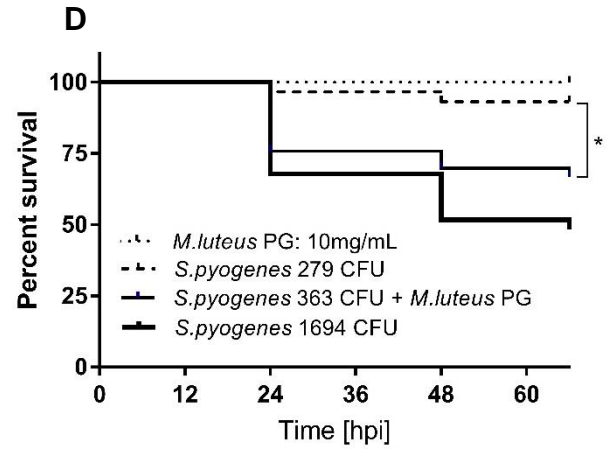


Figure 5.4 Examining the effect of *M. luteus* cell wall peptidoglycan on *S. pyogenes* pathogenesis

M. luteus purified peptidoglycan 5 ng (**A, B, C**) and 10 ng (**D, E**) was co-injected with different doses of *S. pyogenes* H293 as shown, into the zebrafish circulation valley to test for the augmentation phenomenon (n=25-30). (**C**) $p < 0.0001$ (****), (**D**) $p = 0.0111$ (*), (**E**) $p = 0.0002$ (***)).

5.3.2.3.2 Effect of *S. aureus* peptidoglycan on *S. pyogenes* infection

Various doses of *S. pyogenes* H293 and *S. aureus* SH1000 PG were injected into the zebrafish circulation valley to test for the effect of *S. aureus* cell wall peptidoglycan on *S. pyogenes* infection (Figure 5.5). Neither 8 ng nor 16 ng of SH1000 PG injected to the fish yielded any host mortality. Mixed inoculum assays of 8 ng of PG and either 75 or 740 CFU of *S. pyogenes* did not produce any significant differences from infecting the hosts with the pathogen alone (Figure 5.5 A, B). Although there was an increase in mortality with the addition of 16 ng PG into the inoculum, this was not statistically significant (Figure 5.5 C).

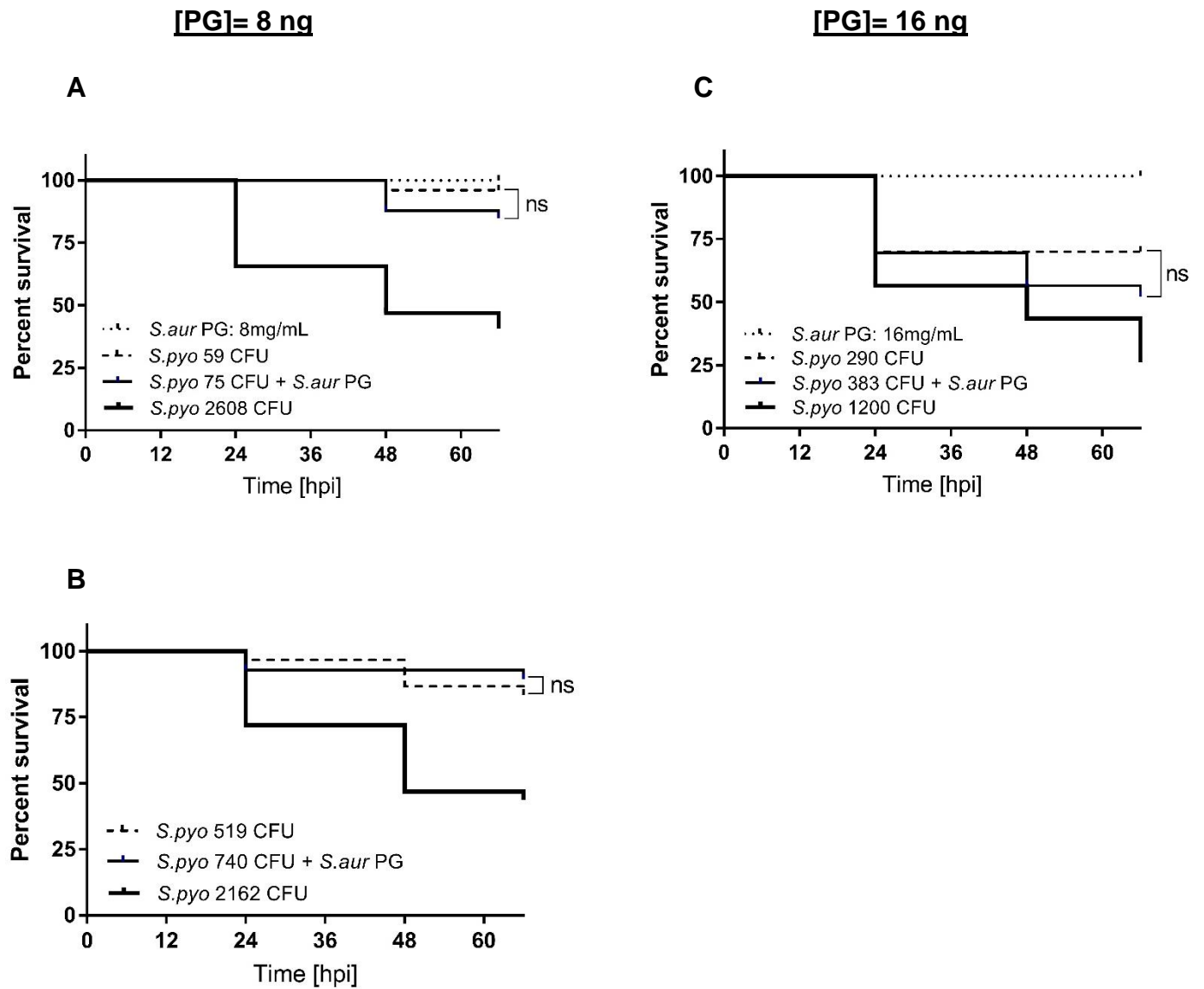


Figure 5.5 *S. aureus* peptidoglycan has no effect on *S. pyogenes* virulence

Testing for the augmentation effect by injecting systemically *S. aureus* SH1000 purified peptidoglycan, 8 ng (**A, B**) and 16 ng (**C**), with *S. pyogenes* H293 (numbers as shown) into zebrafish embryos (n=25-30).

5.3.2.5 *In vivo* zebrafish imaging of *S. pyogenes* co-inoculated with *M. luteus* peptidoglycan

To further investigate any potential immuno-stimulatory role of peptidoglycan, *in vivo* imaging using labelled host macrophages, *S. pyogenes* H293, and *M. luteus* peptidoglycan, was conducted. In order for this experiment to be carried out, the Tg(mpeg1: mCherryCAAX) zebrafish line, with mCherry-labelled macrophages, was used. Three groups of larvae from this line, were injected systemically with 5 ng of *M. luteus* peptidoglycan dyed with AlexaFluor 405 alone, 583 CFU *S. pyogenes* H293 carrying pMV158-GFP alone, and then a mixed inoculum of both 408 CFU of the pathogen and 5 ng of PG. At 0.5, 5.5 and 18.5 hours post bacterial challenge, 5 individual hosts were removed and fixed for imaging. All images were acquired via confocal microscopy.

At 0.5 hpi, albeit, some of the *M. luteus* peptidoglycan could be seen colocalised within macrophages, most of it was not (Figure 5.6). What was observed can be almost described as “a sea” of peptidoglycan. In spite of this experiment being unable to confirm phagocytosis, the shape of PG aggregates that fit the shape of the colocalising macrophage, served as an indirect confirmation. As the fish were fixed, and this was not live imaging, it was not possible to infer if the PG particles were moving or were stuck on surfaces. This excess of peptidoglycan pattern remained throughout all three time-points, including fish that had successfully cleared the infection and were healthy at 66 hpi at the time of culling

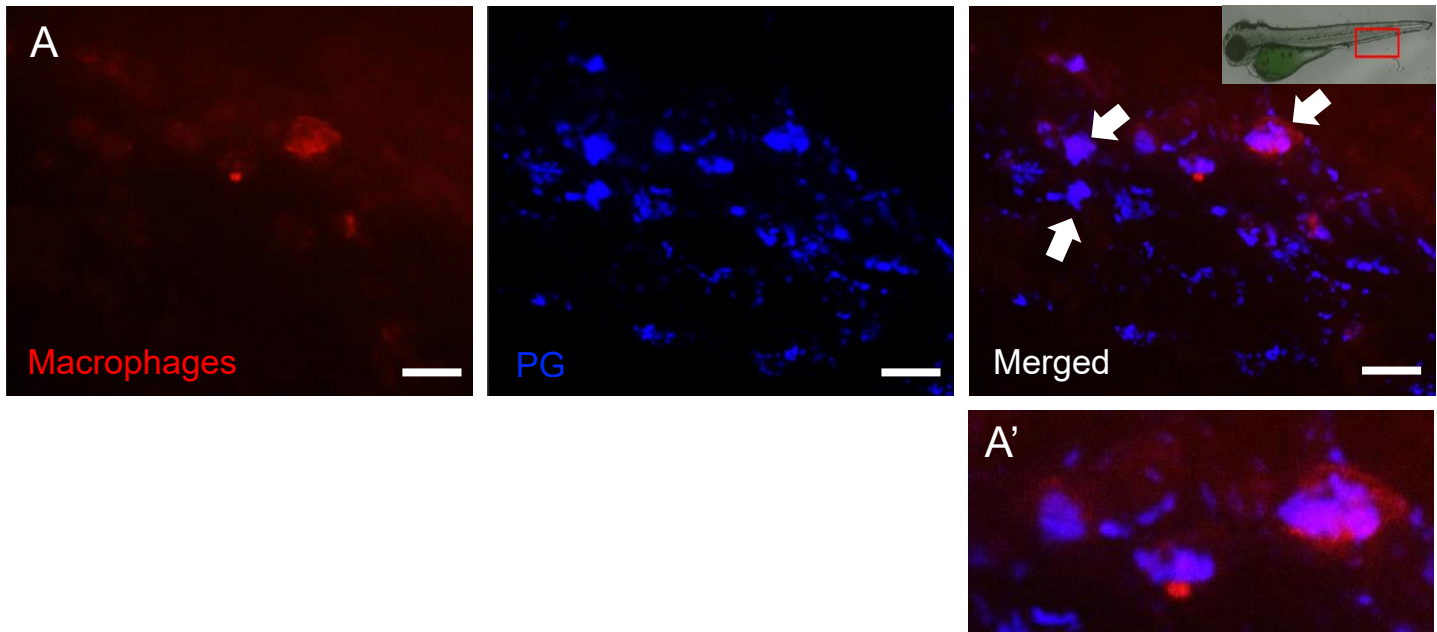


Figure 5.6 Confocal microscopy of labelled *M. luteus* cell wall peptidoglycan in fixed zebrafish embryos

Zebrafish embryos were systemically infected with AlexaFluor 405-labelled *M. luteus* peptidoglycan (5 ng). At 0.5 hpi, five individual hosts were removed and fixed. The image shown here is representative of the five individual hosts. The images were acquired at 40x. The scale bars represent 17 μm . The red box outline on the top, represents the tail area where the imaging took place. **(A')** Blow up of Merged image showing colocalization of macrophages and PG.

(data not shown). In the zebrafish embryos that were co-injected with *S. pyogenes*-GFP and PG, the pattern of excess PG was still observed at 0.5 hpi. *M. luteus* PG, however was found to colocalise with *S. pyogenes* within macrophages, while most of the pathogen was found within the phagocytes (Figure 5.7). At 5.5 hours after challenge, the larvae removed from the ones injected with the mixed inoculum of *S. pyogenes* and PG, had either cleared the infection and barely any bacteria could be seen (Figure 5.8 A) or the bacteria had overcome the host system and had replicated out of control (Figure 5.8 B). The aim of these experiments was to discover whether or not PG colocalised with *S. pyogenes* and macrophages as reported by Boldock et al.

Images from all three groups of embryos at different time-points, were all pooled together into one figure to produce a holistic view of the progression of the infection, taking all the variables into consideration. As shown in Figure 5.9, the distribution and dispersion patterns of PG remain the same regardless of the time-point or the presence of *S. pyogenes*, even at 66 hpi. Most of *S. pyogenes* was phagocytosed by 0.5 hpi, something previously reported in Chapter 4. By 5.5 hours past challenge, the pathogen had either been removed or was on its way to overwhelming the fish while macrophages were still detectable. At 18.5 hpi, the same dichotomy was observed with bacteria either being completely absent or saturating the fish.

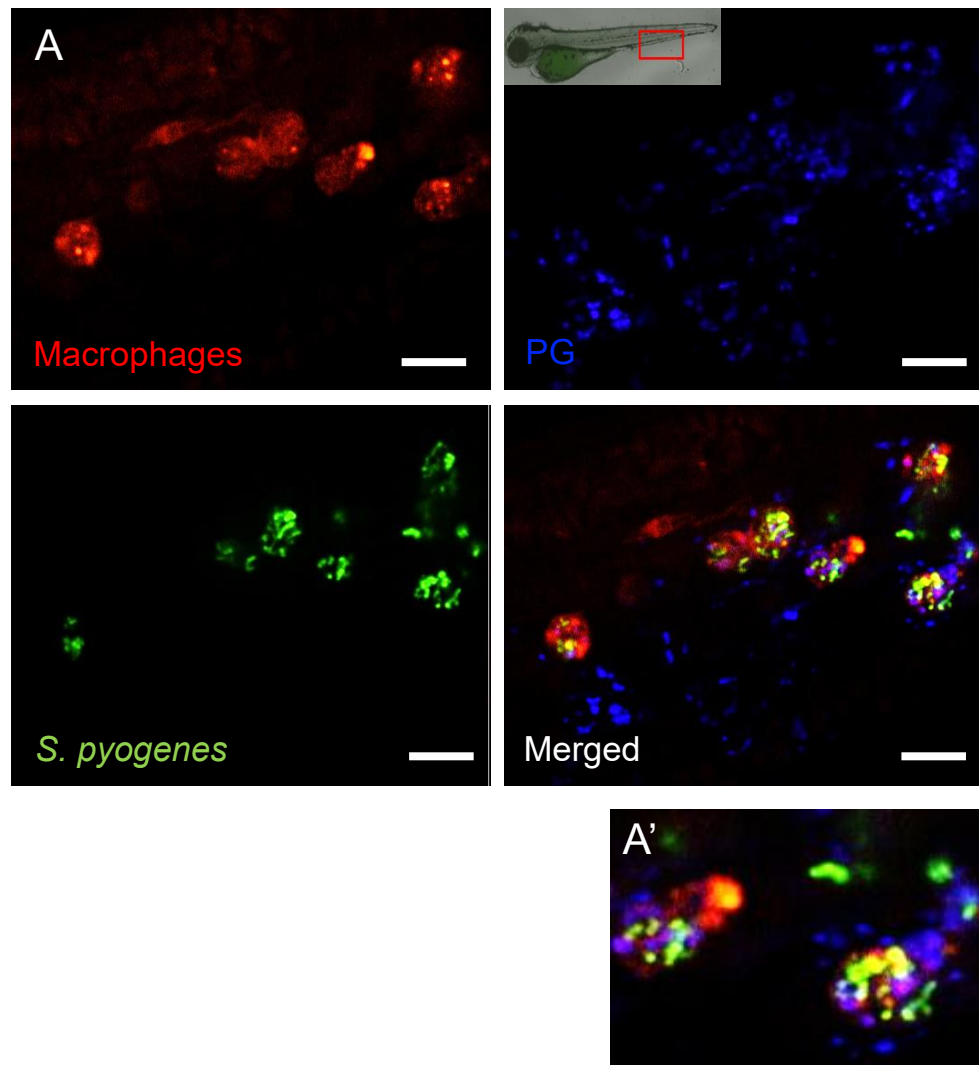


Figure 5.7 *In vivo* microscopy of labelled *M. luteus* peptidoglycan and *S. pyogenes* H293 co-injected in zebrafish larvae

Larvae were challenged with a mixed inoculum of 408 CFU GFP-labelled *S. pyogenes* H293 and AlexaFluor 405(blue)-labelled *M. luteus* purified peptidoglycan (5 ng). At 0.5 hpi, five individual hosts were removed and fixed. Here, one of five fish is shown. The images were acquired at 40x. The scale bars represent 17 μ m. The red box outline on the top, represents the tail area where the imaging took place. **(A')** Enlarged of merged image showing colocalization of macrophages, *S. pyogenes*, and PG.

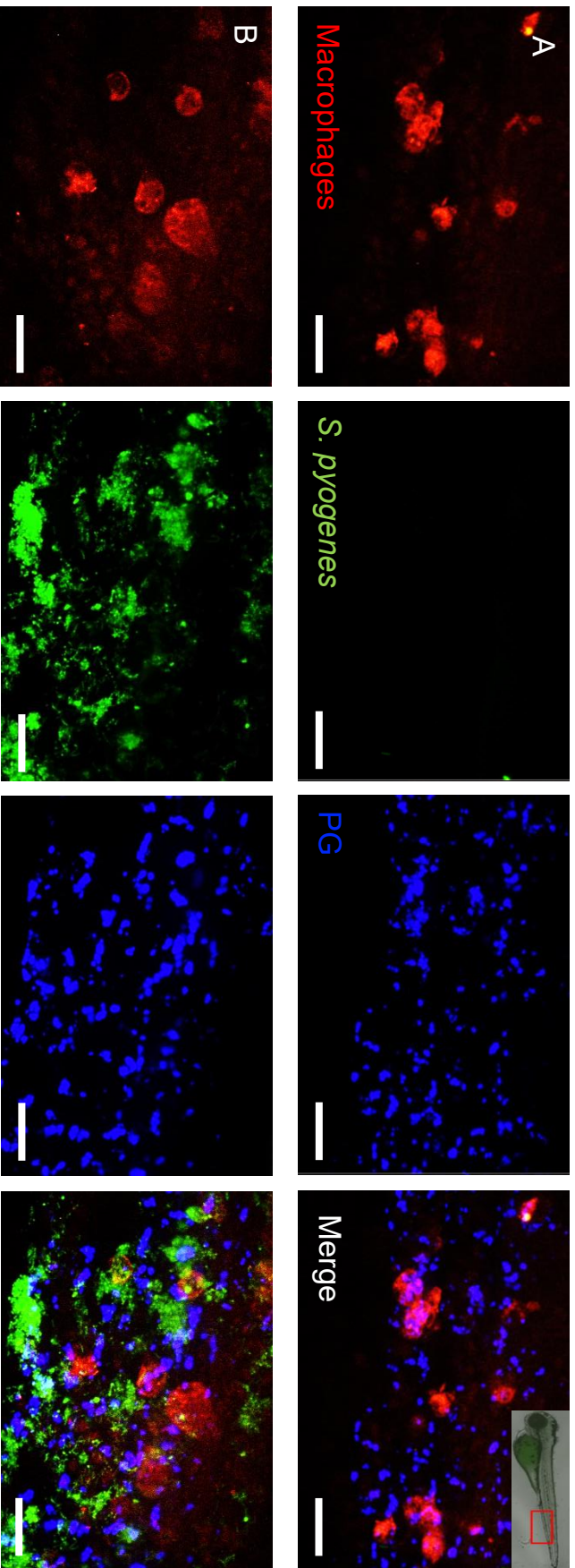


Figure 5.8 Comparative microscopy of overwhelmed and healthy zebrafish embryos after injections with labelled *M. luteus* peptidoglycan and *S. pyogenes*

Hosts were injected with AlexaFluor 405-labelled *M. luteus* peptidoglycan (5 ng) and 408 CFU GFP-labelled *S. pyogenes* H293. At 5.5 hpi, five fish were removed and fixed. Panel A shows a fish that had successfully cleared the infection, whereas panel B represents a fish that was overwhelmed by the infection. The images were acquired at 40x. The scale bars represent 17 μm . The red box outline on the top, represents the tail area were the imaging took place.

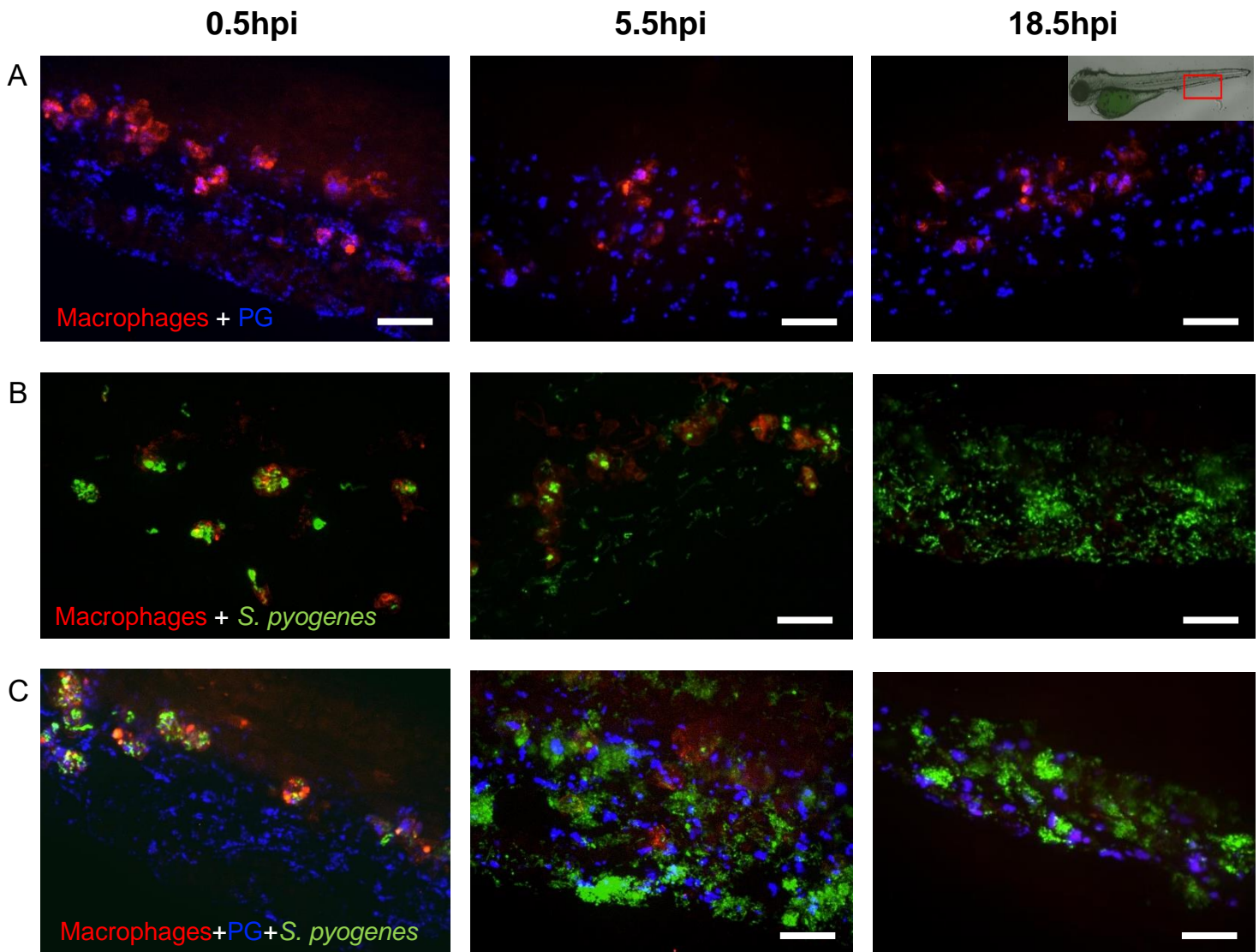


Figure 5.9 Comparative microscopy of zebrafish embryos challenged with a mixed inoculum of *S. pyogenes*-GPF and *M. luteus* peptidoglycan over 0.5, 5.5 and 18.5 hpi

Three groups of embryos were injected systemically at 56 dpf. One group was infected with *M. luteus* cell wall peptidoglycan (5 ng) alone (**A**). The second group was injected with a low dose of GFP-marked *S. pyogenes* H293 (583 CFU) (**B**). The third group was co-injected with both *S. pyogenes* (408 CFU) and 5 ng *M. luteus* peptidoglycan (**C**). At 0.5, 5.5 and 18.5 hpi, five fish were removed, fixed, and subsequently imaged with a spinning disc confocal microscope. Each panel is a different host. The images were acquired at 40x. The scale bars represent 17 μ m. The red box outline on the top, represents the tail area where the imaging took place.

5.4 Discussion

In the *S. aureus* model, in both zebrafish embryos and mice, the infection is monoclonal as individual clones were demonstrated to have formed the abscesses that led to the host being overwhelmed (Prajsnar et al., 2008, McVicker et al., 2014). It was on this premise that this Chapter sought to investigate the clonality of *S. pyogenes* infection. With a 3:1 mCherry:GFP initial dose, the resulting lesions in the fish, showed mixed population ratios at the host terminal stage. A combination of single colour and mixed colour lesions was observed within the same fish, with CFU numbers of the two fluorescent labels being evenly spread in the fish that had succumbed. From the four live fish collected, one of the two labelled strains, was found to be absent from a few fish. This was determined via homogenising and observing CFU numbers under a fluorescent microscope. Taken together, this data suggests that many *S. pyogenes* cells are able to exit the phagocytes, and form lesions, revealing polyclonality. Despite a number of *S. pyogenes* cells losing their plasmid, the question this set of experiments attempted to answer was whether the lesions were founded by one colour or both. As this question was answered regardless of the loss of plasmid, this data constitutes sufficient evidence as a pilot study regarding *S. pyogenes* clonality.

Live *M. luteus*, *M. luteus* and *S. aureus* PG do not augment *S. pyogenes* infection

The second goal of my study was to use *M. luteus* and its purified peptidoglycan, along with *S. aureus* peptidoglycan, to test for the augmentation effect during *S. pyogenes* infection. As previously reported, this effect allows for infectious dose to drop dramatically for *S. aureus*. To that end, low doses of *S. pyogenes* (50 or 500 CFU) were used in combination with live *M. luteus*, *M. luteus* peptidoglycan, or *S. aureus* peptidoglycan. These mixed inocula used low doses of *S. pyogenes*, and 5 ng of *M. luteus* PG as previously described (Boldock et al., 2018). At these doses, no statistically significant increase in mortality was noted. Instead, at the highest *S. pyogenes* dose (1200 CFU), mixed with *M. luteus* PG, a significant decrease in host survival was recorded. Furthermore, the same significant decrease in survival was seen when using twice the PG concentration. This result, as it only occurs at high doses of *S. pyogenes* and other material, is probably due to overwhelming of the phagocytes. In support of a simpler swamping of the phagocytosing capacity of the immune system, it was observed that although PG could be successfully taken up by macrophages at large doses, PG could be seen both inside and outside the cells. Despite a number of *S. pyogenes* bacteria losing their fluorescent label, these experiments still allowed for the visualisation of any potential interactions between phagocytes, pathogen, and peptidoglycan.

Chapter 6: General Discussion

6.1 Introduction

S. pyogenes manifests primarily as minor infections, either associated with the throat or the skin (Carapetis et al., 2005). In the less frequent cases when it develops into a severe invasive infection, treating it is complicated, and the infection often proves fatal. Currently, there is no vaccine available. Although, numerous studies have begun to break down and characterise *S. pyogenes* infections, much is still unknown. For that reason, the development of additional infection models, would likely help further our understanding of *S. pyogenes* infection.

My project has established the zebrafish embryo model as a relatively high-throughput and rapid method of investigating *S. pyogenes* infection. The three *S. pyogenes* strains H293 (*emm89*), H305 (*emm1*), and HSC5 (*emm14*) were initially explored, with the first being chosen due to its amenability to study. Monitoring the H293 bacterial burden *in vivo* over time, revealed the presence of a bottleneck until 8 hpi, after which there was a bifurcation of zebrafish hosts; one group that demonstrated rapid bacterial proliferation and host mortality and one in which a decline in bacterial load was seen. Macrophage depletion showed that this 8-hour bottleneck, was immunological as also seen in the *S. aureus* model (Prajsnar et al., 2012). Real-time visualisation via microscopy of host-pathogen interactions revealed bacterial uptake early on, in potentially greater number by macrophages rather than neutrophils, while by 8 hpi macrophages were found saturated with

bacteria. Population dynamics analysis showed that *S. pyogenes* infection is polyclonal as lesions were founded by many different bacterial cells. Moreover, live commensals, or their cell wall peptidoglycan, were co-injected with *S. pyogenes* in order to investigate the presence of the augmentation effect. This effect was not observed. All in all, this now established model can add to existing animal models, on the way to understanding *S. pyogenes* infection. It can act as a platform to test and refine hypotheses before moving on to a murine, or other host.

One of the shortcomings of this study that needs to be addressed is the loss of the pMV158 plasmid, tagging *S. pyogenes* cells fluorescently, by a number of bacteria. More specifically, Figure 5.1 showed that about a third of the infectious dose, for the population dynamics experiment, lacked any fluorescence. To begin with, these bacteria need to be grown and plated always in the presence of antibiotic, something not carried out in this study. Another idea that could be explored could be the chromosomal integration of the fluorescent tags, or a choice of plasmid previously used in *S. pyogenes* that is known to not be so easily lost. Future experiments require to additionally test for any effects the presence of the plasmid might have on growth or virulence of these new strains when compared to their wild type equivalents. With that being said, much of the data of this study relied on work using these plasmids. Most of the experiments sought to elucidate the basic interactions between phagocytes, pathogen, and augmented material in a heavily qualitative manner, which somewhat addresses this shortcoming. The one experiment that quantified the observed difference in phagocytosis efficiency between macrophages

and neutrophils, *S. pyogenes* was instead labelled with an AlexaFluor dye (Chapter 5).

6.2 Setting up the model

One of the biggest issues when investigating *S. pyogenes* infections is choosing a strain to work with. There are many different *S. pyogenes* strains, and many of them have been characterised to exhibit tissue tropisms, which alludes to differences in the virulence factors deployed during infection (Bessen and Lizano, 2010). Most studies examine *emm1* isolates, as it is the single most successful and widespread type. For my study, three strains were used; H293 (*emm89*), H305 (*emm1*), and HSC5 (*emm14*). They were selected on the premise of prevalence and clinical relevance (*emm89*, *emm1*), as well as being extensively used in zebrafish studies (*emm14*).

6.3 Describing the *S. pyogenes* infection dynamics

S. pyogenes H293, at a dose of about 1500 CFU injected at 2 dpf, yields approximately 50% survival after 3 days. In the case of HSC5, 50% survival was seen at 500 CFU, while H305 showed the highest virulence with 70 CFU resulting in 25% survival. What is interesting, however, is that for H293, bacterial growth was restricted by the host until almost 8 hpi, but at 20 hpi, that was no longer the case. Two distinct host populations formed, with a 10^4 difference in bacterial load. Those

with high bacterial loads were associated with mortality. H293 was subsequently chosen for further studies, due to its amenability to study as well as clinical relevance (Chapters 4, 5). H293 is amenable to studying pathogenesis in the zebrafish embryo model, given the nature of the time window available during fish development.

6.4 Phagocytes mediate a temporary bottleneck during infection

In order to discover the nature of the host-associated bacterial growth restriction (bottleneck), microscopy was used. Data indicated that phagocytes had taken up most of the bacteria as early as 0.5 hpi, with very few if any extracellular bacteria visible. By 6 hpi macrophages completely saturated with bacteria were observed, with the load being almost as big as the cell itself. This would suggest subsequent lysis of the macrophages, and release of live *S. pyogenes*, which matches what was observed at 8 hpi. The pathogen could then disseminate and form multiple lesions, eventually overwhelming the host. Depleting phagocytes, resulted in a dramatically faster host survival drop, and microscopy demonstrated that bacteria were much more spread, when compared to the control. Taken together, this data further suggests that the bottleneck described above, is an immunological one, driven by phagocytes.

6.5 *S. pyogenes* can replicate inside phagocytes

It is apparent that the phagocytes are able to temporarily control *S. pyogenes* growth. Fluorescence images also suggest that the bacterial numbers, within the macrophages, increase over time. Albeit, this study not being able to assess if this increase came from intracellular growth or from continued phagocytosis, it was shown that *S. pyogenes* is able to not only persist, but also replicate within macrophages (Hertzén et al., 2010, O'Neil et al., 2016), neutrophils (Medina et al., 2003), and pharyngeal epithelial cells (Osterlund et al., 1997). However, there is no previous evidence of this in zebrafish macrophages.

Despite the fact that many previous studies worked with *emm1* type *S. pyogenes* strains, there was one that reported that the H293 *emm89*-type strain, could replicate within HeLa cells (Thurston et al., 2009). Another group, investigating severe invasive *S. pyogenes* soft tissue infections, reported macrophages to act as the primary reservoir for viable intracellular *S. pyogenes*, even during antibiotic treatment of the patient. This “trojan horse” approach has also been described for *Streptococcus iniae* (Zlotkin et al., 2003), and *S. aureus* (Gresham et al., 2000). Hence, although phagocytes provide protection of the host against pathogens, they can also be used as a shelter to ensure the survival of the pathogen, that eventually emerges to overwhelm the host. While, *S. pyogenes* has been described to use phagocytes as a reservoir to withstand assault (Thulin et al., 2006), this was not observed in the systemic infection zebrafish embryo model, as it was in the model for *S. aureus*.

6.6 Pathogen population dynamics reveal polyclonality

In the case that the events occurring inside the phagocytes, favour the pathogen, *S. pyogenes* replicates, gets released, and begins forming lesions. In a mixed infection using the same H293 strain with different fluorescent labels, no clonality was observed, as the lesions formed were of mixed colours. Given the nature of this bottleneck, and how adept *S. pyogenes* is at combating the phagocytes, this results in a polyclonal infection.

6.7 Augmenting material does not affect *S. pyogenes* infection

Some *S. pyogenes* infections occur within a polymicrobial environment that is the microbiome. It was therefore tested if other microbes, and their constituent components might alter host-pathogen dynamics. To this end, the effect of different types of peptidoglycan and live *M. luteus* were used to try and emulate the natural instance as much as possible. This choice of augmenting material was reported to increase the mortality of fish, when mixed with an *S. aureus* dose that does not produce such pathogenicity alone (Boldock et al., 2018). Unlike in *S. aureus* however, none of the aforementioned material was able to augment *S. pyogenes* infection. Pathogenesis of *S. pyogenes* was formally augmented by peptidoglycan, but this seems due to overwhelming the immune system rather than a more specific process, as was discovered in *S. aureus*. This highlights differences in the cellular interactions during *S. pyogenes* and *S. aureus* infection. *S. pyogenes* is only held

back by the phagocytes with no clonal expansion ensuing. This suggests that the treatment and outcome of the pathogens by phagocytes is different as the pathogens have different means of infecting.

6.8 *S. pyogenes* infection model hypothesis

Other infection models in zebrafish embryos, have reported bottlenecks before, including *S. enterica*, *Borellia* species, *S. aureus*, *E. faecalis* (Grant et al., 2008, Prajsnar et al., 2012, Prajsnar et al., 2013, Rego et al., 2014). It is hence clear that the bottleneck effect will appear with any immunocompetent host. The following question then is, what kind of bottleneck occurs for each pathogen.

Zebrafish mortality data shows that this is the order of how successfully these strains cause infection: *S. pyogenes* H305 (*emm1*)>*S. pyogenes* HSC5 (*emm14*)>*S. pyogenes* H293 (*emm89*). Only H293 had a distinct bottleneck, whereas for the two first strains no bottleneck was observed at the time-points used. For H293, *S. aureus*, and *E. faecalis*, the population bottleneck within the host is phagocyte-associated (Prajsnar et al., 2012, 2013). The molecular interactions which control this process are unknown for all three species. My study allows me to propose a model for *S. pyogenes* infection dynamics, and to give comparison with other species.

Despite a number of zebrafish embryo studies having been reported, including for *Burkholderia cenocepacia* and *Pseudomonas aeruginosa* (Brannon et al., 2009, Vergunst et al., 2010), their infectious doses and resulting mortality have not been connected to their respective bacterial *in vivo* kinetics and phagocyte behaviour. As a result, I will use the *S. aureus* model for comparison. In *S. aureus*, a dose of 1200 CFU in 1 day old fish results in 50% host mortality after 4 days (Prajsnar et al., 2008). Phagocytes restrict bacterial growth until almost 48 hpi, at which time-point there were two distinct host populations with a 10^3 difference in bacterial load. These higher bacterial numbers were associated with the fish succumbing to infection.

The hypothesis that I suggest here is that the fate of the host is determined within the phagocytes, while the presence of extracellular *S. pyogenes* also exerts additional pressure on the immune system (Figure 6.1). The greater the number of bacteria overcoming the defences of their phagocytes, and managing to replicate intracellularly, the greater the number of extracellular *S. pyogenes* will be to form lesions. Eventually, the amount of extracellular *S. pyogenes* will overwhelm the host.

6.9 Future directions

The effect of neutrophil ablation during *S. pyogenes* infection

Although my study employed techniques to ablate macrophages to investigate the role of phagocytes against *S. pyogenes* infection, ablation of neutrophils was not successful. The prodrug Metronidazole can be used in conjunction with a transgenic

fish line, that has a cell type genetically tagged, to break the prodrug down, into a toxic chemical that will ablate the targeted cell type. This approach was used, as seen in Chapter 4, but it also rendered wildtype more susceptible to infection. An alternative would be to use morpholinos to knock-down the colony-stimulating factor 3 receptor (CSF3R), and its two cytokine ligands coded by *csf3a* and *csf3b*, to reduce neutrophil numbers in zebrafish embryos (Pazhakh et al., 2017). CSF3, also known as the granulocyte colony-stimulating factor (GCSF), is a regulator vital to neutrophil development.

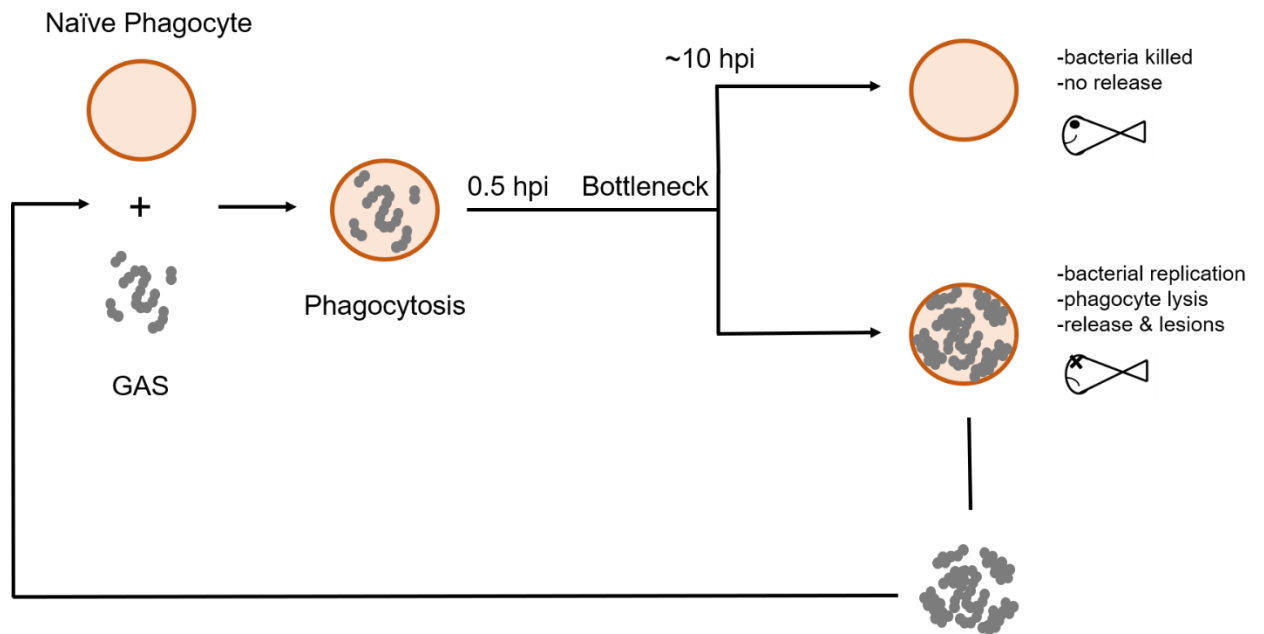


Figure 6.1 Diagram of the *S. pyogenes* systemic model of infection

A conceptual model of the *S. pyogenes* infection based on the results of *S. pyogenes* H293. *S. pyogenes* is phagocytosed within 0.5 hpi. At about 10 hpi, the bottleneck is resolved, and the bacterial numbers begin to alter from the infectious dose. At 24 hpi (75% survival), and until the end of the experiment (66 hpi - 50% survival), two very distinct host populations can be seen in terms of bacterial load. The group with the high bacterial numbers, with the bacteria that managed to pass through the bottleneck, has succumbed. In contrast, the other group has successfully cleared the infection.

Analysis of the host response to *S. pyogenes*

As described in Chapter 1, MyD88 has been found to be required for the host to mount an effective phagocyte-mediated inflammatory response to *S. pyogenes*, and further phagocyte recruitment (Loof et al., 2008, 2010). Levels of TNF, IL-6, IL-12, and type I interferons (IFNs) were significantly lower in mice lacking MyD88 (Gratz et al., 2008, 2011; Loof et al., 2008, 2010). This was shown to render the neutrophils unable to migrate to the site of infection, and make the host more susceptible to *S. pyogenes* infection. Reduced amounts of TNF α were also suggested to be associated with reduced macrophage recruitment (Mishalian et al., 2011). Regardless of MyD88 being reported to be involved in the defence against *S. pyogenes*, and a study showing that TLR2 and TLR13 are not redundant *in vivo*, it is still not clear which human TLRs are deployed (Fieber et al., 2015). This is because although TLR2 is a highly conserved receptor in vertebrates, TLR13 is only present in mice and rats, making them naturally resistant to *S. pyogenes*. Therefore, future experiments would be to interrogate the role of host factors in disease. The *myd88* gene has been successfully identified in zebrafish and disrupted by a loss-of-function morpholino (Meijer et al., 2004, 2005, van der Sar et al., 2006).

Analysis of *S. pyogenes* virulence factors and their interaction with the host

SpeB is considered one of the major *S. pyogenes* virulence factors and has been reported to be secreted by most invasive disease clinical isolates (Olsen et al., 2015, Laabei and Ermert, 2018). It was demonstrated to be able to degrade the C3 component of the complement system, and resist neutrophil killing, with additional complement targets being reported (Kuo et al., 2008, Terao et al., 2008, Honda-

Ogawa et al., 2013). Therefore, combinatorial studies, of *speB* mutants and morpholino knock-down fish of complement components, could be used following this study to elucidate host-pathogen interactions. Other *S. pyogenes* virulence factors that interfere with complement, that could be explored are fibronectin-binding protein Sfb1/PrtF1 (surface bound), ScpA (secreted) and GAPDH (secreted) (Terao et al., 2006, Hyland et al., 2007). Sfb1/PrtF1 was found to decrease C3b deposition, whereas both ScpA and GAPDH degrade C5a.

In vivo infection dynamics

My studies have revealed a complex cellular interaction between *S. pyogenes* and the host. In order to further elucidate this interplay, it is important to follow this in real time. Only the zebrafish embryo model permits this by virtue of the transparent nature of the host, and the ability to visualise bacteria during infection. The light sheet microscope (Amich et al., 2019) allows determination of real-time interactions throughout infection using labelled host and bacterial cells. By studying the phagocytes that control, or do not control, *S. pyogenes*, it will be possible to begin to determine this crucial break point. In the future, unravelling mechanisms of successful host control of pathogens will allow their manipulation as adjuncts to conventional approaches to the prophylaxis and treatment of infectious disease.

Chapter 7: References

Abbot, E.L., Smith, W.D., Siou, G.P., Chiriboga, C., Smith, R.J., Wilson, J.A., et al. (2007). Pili mediate specific adhesion of *Streptococcus pyogenes* to human tonsil and skin. *Cellular Microbiology* 9, 1822-1833.

Adderson, E.E., Shikhman, A.R., Ward, K.E. and Cunningham, M.W. (1998). Molecular analysis of polyreactive monoclonal antibodies from rheumatic carditis: human anti-N-acetylglucosamine/anti-myosin antibody V region genes. *Journal of Immunology* 161, 2020-2031.

Aidley, J., Rajopadhye, S., Akinyemi, N.M., Lango-Scholey, L., Jones, M.A. and Bayliss, C.D. (2017). Nonselective bottlenecks control the divergence and diversification of phase-variable bacterial populations. *MBio* 8, e02311-2316.

Akira, S. and Takeda, K. (2004). Toll-like receptor signalling. *Nature Reviews Immunology* 4, 499-511.

Akira, S., Uematsu, S. and Takeuchi, O. (2006). Pathogen recognition and innate immunity. *Cell* 124, 783-801.

Alam, F.M., Turner, C.E., Smith, K., Wiles, S. and Sriskandan, S. (2013). Inactivation of the CovR/S virulence regulator impairs infection in an improved murine model of *Streptococcus pyogenes* naso-pharyngeal infection. *PLoS One* 8, e61655.

Albertí, S., Ashbaugh, C.D. and Wessels, M.R. (1998). Structure of the *has* operon promoter and regulation of hyaluronic acid capsule expression in group A *Streptococcus*. *Molecular Microbiology* 28, 343-353.

Amelung, S., Nerlich, A., Rohde, M., Spellerberg, B., Cole, J.N., Nizet, V., Chhatwal, G.S. and Talay, S.R. (2011). The FbaB-type fibronectin-binding protein of *Streptococcus pyogenes* promotes specific invasion into endothelial cells. *Cellular Microbiology* 13, 1200-1211.

Amich, J., Mokhtari, Z., Strobel, M., Vialetto, E., Kalleda, N., Jarick, K.J., Brede, C., Jordán-Garrote, A.-L., Thusek, S., Schmiedgen, K., et al. (2019). 3D light sheet fluorescence microscopy of lungs to dissect local host immune - *Aspergillus fumigatus* interactions. *mBio* 11, e02752-27519.

Arango Duque, G. and Descoteaux, A. (2014). Macrophage cytokines: involvement in immunity and infectious diseases. *Frontiers in Immunology* 5, 491.

Ashbaugh, C.D., Alberti, S. and Wessels, M.R. (1998). Molecular analysis of the capsule gene region of group A *Streptococcus*: the *hasAB* genes are sufficient for capsule expression. *Journal of Bacteriology* 180, 4955-4959.

Ashbaugh, C.D., Moser, T.J., Shearer, M.H., White, G.L., Kennedy, R.C. and Wessels, M.R. (2000). Bacterial determinants of persistent throat colonization and the associated immune response in a primate model of human group A streptococcal pharyngeal infection. *Cellular Microbiology* 2, 283-292.

Aziz, R.K., Pabst, M.J., Jeng, A., Kansal, R., Low, D.E., Nizet, V. and Kotb, M. (2003). Invasive M1T1 group A *Streptococcus* undergoes a phase-shift in vivo to prevent proteolytic degradation of multiple virulence factors by SpeB. *Molecular Microbiology* 51, 123-134.

Aziz, R.K., Pabst, M.J., Jeng, A., Kansal, R., Low, D.E., Nizet, V., et al. (2004). Invasive M1T1 group A *Streptococcus* undergoes a phase-shift in vivo to prevent proteolytic degradation of multiple virulence factors by SpeB. *Molecular Microbiology* 51, 123-134.

Aziz, R.K., Edwards, R.A., Taylor, W.W., Low, D.E., McGeer, A. and Kotb, M. (2005). Mosaic prophages with horizontally acquired genes account for the emergence and diversification of the globally disseminated M1T1 clone of *Streptococcus pyogenes*. *Journal of Bacteriology* 187, 3311-3318.

Aziz, R.K. and Kotb, M. (2008). Rise and persistence of global M1T1 clone of *Streptococcus pyogenes*. *Emerging Infectious Diseases* 14, 1511-1517.

Babior, B.M. (2000). Phagocytes and oxidative stress. *The American Journal of Medicine* 109, 33-44.

Banks, D., Porcella, S., Barbian, K., Beres, S., Philips, L., Voyich, J., DeLeo, F., Martin, J., Somerville, G. and Musser, J. (2004). Progress toward characterization of the group A *Streptococcus* metagenome: complete genome sequence of a macrolide-resistant serotype M6 strain. *The Journal of Infectious Diseases* 190, 727-738.

Bao, Y., Liang, Z., Booyjzen, C., Mayfield, J., Li, Y., Lee, S., Ploplis, V., Song, H. and Castellino, F. (2014). Unique genomic arrangements in an invasive serotype M23 strain of *Streptococcus pyogenes* identify genes that induce hypervirulence. *Journal of Bacteriology* 196, 4089-4102.

Bao, Y., Liang, Z., Mayfield, J., Donahue, D., Carothers, K., Lee, S., Ploplis, V. and Castellino, F. (2016). Genomic characterization of a pattern D *Streptococcus pyogenes* *emm53* isolate reveals a genetic rationale for invasive skin tropicity. *Journal of Bacteriology* 198, 1712-1724.

Barbalat, R., Lau, L., Locksley, R.M. and Barton, G.M. (2009). Toll-like receptor 2 on inflammatory monocytes induces type I interferon in response to viral but not bacterial ligands. *Nature Immunology* 10, 1200-1207.

Baruch, M., Belotserkovsky, I., Hertzog, B.B., Ravins, M., Dov, E., McIver, K.S., Le Breton, Y.S., Zhou, Y., Cheng, C.Y., Chen, C.Y., et al. (2014). An extracellular bacterial pathogen modulates host metabolism to regulate its own sensing and proliferation. *Cell* 156, 97-108.

Beall, B., Facklam, R., Hoenes, T. and Schwartz, B. (1997). Survey of *emm* gene sequences and T-antigen types from systemic *Streptococcus pyogenes* infection isolates collected in San Francisco, California; Atlanta, Georgia; and Connecticut in 1994 and 1995. *Journal of Clinical Microbiology* 35, 1231-1235.

Benard, E.L., van der Sar, A.M., Ellett, F., Lieschke, G.J., Spaink, H.P. and Meijer, A.H. (2012). Infection of zebrafish embryos with intracellular bacterial pathogens. *Journal of Visualized Experiments* 61, 3781.

Benavides, F., Oberyszyn, T.M., VanBuskirk, A.M., Reeve, V.E. and Kusewitt, D.F. (2009). The hairless mouse in skin research. *Journal of Dermatological Science* 53, 10-18.

Bensi, G., Mora, M., Tuscano, G., Biagini, M., Chiarot, E., Bombaci, M., Capo, S., Falugi, F., Manetti, A. G. O., Donato, P., et al. (2012). Multi high-throughput approach for highly selective identification of vaccine candidates: the Group A *Streptococcus* case. *Molecular & Cellular Proteomics* 11, M111.015693.

Beres, S.B. and Musser, J.M. (2007). Contribution of exogenous genetic elements to the group A *Streptococcus* metagenome. *PLoS One* 2, e800.

Berggard, K., Johnsson, E., Morfeldt, E., Persson, J., Stalhammar-Carlemalm, M. and Lindahl, G. (2001). Binding of human C4BP to the hypervariable region of M protein: a molecular mechanism of phagocytosis resistance in *Streptococcus pyogenes*. *Molecular Microbiology* 42, 539-551.

Bessen, D.E. (2009). Population biology of the human restricted pathogen, *Streptococcus pyogenes*. *Infection, Genetic and Evolution* 9, 581-593.

Bessen, D.E. (2016). Tissue tropisms in group A *Streptococcus*. *Current Opinion in Infectious Diseases* 29, 295-303.

Bessen, D. and Fischetti, V.A. (1988). Influence of intranasal immunization with synthetic peptides corresponding to conserved epitopes of M protein on mucosal colonization by group A streptococci. *Infection and Immunity* 56, 2666-2672.

Bessen, D.E. and Kalia, A. (2002). Genomic localization of a T serotype locus to a recombinatorial zone encoding extracellular matrix-binding proteins in *Streptococcus pyogenes*. *Infection and Immunity* 70, 1159-1167.

Bessen, D.E. and Lizano, S. (2010). Tissue tropisms in group A streptococcal infections. *Future Microbiology* 5, 623-638.

Bessen, D.E., McGregor, K. F. and Whatmore, A. M. (2008). Relationships between *emm* and multilocus sequence types within a global collection of *Streptococcus pyogenes*. *BMC Microbiology* 8, 59.

Bhakdi, S., Tranum-Jensen, J. and Sziegoleit, A. (1985). Mechanism of membrane damage by streptolysin-O. *Infection and Immunity*, 47, 52-60.

Bisno, A L. and Stevens, D.L. (1996). Streptococcal infections of skin and soft tissues. *The New England Journal of Medicine* 334, 240-246.

Bober, M., Morgelin, M., Olin, A.I., von Pawel-Rammingen, U. and Collin, M. (2011). The membrane bound LRR lipoprotein Slr, and the cell wall-anchored M1 protein from *Streptococcus pyogenes* both interact with type I collagen. *PLoS One* 6, e20345.

Bogaert, D., van Belkum, A., Sluijter, M., Luijendijk, A., de Groot, R., Rümke, H., Verbrugh, H. and Hermans, P. (2004). Colonisation by *Streptococcus pneumoniae* and *Staphylococcus aureus* in healthy children. *The Lancet*, 363, 1871-1872.

Boldock, E., Surewaard, B. G. J., Shamarina, D., Na, M., Fei, Y., Ali, A., Williams, A., Pollitt, E.J.G., Szkuta, P., Morris, P., et al. (2018). Human skin commensals augment *Staphylococcus aureus* pathogenesis. *Nature Microbiology* 3, 881-890.

Bolm, M., Jansen, W.T.M., Schnabel, R., and Chhatwal, G.S. (2004). Hydrogen peroxide-mediated killing of *Caenorhabditis elegans*: a common feature of different streptococcal species. *Infection and Immunity* 72, 1192-1194.

Boucontet, L., Passoni, G., Thiry, V., Maggi, L., Herbomel, P., Levraud, J.-P. and Colucci-Guyon, E. (2018). A model of superinfection of virus-infected zebrafish larvae: increased susceptibility to bacteria associated with neutrophil death. *Frontiers in Immunology* 9, 1084.

Brannon, M.K., Davis, J.M., Mathias, J.R., et al. (2009). *Pseudomonas aeruginosa* Type III secretion system interacts with phagocytes to modulate systemic infection of zebrafish embryos. *Cellular Microbiology* 11, 755-768.

Brenot, A., King, K., Janowiak, B., Griffith, O. and Caparon, M. (2003). Contribution of glutathione peroxidase to the virulence of *Streptococcus pyogenes*. *Infection and Immunity* 72, 408-413.

Brouwer, S., Cork, A. J., Ong, C.-L. Y., Barnett, T. C., West, N. P., Mciver, K. S. and Walker, M. J. (2018). Endopeptidase PepO regulates the SpeB cysteine protease and is essential for the virulence of invasive M1T1 *Streptococcus pyogenes*. *Journal of Bacteriology* 200, e00654-17.

Brouwer, S., Lacey, J.A., You, Y., Davies, M.R. and Walker, M.J. (2019). Scarlet fever changes its spots. *The Lancet Infectious Diseases* 19, 1154-1155.

Buchan, K., Prajsnar, T., Ogryzko, N., de Jong, N., van Gent, M., Kolata, J., Foster, S., van Strijp, J. and Renshaw, S. (2019). A transgenic zebrafish line for in vivo visualisation of neutrophil myeloperoxidase. *PLoS One* 14, e0215592.

Buchanan, J.T., Simpson, A.J., Aziz, R.K., Liu, G.Y., Kristian, S.A., Kotb, M., et al. DNase expression allows the pathogen group A *Streptococcus* to escape killing in neutrophil extracellular traps. *Current Biology* 16, 396-400.

Burrus, V. and Waldor, M.K. (2004). Shaping bacterial genomes with integrative and conjugative elements. *Research in Microbiology* 155, 376-386.

Carapetis, J.R., Steer, A.C., Mulholland, E.K. and Weber, M. (2005). The global burden of group A streptococcal diseases. *The Lancet Infectious Diseases* 5, 685-694.

Carlsson, F., Sandin, C. and Lindahl, G. (2005). Human fibrinogen bound to *Streptococcus pyogenes* M protein inhibits complement deposition via the classical pathway. *Molecular Microbiology* 56, 28-39.

Carroll, R.K. and Musser, J.M. (2011). From transcription to activation: how group A *Streptococcus*, the flesh-eating pathogen, regulates SpeB cysteine protease production. *Molecular Microbiology* 81, 588-601.

Chang, J.C., LaSarre, B., Jimenez, J.C., Aggarwal, C. and Federle, M.J. (2011). Two group A streptococcal peptide pheromones act through opposing Rgg regulators to control biofilm development. *PLoS Pathogens* 7, e1002190.

Chatellier, S., Ihendyane, N., Kansal, R.G., Khambaty, F., Basma, H., Norrby-Teglund, A., Low, D.E., McGeer, A. and Kotb, M. (2000). Genetic relatedness and superantigen expression in Group A *Streptococcus* serotype M1 isolates from patients with severe and nonsevere invasive diseases. *Infection and Immunity* 68, 3523-3534.

Chaussee, M.S., Ajdic, D. and Ferretti, J.J. (1999). The *rgg* gene of *Streptococcus pyogenes* NZ131 positively influences extracellular SPE B production. *Infection and Immunity* 67, 1715-1722.

Chaussee, M.A., Callegari, E.A. and Chaussee, M.S. (2004). Rgg regulates growth phase-dependent expression of proteins associated with secondary metabolism and stress in *Streptococcus pyogenes*. *Journal of Bacteriology* 186, 7091-7099.

Chaussee, M.S., Somerville, G.A., Reitzer, L. and Musser, J.M. (2003). Rgg coordinates virulence factor synthesis and metabolism in *Streptococcus pyogenes*. *Journal of Bacteriology* 185, 6016-6024.

Chaussee, M.S., Sylva, G.L., Sturdevant, D.E., Smoot, L.M., Graham, M.R., Watson, R. O., et al. (2002). Rgg influences the expression of multiple regulatory loci to coregulate virulence factor expression in *Streptococcus pyogenes*. *Infection and Immunity* 70, 762-770.

Clatworthy, A.E., Lee, J.S., Leibman, M., Kostun, Z., Davidson, A.J. and Hung, D.T. (2009). *Pseudomonas aeruginosa* infection of zebrafish involves both host and pathogen determinants. *Infection and Immunity* 77, 1293-1303.

Cleary, P.P., LaPenta, D., Vessela, R., Lam, H. and Cue, D. (1998). A globally disseminated M1 subclone of group A streptococci differs from other subclones by 70 kilobases of prophage DNA and capacity for high-frequency intracellular invasion. *Infection and Immunity* 66, 5592-5597.

Cogen, A., Nizet, V. and Gallo, R. (2008). Skin microbiota: a source of disease or defence? *British Journal of Dermatology* 158, 442-455.

Cole, J.N., Aziz, R.K., Kuipers, K., Timmer, A.M., Nizet, V. and van Sorge, N.M. (2012). A conserved UDP-glucose dehydrogenase encoded outside the *hasABC* operon contributes to capsule biogenesis in group A *Streptococcus*. *Journal of Bacteriology* 194, 6154-6161.

Cole, J.N., Barnett, T.C., Nizet, V. and Walker, M.J. (2011). Molecular insight into invasive group A streptococcal disease. *Nature Reviews Microbiology* 9, 724-736.

Cole, J.N., McArthur, J.D., McKay, F.C., Sanderson-Smith, M.L., Cork, A.J., Ranson, M., Rohde, M., Itzek, A., Sun, H., Ginsburg, D., et al. (2006). Trigger for group A streptococcal M1T1 invasive disease. *FASEB Journal* 20, 1745-1747.

Cole, J.N., Pence, M.A., von Kockritz-Blickwede, M., Hollands, A., Gallo, R.L., Walker, M.J., et al. (2010). M protein and hyaluronic acid capsule are essential for in vivo selection of *covRS* mutations characteristic of invasive serotype M1T1 group A *Streptococcus*. *Mbio* 1, e00191-210.

Collin, M and Olsén, A. (2001). EndoS, a novel secreted protein from *Streptococcus pyogenes* with endoglycosidase activity on human IgG. *EMBO Journal* 20, 3046-3055.

Collin, M. and Olsen, A. (2001b). Effect of SpeB and EndoS from *Streptococcus pyogenes* on human immunoglobulins. *Infection and Immunity* 69, 7187-7189.

Collin, M., Svensson, M. D., Sjöholm, A. G., Jensenius, J. C., Sjöbring, U. and Olsen, A. (2002). EndoS and SpeB from *Streptococcus pyogenes* Inhibit Immunoglobulin-Mediated Opsonophagocytosis. *Infection and Immunity* 70, 6646-6651.

Colucci-Guyon, E., Tinevez, J.-Y., Renshaw, S. A. and Herbomel, P. (2011). Strategies of professional phagocytes in vivo: unlike macrophages, neutrophils engulf only surface-associated microbes. *Journal of Cell Science* 124, 3053-3059.

Csencsits, K.L., Jutila, M.A. and Pascual, D.W. (1999). Nasal-associated lymphoid tissue: phenotypic and functional evidence for the primary role of peripheral node addressin in naive lymphocyte adhesion to high endothelial venules in a mucosal site. *The Journal of Immunology* 163, 1382-1389.

Cue, D., Dombek, P.E., Lam, H. and Cleary, P.P. (1998). *Streptococcus pyogenes* serotype M1 encodes multiple pathways for entry into human epithelial cells. *Infection and Immunity* 66, 4593-4601.

Cunningham, M.W. (2000). Pathogenesis of group A streptococcal infections. *Clinical Microbiology Reviews* 13, 470-511.

Cunningham, M.W. (2014). Rheumatic fever, autoimmunity, and molecular mimicry: The streptococcal connection. *International Reviews of Immunology* 33, 314-329.

Cunningham, M.W. (2016). Post-streptococcal autoimmune sequelae: rheumatic fever and beyond. In *Streptococcus pyogenes: basic biology to clinical manifestations*. Ferretti, J.J., Stevens, D.L., Fischetti, V.A., eds. (Oklahoma City, OK: University of Oklahoma Health Sciences Center).

Cywes, C. and Wessels, M.R. (2001). Group A *Streptococcus* tissue invasion by CD44-mediated cell signalling. *Nature* 414, 648-652.

Dale, J.B., Penfound, T.A., Tamboura, B., Sow, S.O., Nataro, J.P., Tapia, M. and Kotloff, K.L. (2013). Potential coverage of a multivalent M protein-based group A streptococcal vaccine. *Vaccine* 31, 1576-1581.

Dale, J.B. and Beachey, E.H. (1985). Epitopes of streptococcal M proteins shared with cardiac myosin. *Journal of Experimental Medicine* 162, 583-591.

Dale, J.B., Washburn, R.G., Marques and M.B., Wessels, M.R. (1996). Hyaluronate capsule and surface M protein in resistance to opsonization of group A streptococci. *Infection and Immunity* 64, 1495-1501.

Dalton, T.L. and Scott, J.R. (2004). CovS inactivates CovR and is required for growth under conditions of general stress in *Streptococcus pyogenes*. *Journal of Bacteriology* 186, 3928–3937.

Davies, M.R., Holden, M.T., Coupland, P., Chen, J.H.K., Venturini, C., Barnett, T.C., Zakour, N.L.B., Tse, H., Dougan, G., and Yuen, K.-Y., et al. (2015). Emergence of scarlet fever *Streptococcus pyogenes emm12* clones in Hong Kong is associated with toxin acquisition and multidrug resistance. *Nature Genetics* 47, 84-87.

Davis, C.P. (1996). Normal flora. In *medical microbiology*, 4th, S. Baron, ed(s). (Galveston: University of Texas Medical Branch).

Davis, J.M., Clay, H., Lewis, J.L., Ghori, N., Herbomel, P. and Ramakrishnan, L. (2002). Real-time visualization of mycobacterium-macrophage interactions leading to initiation of granuloma formation in zebrafish embryos. *Immunity* 17, 693-702.

Deng, Y., Boon, C., Eberl, L. and Zhang, L.H. (2009). Differential modulation of *Burkholderia cenocepacia* virulence and energy metabolism by the quorum-sensing signal BDSF and its synthase. *Journal of Bacteriology* 191, 7270-7278.

Dileepan, T., Linehan, J.L., Moon, J.J., Pepper, M., Jenkins, M.K. and Cleary, P.P. (2011). Robust antigen specific th17 T cell response to group A *Streptococcus* is Dependent on IL-6 and intranasal route of infection. *PLoS Pathog* 7, e1002252.

Dinkla, K., Rohde, M., Jansen, W.T.M., Carapetis, J.R., Chhatwal, G.S. and Talay, S.R. (2003). *Streptococcus pyogenes* recruits collagen via surface-bound fibronectin: a novel colonization and immune evasion mechanism. *Molecular Microbiology* 47, 861-869.

Dmitriev, A.V., McDowell, E.J., Kappeler, K.V., Chaussee, M.A., Rieck, L.D. and Chaussee, M.S. (2006). The Rgg regulator of *Streptococcus pyogenes* influences utilization of nonglucose carbohydrates, prophage induction, and expression of the NAD-glycohydrolase virulence operon. *Journal of Bacteriology* 188, 7230-7241.

Dombek, P.E., Cue, D., Sedgewick, J., Lam, H., Ruschkowski, S., Finlay, B.B. and Cleary, P.P. (1999). High-frequency intracellular invasion of epithelial cells by serotype M1 group A streptococci: M1 protein-mediated invasion and cytoskeletal rearrangements. *Molecular Microbiology* 31, 859-870.

Dunkelberger, J.R. and Song, W.C. (2010). Complement and its role in innate and adaptive immune responses. *Cell Research* 20, 34-50.

Edwards, R.J., Taylor, G.W., Ferguson, M., Murray, S., Rendell, N., Wrigley, A., Bai, Z., Boyle, J., Finney, S.J., Jones, A., et al. (2005). Specific C-terminal cleavage and inactivation of interleukin-8 by invasive disease isolates of *Streptococcus pyogenes*. *The Journal Infectious Diseases* 192, 783-790.

Egesten, A., Olin, A.I., Linge, H.M., Yadav, M., Morgelin, M., Karlsson, A. and Collin, M. (2009). SpeB of *Streptococcus pyogenes* differentially modulates antibacterial and receptor activating properties of human chemokines. *PLoS One* 4, e4769.

Ehrengruber, M.U., Geiser, T. and Deranleau, D.A. (1994). Activation of human neutrophils by C3a and C5A. Comparison of the effects on shape changes, chemotaxis, secretion, and respiratory burst. *FEBS Letters* 346, 181-184.

Elek, S.D. and Conen, P.E. (1957). The virulence of *Staphylococcus pyogenes* for man; a study of the problems of wound infection. *British Journal of Experimental Pathology* 38, 573-586.

Engleberg, N.C., Heath, A., Miller, A., Rivera, C. and DiRita, V.J. (2001). Spontaneous mutations in the CsrRS two-component regulatory system of *Streptococcus pyogenes* result in enhanced virulence in a murine model of skin and soft tissue infection. *The Journal of Infectious Diseases* 183, 1043-1054.

Engleberg, N.C., Heath, A., Vardaman, K. and DiRita, V.J. (2004). Contribution of CsrR-regulated virulence factors to the progress and outcome of murine skin infections by *Streptococcus pyogenes*. *Infection and Immunity* 72, 623-628.

Facklam, R. (2002). What happened to the Streptococci: overview of taxonomic and nomenclature changes. *Clinical Microbiology Reviews* 15, 613-630.

Federle, M. (2012). Pathogenic *streptococci* speak, but what are they saying? *Virulence* 3, 92-94.

Feil, S.C., Ascher, D.B., Kuiper, M.J., Tweten, R.K. and Parker, M.W. (2014). Structural studies of *Streptococcus pyogenes* streptolysin O provide insights into the early steps of membrane penetration. *Journal of Molecular Biology* 426, 785-792.

Fernie-King, B.A., Seilly, D.J., Willers, C., Würzner, R., Davies, A. and Lachmann, P.J. (2001). Streptococcal inhibitor of complement (SIC) inhibits the membrane attack complex by preventing uptake of C5b7 onto cell membranes. *Immunology* 103, 390-398.

Ferretti, J., McShan, W., Ajdic, D., Savic, D., Savic, G., Lyon, K., Primeaux, C., Sezate, S., Suvorov, A., Kenton, S., Lai, H., Lin, S., Qian, Y., Jia, H., Najjar, F., Ren, Q., Zhu, H., Song, L., White, J., Yuan, X., Clifton, S., Roe, B. and McLaughlin, R. (2001). Complete genome sequence of an M1 strain of *Streptococcus pyogenes*, *Proceedings of the National Academy of Science of the United States of America* 98, 4658-4663.

Fieber, C. and Kovarik, P. (2014). Responses of innate immune cells to group A *Streptococcus*. *Frontiers in Cellular and Infection Microbiology* 4, 140.

Fieber, C., Janos, M., Koestler, T., Gratz, N., Li, X.-D., Castiglia, V., Aberle, M., Sauert, M., Wegner, M., Alexopoulou, L., et al. (2015). Innate immune response to *Streptococcus pyogenes* depends on the combined activation of TLR13 and TLR2. *Plos One* 10, e0119727.

Fisher, M., Huang, Y.-S., Li, X., Mciver, K.S., Toukoki, C. and Eichenbaum, Z. (2008). Shr is a broad-spectrum surface receptor that contributes to adherence and virulence in group A *Streptococcus*. *Infection and Immunity* 76, 5006-5015.

Flores, A.R., Sahasrabhojane, P., Saldaña, M., Galloway-Peña, J., Olsen, R.J., Musser, J.M. and Shelburne, S.A. (2014). Molecular characterization of an invasive phenotype of Group A *Streptococcus* arising during human infection using whole genome sequencing of multiple isolates from the same patient. *The Journal of Infectious Diseases* 209, 1520-1523.

Friou, G.J. (1950). Experimental infection of the upper respiratory tract of young chimpanzees with group A hemolytic *Streptococci*. *The Journal of Infectious Diseases* 86, 264-274.

Frost, L.S., Leplae, R., Summers, A.O. and Toussaint, A. (2005). Mobile genetic elements: the agents of open source evolution. *Nature Reviews Microbiology* 3, 722-732.

Futosi, K., Fodor, S. and Mócsai, A. (2013). Neutrophil cell surface receptors and their intracellular signal transduction pathways. *International Immunopharmacology* 17, 638-650.

Galloway-Pena, J., DebRoy, S., Brumlow, C., Li, X., Tran, T. T., Horstmann, N., et al. (2018). Hypervirulent group A *Streptococcus* emergence in an acapsular background is associated with marked remodeling of the bacterial cell surface. *PLoS ONE* 13, e0207897.

Gerlini, A., Colomba, L., Furi, L., Braccini, T., Manso, A.S., Pammolli, A., Wang, B., Vivi, A., Tassini, M., Rooijen, N.V., et al. (2014). The role of host and microbial factors in the pathogenesis of pneumococcal bacteraemia arising from a single bacterial cell bottleneck. *PLoS Pathogens* 10, e1004026.

Gherardi, G., Vitali, L. A. and Creti, R. (2018). Prevalent *emm* types among invasive *S. pyogenes* in Europe and North America since year 2000. *Frontiers in Public Health* 6, 59.

Gogos, A. and Federle, M. (2019). Modeling *Streptococcus pyogenes* pharyngeal colonization in the mouse. *Frontiers in Cellular and Infection Microbiology* 9, 137.

Goldmann, O., Lengeling, A., Böse, J., Bloecker, H., Geffers, R., Chhatwal, G. S. and Medina, E. (2005). The role of the MHC on resistance to Group A *Streptococci* in Mice. *The Journal of Immunology* 175, 3862-3872.

Goldmann, O., Rohde, M., Chhatwal, G. S. and Medina, E. (2004). Role of macrophages in host resistance to Group A *Streptococci*. *Infection and Immunity* 72, 2956-2963.

Graham, M.R., Smoot, L.M., Migliaccio, C.A.L., Virtaneva, K., Sturdevant, D.E., Porcella, S.F., Federle, M.J., Adams, G.J., Scott, J.R. and Musser, J.M. (2002). Virulence control in group A *Streptococcus* by a two-component gene regulatory system: global expression profiling and in vivo infection modeling. *Proceedings of the National Academy of Sciences of the United States of America* 99, 13855-13860.

Grant, A.J., Restif, O., McKinley, T.J., Sheppard, M., Maskell, D.J. and Mastroeni, P. (2008). Modelling within-host spatiotemporal dynamics of invasive bacterial disease. *PLoS Biology* 6, e74.

Gratz, N., Hartweiger, H., Matt, U., Kratochvill, F., Janos, M., Sigel, S., Drobits, B., Li, X.-D., Knapp, S. and Kovarik, P. (2011). Type I interferon production induced by *Streptococcus pyogenes*-derived nucleic acids is required for host protection. *PLoS Pathogens* 7, e1001345.

Gratz, N., Siller, M., Schaljo, B., Pirzada, Z. A., Gattermeier, I., Vojtek, I., Kirschning, C. J., Wagner, H., Akira, S., Charpentier, E., et al. (2008). Group A *Streptococcus* activates type I interferon production and MyD88-dependent signaling without involvement of TLR2, TLR4, and TLR9. *The Journal of Biological Chemistry* 283, 19879-19887.

Gryllos, I., Cywes, C., Shearer, M.H., Cary, M., Kennedy, R.C. and Wessels, M.R. (2008). Regulation of capsule gene expression by group A *Streptococcus* during pharyngeal colonization and invasive infection. *Molecular Microbiology* 42, 61-74.

Gryllos, I., Levin, J.C. and Wessels, M.R. (2003). The CsrR/CsrS two-component system of group A *Streptococcus* responds to environmental Mg²⁺. *Proceedings of the National Academy of Sciences of the United States of America* 100, 4227-4232.

Gryllos, I., Tran-Winkler, H.J., Cheng, M.F., Chung, H., Bolcome, R.III, Lu, W., et al. (2008). Induction of group A *Streptococcus* virulence by a human antimicrobial peptide. *Proceedings of the National Academy of Sciences of the United States of America* 105, 16755-16760.

Gustafsson, M.C.U., Lannergård, J., Nilsson, O.R., Kristensen, B.M., Olsen, J.E., Harris, C.L., Ufret-Vincenty, R.L., Stålhammar-Carlemalm, M. and Lindahl, G. (2013). Factor H binds to the hypervariable region of many *Streptococcus pyogenes* M proteins but does not promote phagocytosis resistance or acute virulence. *PLoS Pathogens* 9, e1003323.

Haas, T., Metzger, J., Schmitz, F., Heit, A., Muller, T., Latz, E. and Wagner, H. (2008). The DNA sugar backbone 20 deoxyribose determines toll-like receptor 9 activation. *Immunity* 28, 315-323.

Hall, C., Flores, M.V., Storm, T., Crosier, K. and Crosier, P. (2007). The zebrafish lysozyme C promoter drives myeloid-specific expression in transgenic fish. *BMC Developmental Biology* 7, 42.

Hardie, J.M. and Whiley, R.A. (1997). Classification and overview of the genera *Streptococcus* and *Enterococcus*. *Journal of Applied Microbiology* 83, 1S-11S.

Harvie, E.A. and Huttenlocher, A. (2015). Non-invasive imaging of the innate immune response in a zebrafish larval model of *Streptococcus iniae* infection. *Journal of Visualized Experiments* 98, 52788.

Hause, L.L. and McIver, K.S. (2012). Nucleotides critical for the interaction of the *Streptococcus pyogenes* Mga virulence regulator with Mga regulated promoter sequences. *Journal of Bacteriology* 194, 4904-4919.

Heath, A., DiRita, V.J., Barg, N.L. and Engleberg, N.C. (1999). A two-component regulatory system, CsrR-CsrS, represses expression of three *Streptococcus pyogenes* virulence factors, hyaluronic acid capsule, streptolysin S, and pyrogenic exotoxin B. *Infection and Immunity* 67, 5298-5305.

Herbomel, P., Thisse, B. and Thisse, C. (1999). Ontogeny and behaviour of early macrophages in the zebrafish embryo. *Development* 126, 3735-3745.

Hertzén, E., Johansson, L., Wallin, R., Schmidt, H., Kroll, M., Rehn, A.P., Kotb, M., Mörgelin, M. and Norrby-Teglund, A. (2010). M1 protein-dependent intracellular trafficking promotes persistence and replication of *Streptococcus pyogenes* in macrophages. *Journal of Innate Immunity* 2, 534-545.

Hertzén, E., Johansson, L., Kansal, R., Hecht, A., Dahesh, S., Janos, M., et al. (2012). Intracellular *Streptococcus pyogenes* in human macrophages display an altered gene expression profile. *PLoS One* 7, e35218.

Herwald, H., Cramer, H., Morgelin, M., Russell, W., Sollenberg, U., Norrby-Teglund, A., Flodgaard, H., Lindbom, L. and Bjorck, L. (2004). M protein, a classical bacterial virulence determinant, forms complexes with fibrinogen that induce vascular leakage. *Cell* 116, 367-379.

Hidalgo-Grass, C., Mishalian, I., Dan-Goor, M., Belotserkovsky, I., Eran, Y., Nizet, V., Peled, A. and Hanski, E. (2006). A streptococcal protease that degrades CXC chemokines and impairs bacterial clearance from infected tissues. *EMBO Journal* 25, 4628-4637.

Hidmark, A., von Saint Paul, A. and Dalpke, A. H. (2012). Cutting edge: TLR13 is a receptor for bacterial RNA. *The Journal of Immunology* 189, 2717-2721.

Higashi, D.L., Biais, N., Donahue, D.L., Mayfield, J.A., Tessier, C.R., Rodriguez, K., Ashfeld, B.L., Luchetti, J., Ploplis, V.A., Castellino, F.J., et al. (2016). Activation of band 3 mediates group A *Streptococcus* streptolysin S-based beta-haemolysis. *Nature Microbiology* 1, 15004.

Holland, M.C. and Lambris, J.D. (2002). The complement system in teleosts. *Fish Shellfish Immunology* 12, 399-420.

Hollingshead S.K., Simecka J.W. and Michalek S.M. (1993). Role of M protein in pharyngeal colonization by group A streptococci in rats. *Infection and Immunity* 61, 2277-2283.

Hollingshead, S.K., Arnold, J., Readdy, T.L. and Bessen, D.E. (1994). Molecular evolution of a multigene family in group A streptococci. *Molecular Biology and Evolution* 11, 208-219.

Hollingshead, S.K., Readdy, T.L., Yung, D.L. and Bessen, D.E. (1993). Structural heterogeneity of the *emm* gene cluster in group A streptococci. *Molecular Microbiology* 8, 707-717.

Honda-Ogawa, M., Ogawa, T., Terao, Y., Sumitomo, T., Nakata, M., Ikebe, K., Maeda, Y. and Kawabata, S. (2013). Cysteine proteinase from *Streptococcus pyogenes* enables evasion of innate immunity via degradation of complement factors. *The Journal of Biological Chemistry* 288, 15854-15864.

Honda-Ogawa, M., Sumitomo, T., Mori, Y., Hamd, D.T., Ogawa, T., Yamaguchi, M., Nakata, M. and Kawabata, S. (2017). *Streptococcus pyogenes* endopeptidase O contributes to evasion from complement-mediated bacteriolysis via binding to human complement factor C1q. *The Journal of Biological Chemistry* 292, 4244-4254.

Hsu, K., Traver, D., Kutok, J.L., Hagen, A., Liu, T.X., Paw, B.H., Rhodes, J., Berman, J.N., Zon, L.I., Kanki, J.P. and Look, A.T. (2004). The *pu.1* promoter drives myeloid gene expression in zebrafish. *Blood* 104, 1291-1297.

Hu, Y.L., Pan, X.M., Xiang, L.X. and Shao, J.Z. (2010). Characterization of C1q in teleosts: insight into the molecular and functional evolution of C1q family and classical pathway. *The Journal of Biological Chemistry* 285, 28777-28786.

Husmann L.K., Dillehay D.L., Jennings V.M. and Scott J.R. (1996). *Streptococcus pyogenes* infection in mice. *Microbial Pathogenesis* 20, 213-224.

Hyland, K.A., Wang, B. and Cleary, P.P. (2007). Protein F1 and *Streptococcus pyogenes* resistance to phagocytosis. *Infection and Immunity* 75, 3188-3191.

Ibrahim, M., Nicolas, P., Bessières, P., Bolotin, A., Monnet, V. and Gardan, R. (2007). A genome-wide survey of short coding sequences in *streptococci*. *Microbiology* 153, 3631-3644.

James, R.C. and MacLeod, C.J. (1961). Induction of staphylococcal infections in mice with small inocula introduced on sutures. *The British Journal of Experimental Pathology* 42, 266-277.

Janeway, C.A. Jr., Travers, P., Walport, M., et al. (2001). *Induced innate responses to infection*, 5th (New York: Garland Science).

Jansen, W.T.M., Bolm, M., Balling, R., Chhatwal, G.S. and Schnabel, R. (2002). Hydrogen peroxide-mediated killing of *Caenorhabditis elegans* by *Streptococcus pyogenes*. *Infection and Immunity* 70, 5202-5207.

Jault, C., Pichon, L. and Chluba, J. (2004). Toll-like receptor gene family and TIR-domain adapters in *Danio rerio*. *Molecular Immunology* 40, 759-771.

Johnson, D.R., Kaplan, E.L., VanGheem, A., Facklam, R.R. and Beall, B. (2006). Characterization of group A streptococci (*Streptococcus pyogenes*): correlation of M-protein and *emm*-gene type with T-protein agglutination pattern and serum opacity factor. *Journal of Medical Microbiology* 55, 157-164.

Johnsson, E., Berggard, K., Kotarsky, H., Hellwage, J., Zipfel, P. F., Sjobring, U. and Lindahl, G. (1998). Role of the hypervariable region in streptococcal M proteins: binding of a human complement inhibitor. *The Journal of Immunology* 161, 4894-4901.

Johnsson, E., Thern, A., Dahlback, B., Heden, L.O., Wikstrom, M. and Lindahl, G. (1996). A highly variable region in members of the streptococcal M protein family binds the human complement regulator C4BP. *The Journal of Immunology* 157, 3021-3029.

Joiner, K., Brown, E., Hammer, C., Warren, K. and Frank, M. (1983). Studies on the mechanism of bacterial resistance to complement-mediated killing. III. C5b-9 deposits stably on rough and type 7 *S. pneumoniae* without causing bacterial killing. *The Journal of Immunology* 130, 845-849.

Kaito, C., Kurokawa, K., Matsumoto, Y., Terao, Y., Kawabata, S., Hamada, S. and Sekimizu, K. (2005). Silkworm pathogenic bacteria infection model for identification of novel virulence genes. *Molecular Microbiology* 56, 934-944.

Kang, S., Wright, J., Tesorero, R., Lee, H., Beall, B. and Cho, K. (2012). Thermoregulation of capsule production by *Streptococcus pyogenes*. *PLoS One* 7, e37367.

Kansal, R.G., McGeer, A., Low, D.E., Norrby-Teglund, A. and Kotb, M. (2000). Inverse relation between disease severity and expression of the streptococcal cysteine protease, SpeB, among clonal M1T1 isolates recovered from invasive group A streptococcal infection cases. *Infection and Immunity* 68, 6362-6369.

Kansal, R.G., Datta, V., Aziz, R.K., Abdeltawab, N.F., Rowe, S. and Kotb, M. (2010). Dissection of the molecular basis for hypervirulence of an *in vivo*-selected phenotype of the widely disseminated M1T1 strain of group A *Streptococcus* bacteria. *The Journal of Infectious Diseases* 201, 855-865.

Kao, T.T., Tu, H.C., Chang, W.N., et al. (2010). Grape seed extract inhibits the growth and pathogenicity of *Staphylococcus aureus* by interfering with dihydrofolate reductase activity and folate-mediated one-carbon metabolism. *International Journal of Food Microbiology* 141, 17-27.

Kaplan, E.L., Chhatwal, G.S. and Rohde, M. (2006). Reduced ability of penicillin to eradicate ingested group A *streptococci* from epithelial cells: clinical and pathogenetic implications. *Clinical Infectious Diseases* 43, 1398-1406.

Kaplan, E.L. (2009). Some things never change! *Clinical Infectious Diseases* 48, 1220-1222.

Kapur, V., Topouzis, S., Majesky, M.W., Li, L.L., Hamrick, M.R., Hamill, R.J., Patti, J.M. and Musser, J.M. (1993). A conserved *Streptococcus pyogenes* extracellular cysteine protease cleaves human fibronectin and degrades vitronectin. *Microbial Pathogenesis* 15, 327-346.

Kasper, K.J., Zeppa, J.J., Wakabayashi, A.T., Xu, S.X., Mazzuca, D.M., Welch, I., Baroja, M.L., Kotb, M., Cairns, E., Cleary, P.P., Haeryfar, S.M. and McCormick, J.K. (2014). Bacterial superantigens promote acute nasopharyngeal infection by *Streptococcus pyogenes* in a human MHC Class II-dependent manner. *PLoS Pathogens* 10, e1004155.

Kaur, S.J., Nerlich, A., Bergmann, S., Rohde, M., Fulde, M., Zähler, D., Hanski, E., Zinkernagel, A., Nizet, V., Chhatwal, G.S., et al. (2010). The CXC chemokine-degrading protease SpyCep of *Streptococcus pyogenes* promotes its uptake into endothelial cells. *The Journal of Biological Chemistry* 285, 27798-27805.

Kefalides N.A., Pegg N.T., Ohno N., Poon-King T., Zabriskie J.B. and Fillit H. (1986). Antibodies to basement membrane collagen and to laminin are present in sera from patients with poststreptococcal glomerulonephritis. *Journal of Experimental Medicine* 163:588.

Kerakawauchi, H., Kurono, Y. and Mogi, G. (1997). Immune responses against *Streptococcus pyogenes* in human palatine tonsils. *Laryngoscope* 107, 634-639.

Kärre, K., Ljunggren, H.G. and Piontek, G. (1986). Selective rejection of H-2-deficient lymphoma variants suggests alternative immune defence strategy. *Nature* 319, 675-678.

Kleemann, R., Zadelaar, S. and Kooistra, T. (2008) Cytokines and atherosclerosis: a comprehensive review of studies in mice. *Cardiovascular Research* 79, 360-376.

Kolaczkowska, E. and Kubes, P. (2013). Neutrophil recruitment and function in health and inflammation. *Nature Reviews Immunology* 13, 159-75.

Kondo, M. (2010). Lymphoid and myeloid lineage commitment in multipotent hematopoietic progenitors. *Immunological Reviews* 238, 37-46.

Kondo, M., Wagers, A.J., Manz, M.G., Prohaska, S.S., Scherer, D.C., Beilhack, G.F., Shizuru, J.A. and Weissman, I.L. (2003). Biology of hematopoietic stem cells and progenitors: implications for clinical application. *Annual Review of Immunology* 21, 759-806.

Kratovac, Z., Manoharan, A., Luo, F., Lizano, S. and Bessen, D.E. (2007). Population genetics and linkage analysis of loci within the FCT region of *Streptococcus pyogenes*. *Journal of Bacteriology* 189, 1299-1310.

Krause, R.M. (2002). Evolving microbes and re-emerging streptococcal disease. *Clinics in Laboratory Medicine* 22, 835-848.

Kreikemeyer, B, Beckert, S., Braun-Kiewnick, A. and Podbielski, A. (2002). Group A streptococcal RofA-type global regulators exhibit a strain-specific genomic presence and regulation pattern. *Microbiology* 148, 1501-1511.

Kreikemeyer, B, Boyle, M.D., Buttaro, B.A., Heinemann, M. and Podbielski, A. (2001). Group A streptococcal growth phase-associated virulence factor regulation by a novel operon (Fas) with homologies to two-component-type regulators requires a small RNA molecule. *Molecular Microbiology* 39, 392-406.

Kreikemeyer, B., McIver, K.S. and Podbielski A. (2003). Virulence factor regulation and regulatory networks in *Streptococcus pyogenes* and their impact on pathogen-host interactions. *Trends in Microbiology* 11, 224-232.

Kreikemeyer, B., Nakata, M., Köller, T., Hildisch, H., Kourakos, V., Standar, K., et al. (2007). The *Streptococcus pyogenes* serotype M49 Nra-Ralp3 transcriptional regulatory network and its control of virulence factor expression from the novel *eno ralp3 epf sagA* pathogenicity region. *Infection and Immunity* 75, 5698-5710.

Kumar, V. and Sharma, A. (2010). Neutrophils: Cinderella of innate immune system. *International Immunopharmacology* 10, 1325-1334.

Kuo, C.F., Lin, Y.S., Chuang, W.J., Wu, J.J. and Tsao, N. (2008). Degradation of complement 3 by streptococcal pyrogenic exotoxin B inhibits complement activation and neutrophil opsonophagocytosis. *Infection and Immunity* 76, 1163-1169.

Kurupati, P., Turner, C. E., Tziona, I., Lawrenson, R. A., Alam, F. M., Nohadani, M., Stamp, G. W., Zinkernagel, A. S., Nizet, V., Edwards, R. J., et al. (2010). Chemokine-cleaving *Streptococcus pyogenes* protease SpyCEP is necessary and sufficient for bacterial dissemination within soft tissues and the respiratory tract. *Molecular Microbiology* 76, 1387-1397.

Laabei, M. and Ermert, D. (2018). Catch me if you can: *Streptococcus pyogenes* complement evasion strategies. *Journal of Innate Immunity* 11, 3-12.

Laborel-Préneron, E., Bianchi, P., Boralevi, F., Lehours, P., Fraysse, F., Morice-Picard, F., Sugai, M., Satoo, Y., Badiou, C., Lina, G., et al. (2015). Effects of the *Staphylococcus aureus* and *Staphylococcus epidermidis* secretomes isolated from the skin microbiota of atopic children on CD4 T cell activation. *Plos One* 10, e0141067.

Lam, S.H., Chua, H.L., Gong, Z., Lam, T.J. and Sin, Y.M. (2004). Development and maturation of the immune system in zebrafish, *Danio rerio*: a gene expression profiling, *in situ* hybridization and immunological study. *Developmental and Comparative Immunology* 28, 9-28.

Lamb, L.E., Zhi, X., Alam, F., Pyzio, M., Scudamore, C.L., Wiles, S. and Sriskandan, S. (2018). Modelling invasive group A streptococcal disease using bioluminescence. *BMC Microbiology* 18, 60.

Lancefield, R.C. (1933). A serological differentiation of human and other groups of hemolytic streptococci. *Journal of Experimental Medicine* 57, 571-595.

Lancefield, R.C. (1962). Current knowledge of type-specific M antigens of group A *streptococci*. *The Journal of Immunology* 89, 307-313.

Lancefield, R.C. and Dole, V.P. (1946). The properties of T antigens extracted from group A hemolytic *streptococci*. *Journal of Experimental Medicine* 84, 449-471.

Laskin, L., Weinberger, B. and Laskin, J. (2001). Functional heterogeneity in liver and lung macrophages. *Journal of Leukocyte Biology* 70, 163-170.

Le Guyader, D., Redd, M.J., Colucci-Guyon, E., Murayama, E., Kissa, K., Briolat, V., et al. (2008). Origins and unconventional behavior of neutrophils in developing zebrafish. *Blood* 111, 132-141.

Leday, T.V., Gold, K.M., Kinkel, T.L., Roberts, S.A., Scott, J.R. and Mciver, K.S. (2008). TrxR, a new CovR-repressed response regulator that activates the Mga virulence regulon in Group A *Streptococcus*. *Infection and Immunity* 76, 4659-4668.

Lei, B., Deleo, F. R., Hoe, N. P., Graham, M. R., Mackie, S. M., Cole, R. L., Liu, M., Hill, H. R., Low, D. E., Federle, M. J., et al. (2001). Evasion of human innate and acquired immunity by a bacterial homolog of CD11b that inhibits opsonophagocytosis. *Nature Medicine* 7, 1298-1305.

Levin, J.C. and Wessels, M.R. (1998). Identification of *csrR/csrS*, a genetic locus that regulates hyaluronic acid capsule synthesis in group A *Streptococcus*. *Molecular Microbiology* 30, 209-219.

Li, X., Wang, S., Qi, J., et al. (2007). Zebrafish peptidoglycan recognition proteins are bactericidal amidases essential for defense against bacterial infections. *Immunity* 27, 518-529.

Li, P., Wong, J., Sum, C., Sin, W. and Chin, K. (2011). IRF8 and IRF3 cooperatively regulate rapid interferon- β induction in human blood monocytes. *Blood* 4, 2847-2854.

Li, X.D. and Chen, Z.J. (2012). Sequence specific detection of bacterial 23S ribosomal RNA by TLR13. *elife* 1, e00102.

Li, J., Zhu, H., Feng, W., Liu, M., Song, Y., Zhang, X., et al. (2013). Regulation of inhibition of neutrophil infiltration by the two-component regulatory system CovRS in subcutaneous murine infection with group A *streptococcus*. *Infection and Immunity* 81, 974-983.

Li, J., Liu, G., Feng, W., Zhou, Y., Liu, M., Wiley, J.A., et al. (2014). Neutrophils select hypervirulent CovRS mutants of M1T1 group A *Streptococcus* during subcutaneous infection of mice. *Infection and Immunity* 82, 1579-1590.

Liang, Z., Zhang, Y., Agrahari, G., Chandrabhas, V., Glinton, K., Donahue, D. L., et al. (2013). A natural inactivating mutation in the CovS component of the CovRS regulatory operon in a pattern D *Streptococcal pyogenes* strain influences virulence-associated genes. *Journal of Biological Chemistry* 288, 6561-6573.

Lieschke, G.J., Oates, A.C., Crowhurst, M.O., Ward, A.C. and Layton, J.E. (2001). Morphologic and functional characterization of granulocytes and macrophages in embryonic and adult zebrafish. *Blood* 98, 3087-3096.

Lim, C.H., Voedisch, S., Wahl, B., Rouf, S.F., Geffers, R., Rhen, M. and Pabst, O. (2014). Independent bottlenecks characterize colonization of systemic compartments and gut lymphoid tissue by *Salmonella*. *PLoS Pathogens* 10, e1004270.

Lin, B., Chen, S., Cao, Z., et al. (2007). Acute phase response in zebrafish upon *Aeromonas salmonicida* and *Staphylococcus aureus* infection: striking similarities and obvious differences with mammals. *Molecular Immunology* 44, 295-301.

Lin, A., Loughman, J. A., Zinselmeyer, B. H., Miller, M. J. and Caparon, M. G. (2009). Streptolysin S inhibits neutrophil recruitment during the early stages of *Streptococcus pyogenes* infection. *Infection and Immunity* 77, 5190-5201.

Lin, W.H. and Kussell, E. (2011). Evolutionary pressures on simple sequence repeats in prokaryotic coding regions. *Nucleic Acids Research* 40, 2399-2413.

Linder, A., Christensson, B., Herwald, H., Bjorck, L. and Akesson, P. (2009). Heparin-binding protein: an early marker of circulatory failure in sepsis. *Clinical Infectious Diseases* 49, 1044-1050.

Liu, Z., Treviño, J., Ramirez-Peña, E. and Sumby, P. (2012). The small regulatory RNA FasX controls pilus expression and adherence in the human bacterial pathogen group A *Streptococcus*. *Molecular Microbiology* 86,140-154.

Loh J.M., Adenwalla N., Wiles S. and Proft T. (2013). *Galleria mellonella* larvae as an infection model for group A *streptococcus*. *Virulence* 4, 419-428.

Loof, T. G., Goldmann, O. and Medina, E. (2008). Immune recognition of *Streptococcus pyogenes* by dendritic cells. *Infection and Immunity* 76, 2785-2792.

Loof, T. G., Goldmann, O., Gessner, A., Herwald, H. and Medina, E. (2010). Aberrant inflammatory response to *Streptococcus pyogenes* in mice lacking myeloid differentiation factor 88. *The American Journal of Pathology* 176, 754-763.

Loynes, C.A., Lee, J.A., Robertson, A.L., Steel, M.J., Ellett, F., Feng, Y., Levy, B.D., Whyte, M.K. and Renshaw, S.A. (2018). PGE2 production at sites of tissue injury promotes an anti-inflammatory neutrophil phenotype and determines the outcome of inflammation resolution *in vivo*. *Science Advances* 117, 2847-2854.

Lü, A., Hu, X., Xue, J., Zhu, J., Wang, Y. and Zhou, G. (2012). Gene expression profiling in the skin of zebrafish infected with *Citrobacter freundii*. *Fish Shellfish Immunology* 32, 273-283.

Luca-Harari, B., Darenberg, J., Neal, S., Siljander, T., Strakova, L., Tanna, A., Creti, R., Ekelund, K., Koliou, M., Tassios, P.T., et al. (2009). Clinical and microbiological characteristics of severe *Streptococcus pyogenes* disease in Europe. *Journal of Clinical Microbiology* 47, 1155-1165.

Lukomski, S., Montgomery, C.A., Rurangirwa, J., Geske, R.S., Barrish, J.P., Adams, G.J., et al. (1999). Extracellular cysteine protease produced by *Streptococcus pyogenes* participates in the pathogenesis of invasive skin infection and dissemination in mice. *Infection and Immunity* 67,1779-1788.

Lynskey, N.N., Jauneikaite, E., Li, H.K., Zhi, X., Turner, C.E., Mosavie, M., Pearson, M., Asai, M., Lobkowitz, L., Chow, J.Y., Parkhill, J., Lamagni, T., Chalker, V.J. and Sriskandan, S. (2019). Emergence of dominant toxigenic M1T1 *Streptococcus pyogenes* clone during increased scarlet fever activity in England: a population-based molecular epidemiological study. *Lancet Infectious Diseases* 19, 1209-1218.

Lyon, W.R., Gibson, C.M. and Caparon, M.G. (1998). A role for trigger factor and an *rgg*-like regulator in the transcription, secretion and processing of the cysteine proteinase of *Streptococcus pyogenes*. *EMBO Journal* 17, 6263-6275.

Macheboeuf, P., Buffalo, C., Fu, C., Zinkernagel, A.S., Cole, J.N., Johnson, J.E., Nizet, V. and Ghosh, P. (2011). Streptococcal M1 protein constructs a pathological host fibrinogen network. *Nature* 472, 64-68.

Makthal, N., Do, H., VanderWal, A. R., Olsen, R. J., Musser, J. M. and Kumaraswami, M. (2018). Signaling by a conserved quorum sensing pathway contributes to growth ex vivo and oropharyngeal colonization of human pathogen group A *Streptococcus*. *Infection and Immunity* 86, e00169-18.

Maier, L., Diard, M., Sellin, M.E., Chouffane, E.-S., Trautwein-Weidner, K., Periaswamy, B., Slack, E., Dolowschiak, T., Stecher, B., Loverdo, C., et al. (2014). Granulocytes impose a tight bottleneck upon the gut luminal pathogen population during *Salmonella Typhimurium* colitis. *PLoS Pathogens* 11, e1005047

Mandell, G., Bennett J., Dolin, R. (2005). Mandell, Douglas, and Bennett's principles and practice of infectious diseases. (Philadelphia: Churchill Livingstone).

Margolis, E. and Levin, B. R. (2007). Within-host evolution for the invasiveness of commensal bacteria: an experimental study of bacteremias resulting from *Haemophilus influenzae* nasal carriage. *The Journal of Infectious Diseases* 196, 1068-1075.

Marouni, M.J. and Sela, S. (2004). Fate of *Streptococcus pyogenes* and epithelial cells following internalization. *Journal of Medical Microbiology* 53, 1-7.

Martin, J.M. (2004). Group A *Streptococci* among school-aged children: clinical characteristics and the carrier state. *Pediatrics* 114, 1212-1219.

Mashburn, L. M., Jett, A. M., Akins, D. R. and Whiteley, M. (2005). *Staphylococcus aureus* serves as an iron source for *Pseudomonas aeruginosa* during *in vivo* coculture. *Journal of Bacteriology* 187, 554-566.

Matsui, T. and Amagai, M. (2015). Dissecting the formation, structure and barrier function of the stratum corneum. *International Immunology* 27, 269-280.

McDonald, C., Inohara, N. and Nuñez, G. (2005). Peptidoglycan signaling in innate immunity and inflammatory disease. *Journal of Biological Chemistry* 280, 20177-20180.

McGregor, K. F., Spratt, B. G., Kalia, A., Bennett, A., Bilek, N., Beall, B. and Bessen, D. E. (2004). Multilocus sequence typing of *Streptococcus pyogenes* representing most known *emm* types and distinctions among subpopulation genetic structures. *Journal of Bacteriology* 186, 4285-4294.

McNamara, C., Zinkernagel, A.S., Macheboeuf, P., Cunningham, M.W., Nizet, V. and Ghosh, P. (2008). Coiled-coil irregularities and instabilities in Group A *Streptococcus* M1 are required for virulence. *Science* 319, 1405-1408.

McShan, W.M. and Nguyen, S.V. (2016). The bacteriophages of *Streptococcus pyogenes*. In *Streptococcus pyogenes: basic biology to clinical manifestations*, J.J. Ferretti, D.L. Stevens and V.A. Fischetti eds. (Oklahoma City: University of Oklahoma Health Sciences Center).

McVicker, G., Prajsnar, T.K., Williams, A., Wagner, N.L., Boots, M., Renshaw, S.A. and Foster, S.J. (2014). Clonal expansion during *Staphylococcus aureus* infection dynamics reveals the effect of antibiotic intervention. *PLoS Pathogens* 10, e1003959.

Medina, E., Goldmann, O., Rohde, M., Lengeling, A. and Chhatwals, G. S. (2001). Genetic control of susceptibility to group A streptococcal infection in mice. *The Journal of Infectious Disease* 184, 846-852.

Medina, E., Rohde, M. and Chhatwal, G.S. (2003). Intracellular survival of *Streptococcus pyogenes* in polymorphonuclear cells results in increased bacterial virulence. *Infection and Immunity* 71, 5376-5380.

Meehl, M., Pinkner, J., Anderson, P., Hultgren, S. and Caparon, M. (2005). A novel endogenous inhibitor of the secreted streptococcal NAD-glycohydrolase. *PLoS Pathogens* 1, e35.

Meijer, A. H., Gabby Krens, S. F., Medina Rodriguez, I. A., He, S., Bitter, W., Ewa Snaar-Jagalska, B. and Spaink, H. P. (2004). Expression analysis of the Toll-like receptor and TIR domain adaptor families of zebrafish. *Molecular Immunology* 40, 773-783.

Meijer, A.H., Verbeek, F.J., Salas-Vidal, E., Corredor-Adamez, M., Bussman, J., van der Sar, A.M., et al. (2005). Transcriptome profiling of adult zebrafish at the late stage of chronic tuberculosis due to *Mycobacterium marinum* infection. *Molecular Immunology* 42, 1185-1203.

Merle, N.S., Church, S.E., Fremeaux-Bacchi, V. and Roumenina, L.T. (2015). Complement system part I - molecular mechanisms of activation and regulation. *Frontiers in Immunology* 6, 262.

Merle, N.S., Noe, R., Halbwachs-Mecarelli, L., Fremeaux-Bacchi, V. and Roumenina, L.T. (2015). Complement system part II: role in immunity. *Frontiers in Immunology* 6, 257.

Michael A.F. Jr., Drummond K.N., Good R.A. and Vernier R.L. (1966). Acute poststreptococcal glomerulonephritis: immune deposit disease. *The Journal of Clinical Investigation* 45:237-248.

Miller, J. and Neely, M. (2004). Zebrafish as a model host for streptococcal pathogenesis. *Acta Tropica* 91, 53-68.

Mishalian, I., Ordan, M., Peled, A., Maly, A., Eichenbaum, M. B., Ravins, M., Aychek, T., Jung, S. and Hanski, E. (2011). Recruited macrophages control dissemination of group A *Streptococcus* from infected soft tissues. *The Journal of Immunology* 187, 6022-6031.

Mora, M., Bensi, G., Capo, S., Falugi, F., Zingaretti, C., Manetti, A.G., et al. (2005). Group A *Streptococcus* produce pilus-like structures containing protective antigens and Lancefield T antigens. *Proceedings of the National Academy of Sciences of the United States of America* 102, 15641-15646.

Naik, S., Bouladoux, N., Linehan, J.L., Han, S.-J., Harrison, O.J., Wilhelm, C., Conlan, S., Himmelfarb, S., Byrd, A.L., Deming, C., et al. (2015). Commensal-dendritic-cell interaction specifies a unique protective skin immune signature. *Nature* 520, 104-108.

Nasevicius, A. and Ekker, S.C. (2000). Effective targeted gene 'knockdown' in zebrafish. *Nature Genetics* 26, 216-220.

Nauseef, W.M. (2007). How human neutrophils kill and degrade microbes: an integrated view. *Immunological Reviews* 219, 88-102.

Neely, M.N., Lyon, W.R., Runft, D.L. and Caparon, M. (2003). Role of RopB in growth phase expression of the SpeB cysteine protease of *Streptococcus pyogenes*. *Journal of Bacteriology* 185, 5166-5174.

Neely, M.N., Pfeifer, J.D. and Caparon, M. (2002). *Streptococcus*-zebrafish model of bacterial pathogenesis. *Infection and Immunity* 70, 3904-3914.

Nelson, D. C., Garbe, J. and Collin, M. (2011). Cysteine proteinase SpeB from *Streptococcus pyogenes* - a potent modifier of immunologically important host and bacterial proteins. *Biological Chemistry* 392, 1077-1088.

Nguyen-Chi, M., Laplace-Builhé, B., Travnickova, J., Luz-Crawford, P., Tejedor, G., Lutfalla, G., Kissa, K., Jorgensen, C. and Djouad, F. (2017). TNF signaling and macrophages govern fin regeneration in zebrafish larvae. *Cell Death & Disease* 8.

Noris, M. and Remuzzi, G. (2013). Overview of complement activation and regulation. *Seminars in Nephrology* 33, 479-492.

O'Loughlin, R.E., Roberson, A., Cieslak, P.R., Lynfield, R., Gershman, K., Craig, A., Albanese, B.A., Farley, M.M., Barrett, N.L., Spina, N.L., et al. (2007). The epidemiology of invasive group A streptococcal infection and potential vaccine implications: United States, 2000-2004. *Clinical Infectious Diseases* 45, 853-862.

O'Neill, A.M., Thurston, T.L.M. and Holden, D.W. (2016). Cytosolic replication of group A *Streptococcus* in human macrophages. *mBio* 7, e00020.

O'Shea, J.J., Ma, A. and Lipsky, P. (2002). Cytokines and autoimmunity. *Nature Reviews Immunology* 2, 37-45.

Okada, N., Pentland, A.P., Falk, P. and Caparon, M.G. (1994). M protein and protein F act as important determinants of cell-specific tropism of *Streptococcus pyogenes* in skin tissue. *The Journal of Clinical Investigation*, 94, 965-977.

Okumura, C.Y.M., Anderson, E.L., Döhrmann, S., Tran, D.N., Olson, J., Pawel-Rammingen, U.V. and Nizet, V. (2013). IgG protease Mac/IdeS is not essential for phagocyte resistance or mouse virulence of M1T1 group A *Streptococcus*. *MBio* 4, e00499-13.

Oldenburg, M., Kruger, A., Ferstl, R., Kaufmann, A., Nees, G., Sigmund, A., Bathke, B., Lauterbach, H., Suter, M., Dreher, S., et al. (2012). TLR13 recognizes bacterial 23S rRNA devoid of erythromycin resistance-forming modification. *Science* 337, 1111-1115.

Olive, C., Clair, T., Yarwood, P. and Good, M.F. (2002). Protection of mice from group A streptococcal infection by intranasal immunisation with a peptide vaccine that contains a conserved M protein B cell epitope and lacks a T cell autoepitope. *Vaccine* 20, 2816-2825.

Olive, C., Sun, H.K., Ho, M.F., Dyer, J., Horváth, A., Toth, I. and Good, M.F. (2006). Intranasal administration is an effective mucosal vaccine delivery route for self-adjuvanting lipid core peptides targeting the group A streptococcal M protein. *The Journal of Infectious Diseases* 194, 316-324.

Olsen, R. J., Raghuram, A., Cantu, C., Hartman, M. H., Jimenez, F. E., Lee, S., Ngo, A., Rice, K. A., Saddington, D., Spillman, H., et al. (2015). The majority of 9,729 group A *Streptococcus* strains causing disease secrete SpeB cysteine protease: pathogenesis implications. *Infection and Immunity* 83, 4750-4758.

Olsen, R.J., Ashraf, M., Gonulal, V.E., Ayeras, A.A., Cantu, C., Shea, P.R., Carroll, R.K., Humbird, T., Greaver, J.L., Swain, J.L., et al. (2010). Lower respiratory tract infection in cynomolgus macaques (*Macaca fascicularis*) infected with group A *Streptococcus*. *Microbial Pathogenesis* 49, 336-347.

Osterlund, A., Popa, R., Nikkila, T., Scheynius, A. and Engstrand, L. (1997). Intracellular reservoir of *Streptococcus pyogenes in vivo*: a possible explanation for recurrent pharyngotonsillitis. *Laryngoscope* 107, 640-647.

Pahlman, L.I., Morgelin, M., Eckert, J., Johansson, L., Russell, W., Riesbeck, K., Soehnlein, O., Lindbom, L., Norrby-Teglund, A., Schumann, R.R., Bjorck, L. and Herwald, H. (2006). Streptococcal M protein: a multipotent and powerful inducer of inflammation. *The Journal of Immunology* 177, 1221-1228.

Pahlman, L.I., Olin, A.I., Darenberg, J., Morgelin, M., Kotb, M., Herwald, H. and Norrby-Teglund, A. (2008). Soluble M1 protein of *Streptococcus pyogenes* triggers potent T cell activation. *Cellular Microbiology* 10, 404-414.

Pandey, M., Sekuloski, S. and Batzloff, M.R. (2009). Novel strategies for controlling *Streptococcus pyogenes* infection and associated diseases: from potential peptide vaccines to antibody immunotherapy. *Immunology and Cell Biology* 87, 391-399.

Panchaud, A., Guy, L., Collyn, F., Haenni, M., Nakata, M., Podbielski, A., et al. (2009). M-protein and other intrinsic virulence factors of *Streptococcus pyogenes* are encoded on an ancient pathogenicity island. *BMC Genomics* 10, 198.

Park, H.S., Costalonga, M., Reinhardt, R.L., Dombek, P.E., Jenkins, M.K. and Cleary, P.P. (2004). Primary induction of CD4 T cell responses in nasal associated lymphoid tissue during group A streptococcal infection. *European Journal of Immunology* 34, 2843-2853.

Pazhakh, V., Clark, S., Keightley, M.C. and Lieschke, G.J. (2017). A GCSFR/CSF3R zebrafish mutant models the persistent basal neutrophil deficiency of severe congenital neutropenia. *Scientific Reports* 7, 44455.

Phelps, H.A., Runft, D.L. and Neely, M.N. (2009). Adult zebrafish model of streptococcal infection. *Current Protocols in Microbiology*, Chapter 9:Unit 9D.1.

Phennicie, R.T., Sullivan, M.J., Singer, J.T., Yoder, J.A. and Kim, C.H. (2010). Specific resistance to *Pseudomonas aeruginosa* infection in zebrafish is mediated by the cystic fibrosis transmembrane conductance regulator. *Infection and Immunity* 78, 4542-4550.

Podbielski, A., Woischnik, M., Leonard, B.A. and Schmidt, K.H. (1999). Characterization of *nra*, a global negative regulator gene in group A *streptococci*. *Molecular Microbiology* 31, 1051-1064.

Postlethwait, J., Amores, A., Force, A. and Yan, Y.L. (1999). The zebrafish genome. *Methods in Cell Biology* 60, 149-163.

Prajsnar, T.K., Cunliffe, V.T., Foster, S.J. and Renshaw, S.A. (2008). A novel vertebrate model of *Staphylococcus aureus* infection reveals phagocyte-dependent resistance of zebrafish to non-host specialized pathogens. *Cellular Microbiology* 10, 2312-2325.

Prajsnar, T.K., Hamilton, R., Garcia-Lara, J., Mcvicker, G., Williams, A., Boots, M., Foster, S.J. and Renshaw, S.A. (2012). A privileged intraphagocyte niche is responsible for disseminated infection of *Staphylococcus aureus* in a zebrafish model. *Cellular Microbiology* 14, 1600-1619.

Prajsnar, T.K., Renshaw, S.A., Ogryzko, N.V., Foster, S.J., Serror, P. and Mesnage, S. (2013). Zebrafish as a novel vertebrate model to dissect enterococcal pathogenesis. *Infection and Immunity* 81, 4271-4279.

Prouty, M.G., Correa, N.E., Barker, L.P., Jagadeeswaran, P. and Klose, K.E. (2003). Zebrafish-*Mycobacterium marinum* model for mycobacterial pathogenesis. *FEMS Microbiology Letters* 225, 177-182.

Raeder, R.H., Barker-Merrill, L., Lester, T., Boyle, M.D.P. and Metzger, D.W. (2000). A pivotal role for interferon- γ in protection against group A streptococcal skin infection. *The Journal of Infectious Diseases* 181, 639-645.

Rakers, S., Niklasson, L., Steinhagen, D., Kruse, C., Schauber, J., Sundell, K. and Paus, R. (2013). Antimicrobial peptides (AMPs) from fish epidermis: perspectives for investigative dermatology. *The Journal of Investigative Dermatology* 133, 1140-1149.

Ramirez-Peña, E., Treviño, J., Liu, Z., Perez, N. and Sumbly, P. (2010). The group A *Streptococcus* small regulatory RNA FasX enhances streptokinase activity by increasing the stability of the ska mRNA transcript. *Molecular Microbiology* 78, 1332-1347.

Reglinski, M. and Sriskandan, S. (2014). The contribution of group A streptococcal virulence determinants to the pathogenesis of sepsis. *Virulence* 5, 127-136.

Reglinski, M. and Sriskandan, S. (2015). *Streptococcus pyogenes*. In *Molecular medical microbiology*, 2nd, Y-W. Tang, D. Liu, J. Scharzman, M. Sussman, I. Poxton, eds. (Academic Press), 675-716.

Reglinski, M., Gierula, M., Lynskey, N., Edwards, R. and Sriskandan, S. (2015). Identification of the *Streptococcus pyogenes* surface antigens recognised by pooled human immunoglobulin. *Scientific Reports* 5.

Reglinski, M., Lynskey, N., Choi, Y., Edwards, R. and Sriskandan, S. (2016). Development of a multicomponent vaccine for *Streptococcus pyogenes* based on the antigenic targets of IVIG. *The Journal of Infection* 72, 450-459.

Rego, R.O.M., Bestor, A., Štefka, J. and Rosa, P.A. (2014). Population bottlenecks during the infectious cycle of the Lyme disease spirochete *Borrelia burgdorferi*. *PLoS ONE* 9, e101009.

Renshaw, S.A. and Trede, N.S., (2012). A model 450 million years in the making: zebrafish and vertebrate immunity. *Disease Models & Mechanisms* 5, 38-47.

Renshaw, S.A., Loynes, C.A., Trushell, D.M., Elworthy, S., Ingham, P.W. and Whyte, M.K. (2006). A transgenic zebrafish model of neutrophilic inflammation. *Blood* 108, 3976-3978.

Rhodes, J., Hagen, A., Hsu, K., Deng, M., Liu, T.X., Look, A.T. and Kanki, J.P. (2005). Interplay of pu.1 and gata1 determines myelo-erythroid progenitor cell fate in zebrafish. *Developmental Cell* 8, 97-108.

Ribardo, D.A. and McIver, K.S. (2006). Defining the Mga regulon: comparative transcriptome analysis reveals both direct and indirect regulation by Mga in the group A *Streptococcus*. *Molecular Microbiology* 62, 491-508.

Roberts, S., Scott, J.R., Husmann, L.K. and Zurawski, C.A. (2006). Murine models of *Streptococcus pyogenes* infection. *Current Protocols in Microbiology*, Chapter 9, 5.

Roca, F.J., Mulero, I., Lopez-Munoz, A., et al. (2008). Evolution of the inflammatory response in vertebrates: fish TNF-alpha is a powerful activator of endothelial cells but hardly activates phagocytes. *The Journal of Immunology* 181, 5071-5081.

Romo, M.R., Pérez-Martínez, D. and Ferrer, C.C. (2016). Innate immunity in vertebrates: an overview. *Immunology* 148, 125-139.

Rosch, J.W., Vega, L.A., Beyer, J.M., Lin, A. and Caparon, M.G. (2008). The signal recognition particle pathway is required for virulence in *Streptococcus pyogenes*. *Infection and Immunity* 76, 2612-2619.

Rowley, D. (1956). Rapidly induced changes in the level of non-specific immunity in laboratory animals. *The British Journal of Experimental Pathology* 37, 223-234.

Sakurai, A., Maruyama, F., Funao, J., Nozawa, T., Aikawa, C., Okahashi, N., Shintani, S., Hamada, S., Ooshima, T., and Nakagawa, I. (2010). Specific behavior of intracellular *Streptococcus pyogenes* that has undergone autophagic degradation is associated with bacterial streptolysin O and host small G proteins Rab5 and Rab7. *Journal of Biological Chemistry* 285, 22666-22675.

Sanderson-Smith, M.L., Dinkla, K., Cole, J.N., Cork, A.J., Maamary, P.G., McArthur, J.D., Chhatwal, G.S. and Walker, M.J. (2008). M protein-mediated plasminogen binding is essential for the virulence of an invasive *Streptococcus pyogenes* isolate. *FASEB Journal* 22, 2715–2722.

Saralahti, A. and Rämetsä, M. (2015). Zebrafish and streptococcal infections. *Scandinavian Journal of Immunology* 82, 174-183.

Schmidtchen, A., Frick, I.M., Andersson, E., Tapper, H. and Björck, L. (2002). Proteinases of common pathogenic bacteria degrade and inactivate the antibacterial peptide LL-37. *Molecular Microbiology* 46, 157-168.

Schrager, H.M., Alberti, S., Cywes, C., Dougherty, G.J. and Wessels, M.R. (1998). Hyaluronic acid capsule modulates M protein-mediated adherence and acts as a ligand for attachment of group A *Streptococcus* to CD44 on human keratinocytes. *The Journal of Clinical Investigation* 101, 1708-1716.

Schrager, H.M., Rheinwald, J.G. and Wessels, M.R. (1996). Hyaluronic acid capsule and the role of streptococcal entry into keratinocytes in invasive skin infection. *The Journal of Clinical Investigation* 98, 1954-1958.

Segal, A.W., Geisow, M., Garcia, R., Harper, A. and Miller, R. (1981). The respiratory burst of phagocytic cells is associated with a rise in vacuolar pH. *Nature* 290, 406-409.

Shah, S.S., Hall, M., Srivastava, R., Subramony, A. and Levin, J.E. (2009). Intravenous immunoglobulin in children with streptococcal toxic shock syndrome. *Clinical Infectious Diseases* 49, 1369-1376.

Shaikh, N., Leonard, E. and Martin, J. M. (2010). Prevalence of Streptococcal pharyngitis and Streptococcal carriage in children: a meta-analysis. *Pediatrics* 126.

Shelburne, S.A. III, Granville, C., Tokuyama, M., Sitkiewicz, I., Patel, P. and Musser, J.M. (2005). Growth characteristics of and virulence factor production by group A *Streptococcus* during cultivation in human saliva. *Infection and Immunity* 73, 4723-4731.

Shelburne, S.A., Keith, D., Horstmann, N., Sumby, P., Davenport, M.T., Graviss, E.A., et al. (2008). A direct link between carbohydrate utilization and virulence in the major human pathogen group A *Streptococcus*. *Proceedings of the National Academy of Sciences of the United States of America* 105, 1698-1703.

Shewell, L.K., Harvey, R.M., Higgins, M.A., Day, C.J., Hartley-Tassell, L.E., Chen, A.Y., Gillen, C.M., James, D.B.A., Alonzo, F., Torres, V.J., et al. (2014). The cholesterol-dependent cytolysins pneumolysin and streptolysin O require binding to red blood cell glycans for hemolytic activity. *Proceedings of the National Academy of Sciences of the United States of America* 111, 5312-5320.

Shulman, S.T., Tanz, R.R., Dale, J.B., Beall, B., Kabat, W., Kabat, K., Cederlund, E., Patel, D., Rippe, J., Li, Z., et al. (2009). Seven-year surveillance of north American paediatric group A streptococcal pharyngitis isolates. *Clinical Infectious Diseases* 49, 78-84.

Siemens, N., Fiedler, T., Normann, J., Klein, J., Munch, R., Patenge, N., et al. (2012). Effects of the ERES pathogenicity region regulator Ralp3 on *Streptococcus pyogenes* serotype M49 virulence factor expression. *Journal of Bacteriology* 194, 3618-3626.

Sifri, C.D., Begun, J., Ausubel, F.M. and Calderwood, S.B. (2003). *Caenorhabditis elegans* as a model host for *Staphylococcus aureus* pathogenesis. *Infection and Immunity* 71, 2208-2217.

Slade, H.D. and Slamp, W.C. (1962). Cell-wall composition and the grouping antigens of streptococci. *Journal of Bacteriology* 84, 345-351.

Sloan, C.D. and Haslam, J.R. (1997). Protein kinase C-dependent and Ca²⁺-dependent mechanisms of secretion from streptolysin O-permeabilized platelets: effects of leakage of cytosolic proteins. *Biochemistry Journal* 328, 13-21.

Smeesters, P.R., McMillan, D.J. and Sriprakash, K.S. (2010). The streptococcal M protein: a highly versatile molecule. *Trends in Microbiology* 18, 275-282.

Sriskandan, S., Unnikrishnan, M., Krausz, T. and Cohen, J. (2000). Mitogenic factor (MF) is the major DNase of serotype *emm89 Streptococcus pyogenes*. *Microbiology* 146, 2785-2792.

Staal, L., Bauer, S., Mörgelin, M., Björck, L. and Tapper, H. (2006). *Streptococcus pyogenes* bacteria modulate membrane traffic in human neutrophils and selectively inhibit azurophilic granule fusion with phagosomes. *Cellular Microbiology* 8, 690-703.

Steer, A. C., Batzloff, M. R., Mulholland, K. and Carapetis, J. R. (2009). Group A streptococcal vaccines: facts versus fantasy. *Current Opinion in Infectious Diseases* 22, 544-552.

Steer, A.C., Jenney, A.W.J., Kado, J., Good, M.F., Batzloff, M., Magor, G., Ritika, R., Mulholland, K.E. and Carapetis, J.R. (2009). Prospective surveillance of streptococcal sore throat in a tropical country. *The Pediatric Infectious Disease Journal* 28, 477-482.

Stein, C., Caccamo, M., Laird, G. and Leptin, M. (2007). Conservation and divergence of gene families encoding components of innate immune response systems in zebrafish. *Genome Biology* 8, R251

Stevens, D.L. (2000). Streptococcal toxic shock syndrome associated with necrotizing fasciitis. *Annual Review of Medicine* 51, 271-288.

Stevens, D.L., Bryant, A.E., Hackett, S.P., Chang, A., Peer, G., Kosanke, S., Emerson, T. and Hinshaw, L. (1996). Group A streptococcal bacteremia: the role of tumor necrosis factor in shock and organ failure. *The Journal of Infectious Diseases* 173, 619-626.

Stock, A.M., Robinson, V.L. and Goudreau, P.N. (2000). Two-component signal transduction. *Annual Review of Biochemistry* 69,183-215.

Stulberg, D.L., Penrod, M.A. and Blatny, R.A. (2002). Common bacterial skin infections. *American Family Physician* 66, 119-125.

Sullivan, C., Matty, M., Jurczynszak, D., Gabor, K., Millard, P., Tobin, D. and Kim, C. (2017). Infectious disease models in zebrafish. *Methods in Cell Biology* 138, 101-136.

Sullivan, C., Matty, M.A., Jurczynszak, D., Gabor, K.A., Millard, P.J., Tobin, D.M. and Kim, C.H. (2017). Infectious disease models in zebrafish. In *The zebrafish disease models and chemical screens*, H.W. Detrich III, M. Westerfield, and L.I. Zon, eds. (Elsevier), pp. 101-136.

Sumby, P., Barbian, K.D., Gardner, D.J., Whitney, A.R., Welty, D.M., Long, R.D., et al. (2005). Extracellular deoxyribonuclease made by group A *Streptococcus* assists pathogenesis by enhancing evasion of the innate immune response. *Proceedings of the National Academy of Sciences of the United States of America* 102, 1679-1684.

Sumby, P., Porcella, S.F., Madrigal, A.G., Barbian, K.D., Virtaneva, K., Ricklefs, S.M., et al. (2005). Evolutionary origin and emergence of a highly successful clone of serotype M1 group A *Streptococcus* involved multiple horizontal gene transfer events. *The Journal of Infectious Diseases* 192, 771-782.

Sumby, P., Whitney, A.R., Graviss, E.A., DeLeo, F.R. and Musser, J.M. (2006). Genome-wide analysis of group a *streptococci* reveals a mutation that modulates global phenotype and disease specificity. *PLoS Pathogens* 2, e5.

Sumitomo, T., Nakata, M., Higashino, M., Jin, Y., Terao, Y., Fujinaga, Y. and Kawabata, S. (2011). Streptolysin S contributes to group A Streptococcal translocation across an epithelial barrier. *Journal of Biological Chemistry* 286, 2750-2761.

Sumitomo, T., Nakata, M., Higashino, M., Terao, Y. and Kawabata, S. (2013). Group A streptococcal cysteine protease cleaves epithelial junctions and contributes to bacterial translocation. *Journal of Biological Chemistry* 288,13317-13324.

Sun, C., Wu, J., Liu, S., Li, H. and Zhang, S., (2013). Zebrafish CD59 has both bacterial binding and inhibiting activities. *Developmental and Comparative Immunology* 41, 178-188.

Sun, H. (2004). Plasminogen is a critical host pathogenicity factor for group A streptococcal infection. *Science* 305, 1283-1286.

Svensson, M.D., Sjobring, U., Luo, F. and Bessen, D.E. (2002). Roles of the plasminogen activator streptokinase and the plasminogen-associated M protein in an experimental model for streptococcal impetigo. *Microbiology* 148, 3933-3945.

Swaim, L.E., Connolly, L.E., Volkman, H.E., Humbert, O., Born, D.E. Ramakrishnan, L. (2006). *Mycobacterium marinum* infection of adult zebrafish causes caseating granulomatous tuberculosis and is moderated by adaptive immunity. *Infection and Immunity* 74, 6108-6117.

Takeuchi, O. and Akira, S. (2010). Pattern recognition receptors and inflammation. *Cell* 140, 805-820.

Telford, J.L., Barocchi, M.A., Margarit, I., Rappuoli, R. and Grandi, G. (2006). Pili in gram-positive pathogens. *Nature Reviews Microbiology* 4, 509-519.

Terao, Y., Mori, Y., Yamaguchi, M., Shimizu, Y., Ooe, K., Hamada, S. and Kawabata, S. (2008). Group A streptococcal cysteine protease degrades C3 (C3b) and contributes to evasion of innate immunity. *Journal of Biological Chemistry* 283, 6253-6260.

Terao, Y., Yamaguchi, M., Hamada, S. and Kawabata, S. (2006). Multifunctional glyceraldehyde-3-phosphate dehydrogenase of *Streptococcus pyogenes* is essential for evasion from neutrophils. *Journal of Biological Chemistry* 281, 14215-14223.

Tewodros, W. and Kronvall, G. (2005). M protein gene (*emm* type) analysis of group A beta-hemolytic streptococci from Ethiopia reveals unique patterns. *Journal of Clinical Microbiology* 43, 4369-4376.

Thomas, C.J. and Schroder, K. (2013). Pattern recognition receptor function in neutrophils. *Trends in Immunology* 34, 317-328.

Thulin, P., Johansson, L., Low, D.E., Gan, B.S., Kotb, M., McGeer, A. and Norrby-Teglund, A. (2006). Viable group A *streptococci* in macrophages during acute soft tissue infection. *PLoS Medicine* 3, e53.

Thurston, T. L. M., Ryzhakov, G., Bloor, S., von Muhlinen, N. and Randow, F. (2009). The TBK1 adaptor and autophagy receptor NDP52 restricts the proliferation of ubiquitin-coated bacteria. *Nature Immunology* 10, 1215-1221.

Treviño, J., Perez, N., Ramirez-Peña, E., Liu, Z., Shelburne, S.A.III, Musser, J.M., et al. (2009). CovS simultaneously activates and inhibits the CovR-mediated repression of distinct subsets of group A *Streptococcus* virulence factor-encoding genes. *Infection and Immunity* 77, 3141-3149.

Turner, C., Kurupati, P., Jones, M., Edwards, R. and Sriskandan, S. (2009). Emerging role of the interleukin-8 cleaving enzyme SpyCEP in clinical *Streptococcus pyogenes* infection. *The Journal of Infectious Diseases* 200, 555-563.

Turner, C.E., Sommerlad, M., McGregor, K., Davies, F.J., Pichon, B., Chong, D.L., Farzaneh, L., Holden, M.T., Spratt, B.G., Efstratiou, A. and Sriskandan S. (2012). Superantigenic activity of *emm3* *Streptococcus pyogenes* is abrogated by a conserved, naturally occurring *smeZ* mutation. *PLoS One* 7, e46376.

Turner, C.E., Abbott, J., Lamagni, T., Holden, M.T.G., David, S., Jones, M.D., Game, L., Efstratiou, A. and Sriskandan, S. (2015). Emergence of a new highly successful acapsular group A *Streptococcus* clade of genotype *emm89* in the United Kingdom. *mBio* 6, e00622.

Underhill, D.M. and Ozinsky, A. (2002). Phagocytosis of microbes: complexity in action. *Annual Review of Immunology* 20, 825-852.

Unnikrishnan, M., Cohen J. and Sriskandan S. (1999). Growth-phase-dependent expression of virulence factors in an M1T1 clinical isolate of *Streptococcus pyogenes*. *Infection and Immunity* 67, 5495-5499.

Uribe, C., Folch, H., Enriquez, R. and Moran, G. (2011). Innate and adaptive immunity in teleost fish: a review. *Veterinárni Medicína* 56, 486-503.

van der Sar, A.M., Musters, R.J., van Eeden, F.J., Appelmelk, B.J., Vandenbroucke-Grauls, C.M. and Bitter, W. (2003). Zebrafish embryos as a model host for the real time analysis of *Salmonella typhimurium* infections. *Cellular Microbiology* 5, 601-611.

van der Sar, A.M., Appelmelk, B.J., Vandenbroucke-Grauls, C.M. and Bitter, W. (2004). A star with stripes: zebrafish as an infection model. *Trends in Microbiology* 12, 451-457.

van der Sar, A.M., Stockhammer, O.W., van der Laan, C., Spaink, H.P., Bitter, W. and Meijer, A.H. (2006). MyD88 innate immune function in a zebrafish embryo infection model. *Infection and Immunity* 74, 2436-2441.

van der Vaart, M., Spaink, H.P. and Meijer, A.H. (2012). Pathogen recognition and activation of the innate immune response in zebrafish. *Advances in Hematology* 2012, e159807.

van Rooijen, N., Sanders, A. and Berg, T.K.V.D. (1996). Apoptosis of macrophages induced by liposome-mediated intracellular delivery of clodronate and propamidine. *Journal of Immunological Methods* 193, 93-99.

van Rooijen, N. and Hendrikx, E. (2010). Liposomes for specific depletion of macrophages from organs and tissues. *Methods in Molecular Biology* 189-203.

Vandecandelaere, I., Depuydt, P., Nelis, H. J. and Coenye, T. (2014). Protease production by *Staphylococcus epidermidis* and its effect on *Staphylococcus aureus* biofilms. *Pathogens and Disease* 70, 321-331.

Vega, L.A., Malke, H. and McIver, K.S. (2016). Virulence-related transcriptional regulators of *Streptococcus pyogenes*. In *Streptococcus pyogenes: basic biology to clinical manifestations*, J.J. Ferretti, D.L. Stevens and V.A. Fischetti eds. (Oklahoma City: University of Oklahoma Health Sciences Center).

Vergunst, A.C., Meijer, A.H., Renshaw, S.A. and O'Callaghan, D. (2010). *Burkholderia cenocepacia* creates an intramacrophage replication niche in zebrafish embryos, followed by bacterial dissemination and establishment of systemic infection. *Infection and Immunity* 78, 1495-1508.

Virtaneva, K., Graham, M.R., Porcella, S.F., Hoe, N.P., Su, H., Graviss, E.A., Gardner, T.J., Allison, J.E., Lemon, W.J., Bailey, J.R., et al. (2003). Group A *Streptococcus* gene expression in humans and cynomolgus macaques with acute pharyngitis. *Infection and Immunity* 71, 2199-2207.

Von Bernuth, H., Picard, C., Jin, Z., Pankla, R., Xiao, H., Ku, C.L., et al. (2008). Pyogenic bacterial infections in humans with MyD88 deficiency. *Science* 321, 691-696.

von Pawel-Rammingen, U. (2012) *Streptococcal* IdeS and its impact on immune response and inflammation. *Journal of Innate Immunity* 4, 132-140.

Voyich, J.M., Sturdevant, D.E., Braughton, K.R., Kobayashi, S.D., Lei, B., Virtaneva, K., et al. (2003). Genome-wide protective response used by group A *Streptococcus* to evade destruction by human polymorphonuclear leukocytes. *Proceedings of the National Academy of Sciences of the United States of America* 100, 1996-2001.

Voyich, J.M., Braughton, K.R., Sturdevant, D.E., Vuong, C., Kobayashi, S.D., Porcella, S.F., et al. (2004). Engagement of the pathogen survival response used by group A *Streptococcus* to avert destruction by innate host defense. *The Journal of Immunology* 173, 1194-1201.

Walker, M. J., Barnett, T. C., McArthur, J. D., Cole, J. N., Gillen, C. M., Henningham, A., Sriprakash, K. S., Sanderson-Smith, M. L. and Nizet, V. (2014). Disease manifestations and pathogenic mechanisms of Group A *Streptococcus*. *Clinical Microbiology Reviews* 27, 264-301.

Walker, M.J., Hollands, A., Sanderson-Smith, M.L., Cole, J.N., Kirk, J.K., Henningham, A., McArthur, J.D., Dinkla, K., Aziz, R.K., Kansal, R.G., Simpson, A.J., Buchanan, J.T., Chhatwal, G.S., Kotb, M. and Nizet, V. (2007). DNase Sda1 provides selection pressure for a switch to invasive group A streptococcal infection. *Nature Medicine* 13, 981-985.

Wang, B., Dileepan, T., Briscoe, S., Hyland, K. A., Kang, J., Khoruts, A. and Cleary, P. P. (2010). Induction of TGF-1 and TGF-1-dependent predominant Th17 differentiation by group A streptococcal infection. *Proceedings of the National Academy of Sciences of the United States of America* 107, 5937-5942.

Wang, Z., Zhang, S. and Wang, G. (2008). Response of complement expression to challenge with lipopolysaccharide in embryos/larvae of zebrafish *Danio rerio*: Acquisition of immunocompetent complement. *Fish Shellfish Immunology* 25, 264–270.

Watson, M.E., Neely, M.N. and Caparon, M.G. (2016). Animal models of *Streptococcus pyogenes* infection. In *Streptococcus pyogenes: basic biology to clinical manifestations*. Ferretti, J.J., Stevens, D.L., Fischetti, V.A., eds. (Oklahoma City, OK: University of Oklahoma Health Sciences Center).

Weiss, G. and Schaible, U.E. (2015). Macrophage defense mechanisms against intracellular bacteria. *Immunological Reviews* 264, 182-203.

Westman, J., Chakrakodi, B., Snäll, J., Mörgelin, M., Madsen, M. B., Hyldegaard, O., Neumann, A., Frick, I.-M., Norrby-Teglund, A., Björck, L., et al. (2018). Protein SIC secreted from *Streptococcus pyogenes* forms complexes with extracellular histones that boost cytokine production. *Frontiers in Immunology* 9, 236.

Wong, C.J. and Stevens, D.L. (2013). Serious group A streptococcal infections. *The Medical Clinics of North America* 97, 721-736.

Wu, Z., Zhang, W. and Lu, C. (2008). Comparative proteome analysis of secreted proteins of *Streptococcus suis* serotype 9 isolates from diseased and healthy pigs. *Microbial Pathogenesis* 45, 159-166.

Yazdankhah, S.P. (2004). *Neisseria meningitidis*: an overview of the carriage state. *Journal of Medical Microbiology* 53, 821-832.

Yona, S., Kim, K.-W., Wolf, Y., Mildner, A., Varol, D., Breker, M., Strauss-Ayali, D., Viukov, S., Guilliams, M., Misharin, A., et al. (2013). Fate mapping reveals origins and dynamics of monocytes and tissue macrophages under homeostasis. *Immunity* 38, 1073-1079.

Zhang, S. and Cui, P. (2014). Complement system in zebrafish. *Developmental and Comparative Immunology* 46, 3-10.

Zhu, F., Zhou, Y., Jiang, C. and Zhang, X. (2015). Role of JAK-STAT signaling in maturation of phagosomes containing *Staphylococcus aureus*. *Scientific Reports* 5, 14854.

Zimmerman, L.M., Vogel, L.A. and Bowden, R.M. (2010). Understanding the vertebrate immune system: insights from the reptilian perspective. *The Journal of Experimental Biology* 213, 661-671.

Zinkernagel, A.S., Timmer, A.M., Pence, M.A., Locke, J.B., Buchanan, J.T., Turner, C.E., Mishalian, I., Sriskandan, S., Hanski, E. and Nizet, V. (2008). The IL-8 protease SpyCEP/ScpC of Group A *Streptococcus* promotes resistance to neutrophil killing. *Cell Host & Microbe* 4, 170-178.

Zlotkin, A., Chilmonczyk, S., Eyngor, M., Hurvitz, A., Ghittino, C. and Eldar, A. (2003). Trojan horse effect: phagocyte-mediated *Streptococcus iniae* infection of fish. *Infection and Immunity* 71, 2318-2325.